INVESTIGATION OF SPECTRUM-MATCHING SENSING IN AGRICULTURE

Semiannual Report
1 December 1965 Through 30 September 1966
Volume I

Fabian C. Polcyn

September 1967

Prepared under NASA Grant NsG 715/23-05-071
by
INFRARED AND OPTICAL SENSOR LABORATORY
WILLOW RUN LABORATORIES
INSTITUTE OF SCIENCE AND TECHNOLOGY
THE UNIVERSITY OF MICHIGAN
Ann Arbor, Michigan

NATIONAL AERONAUTICS AND SPACE ADMINISTRATION

FOREWORD

This report is one of several in a program to determine the feasibility of developing an imaging sensor which uses the spectral characteristics of a scene point to identify materials of interest or to enhance the contrast of selected objects. Multispectral imagery and video data are being generated over scenes of interest from an airborne platform. Multiband images are analyzed and interpreted using conventional photo-interpretation techniques, and the spectral characteristics of targets and background objects are analyzed to determine how to electronically process the spectral information from a scene in real time for improved remote sensing. The general goal of this program is to develop methods of improving and extending current aerial-survey capabilities; improvements are sought in the kinds and quantity of data obtainable and in the quality and economy of imagery interpretation.

This multispectral program was initiated and is being guided by Marvin R. Holter, Head of the Infrared and Optical Sensor Laboratory of Willow Run Laboratories, a unit of The University of Michigan's Institute of Science and Technology. Previous reports issued by the Infrared and Optical Sensor Laboratory under this and related programs are given in the list of related reports which immediately follows.

This report was prepared by the Willow Run Laboratories under Amendment No. 3 of NASA Grant NsG 715/23-05-071, "The Investigation of a Method for Remote Detection and Analysis of Life on a Planet." The Principal Investigator for the research is D. S. Lowe, Head of the Sensory Systems Group of the Infrared and Optical Sensor Laboratory. Contributions to this report were made by

F. Polcyn, Project Leader

P. Hasell, Sensory Instrumentation and Data Acquisition

L. Larsen, Calibration Procedures

E. Work, 12-Channel Spectrometer Fabrication

R. Marshall, Electronic Signal-Processing Schemes for Spectrum Matching

W. Malila, Analysis of Data for Angle Effects

J. Braithwaite, Altitude Studies

The following personnel also contributed to work on the project during this period: R. Horvath, T. Pierce, L. Miller, J. Beard, M. Salata, J. Boyse, N. Spansail, J. Drake, F. Thomson, P. Lowry, J. Lennington, L. Mumford, J. Ladd, R. Jenks, and H. Spring.

This volume makes reference to a supplement containing classified imagery which appears as a separate volume and is available to those holding the required security clearances and need to know.

RELATED REPORTS

COMPARATIVE MULTISPECTRAL SENSING (U), M. R. Holter and F. C. Polcyn, Report No. 2900-484-R, Willow Run Laboratories of the Institute of Science and Technology, The University of Michigan, Ann Arbor, June 1965, AD 362 283 (CONFIDENTIAL).

DIURNAL AND SEASONAL VARIATIONS IN RADIATION OF OBJECTS AND BACKGROUNDS, 4.5-5.5-μ SPECTRAL REGION (U), L. D. Miller and R. Horvath, Report No. 6400-32-T, Willow Run Laboratories of the Institute of Science and Technology, The University of Michigan, Ann Arbor, June 1965, AD 362 620 (CONFIDENTIAL).

THE INVESTIGATION OF A METHOD FOR REMOTE DETECTION AND ANALYSIS OF LIFE ON A PLANET, M. R. Holter, D. S. Lowe, and R. J. Shay, Report No. 6590-1-P, Institute of Science and Technology, The University of Michigan, Ann Arbor, November 1964.

SPECTRUM MATCHING (U), R. E. Hamilton, Report No. 6400-18-T, Willow Run Laboratories of the Institute of Science and Technology, The University of Michigan, Ann Arbor, June 1965, AD 363 001 (CONFIDENTIAL).

TARGET SIGNATURE STUDY, INTERIM REPORT, VOLUME I: SURVEY (U), R. R. Legault and T. Limperis, Report No. 5698-22-T(I), Institute of Science and Technology, The University of Michigan, Ann Arbor, October 1964, AD 354 166 (CONFIDENTIAL).

TARGET SIGNATURE STUDY, INTERIM REPORT, VOLUME II: RECOMMENDATIONS (U), R. R. Legault and T. Limperis, Report No. 5698-22-T(II), Institute of Science and Technology, The University of Michigan, Ann Arbor, October 1964 (CONFIDENTIAL).

TARGET SIGNATURE STUDY, INTERIM REPORT, VOLUME III: POLARIZATION (U), R. R. Legault and T. Limperis, Report No. 5698-22-T(III), Institute of Science and Technology, The University of Michigan, Ann Arbor, October 1964, AD 354 025 (CONFIDENTIAL).

TARGET SIGNATURE STUDY, INTERIM REPORT, VOLUME IV: BIBLIOGRAPHY (ACOUSTIC, ULTRAVIOLET, VISIBLE, INFRARED, AND RADAR) (U), T. Limperis and R. S. Gould, Report No. 5698-22-T(IV), Institute of Science and Technology, The University of Michigan, Ann Arbor, October 1964, AD 354 232 (SECRET).

TARGET SIGNATURE STUDY, INTERIM REPORT, VOLUME V: CATALOG OF SPECTRAL REFERENCE DATA, R. R. Legault, R. S. Gould, and T. Limperis, Report No. 5698-22-T(V), Institute of Science and Technology, The University of Michigan, Ann Arbor, October 1964.

THE INVESTIGATION OF A METHOD FOR REMOTE DETECTION AND ANALYSIS OF LIFE ON A PLANET, L. D. Miller, Report No. 6590-4-F, Willow Run Laboratories of the Institute of Science and Technology, The University of Michigan, Ann Arbor, November 1965.

A COMPREHENSIVE TARGET-SIGNATURE MEASUREMENT PROGRAM, FIRST INTERIM TECHNICAL REPORT, VOLUME I: TECHNICAL DISCUSSION (U), Report No. 7251-3-P(I), Willow Run Laboratories of the Institute of Science and Technology, The University of Michigan, Ann Arbor, December 1965 (CONFIDENTIAL).

A COMPREHENSIVE TARGET-SIGNATURE MEASUREMENT PROGRAM, SECOND INTERIM TECHNICAL REPORT, VOLUME I: DATA PROCESSING, STORAGE, AND ANALYSIS (U), Report No. 7251-9-P(I), Willow Run Laboratories of the Institute of Science and Technology, The University of Michigan, Ann Arbor, June 1966 (CONFIDENTIAL).

A COMPREHENSIVE TARGET-SIGNATURE MEASUREMENT PROGRAM, SECOND INTERIM TECHNICAL REPORT, VOLUME II: MEASUREMENT IMPLEMENTATION (U), Report No. 7251-9-P(II), Willow Run Laboratories of the Institute of Science and Technology, The University of Michigan, Ann Arbor, June 1966 (CONFIDENTIAL).

A COMPREHENSIVE TARGET-SIGNATURE MEASUREMENT PROGRAM, THIRD INTERIM TECHNICAL REPORT (U), Report No. 7251-15-P, Willow Run Laboratories of the Institute of Science and Technology, The University of Michigan, Ann Arbor, February 1966 (CONFIDENTIAL).

A COMPREHENSIVE TARGET-SIGNATURE MEASUREMENT PROGRAM, FINAL REPORT (U), T. Limperis, Report No. 7251-21-F, Willow Run Laboratories of the Institute of Science and Technology, The University of Michigan, Ann Arbor, December 1966, AD 378 112 (CONFIDENTIAL).

DISPERSIVE MULTISPECTRAL SCANNING: A FEASIBILITY STUDY, FINAL REPORT, J. Braithwaite, Report No. 7610-5-F, Willow Run Laboratories of the Institute of Science and Technology, The University of Michigan, Ann Arbor, September 1966.

AN INVESTIGATIVE STUDY OF A SPECTRUM-MATCHING IMAGING SYSTEM, FINAL REPORT, D. S. Lowe, J. Braithwaite, and V. L. Larrowe, Report No. 8201-1-F, Willow Run Laboratories of the Institute of Science and Technology, The University of Michigan, Ann Arbor, October 1966.

TARGET SIGNATURES ANALYSIS CENTER: DATA COMPILATION, D. G. Earing and J. A. Smith, Report No. 7850-2-B, Willow Run Laboratories of the Institute of Science and Technology, The University of Michigan, Ann Arbor, July 1966, AD 489 968.

ABSTRACT

A spectrum-matching imaging system for agricultural survey purposes is being evaluated. A 12-channel spectrometer for the visible region was combined with an optical-mechanical scanner to obtain calibrated simultaneous multispectral data in the same electronic format so that real-time automatic recognition processes might be used. Multispectral data in 18 channels from the 0.3- to 15-μ region have been obtained with a combination of two scanners mounted in a C-47 aircraft. The research data are tape recorded to facilitate the development of spectrum-matching schemes and to permit subsequent extraction of the signatures of vegetation types of interest. Analysis of data collected in 1964 over agricultural sites has shown the non-Lambertian reflection characteristics of different crop species and the importance of the scanner calibration techniques for current data-acquisition programs. Statistical variations of crop signatures and the effects of reflectance geometry and instrumental parameters on the reliability of a spectrum-matching system are being investigated.

CONTENTS

FIGURES

TABLES

INVESTIGATION OF SPECTRUM-MATCHING SENSING IN AGRICULTURE
Semiannual Report
1 December 1965 Through 30 September 1966
Volume I

1
INTRODUCTION

1.1. STATUS OF WORK PRIOR TO THIS REPORTING PERIOD

Under the initial NASA grant for this work, The University of Michigan and Purdue University began investigations to determine whether there existed spectral differences in the reflectance and emittance of cultivated vegetation which would permit discrimination and identification of different species of vegetation cover. Currently, The University of Michigan is concentrating on the development of airborne spectrum-matching imaging systems with their associated electronic subsystems used in spectral signature extraction, the development of spectrum-matching techniques, and analysis of the relation of such systems to the geometry of the sensing operation. Purdue University is concentrating on obtaining ground-truth data, obtaining and analyzing ground spectra, and forming agricultural interpretations.

The technique of multispectral sensing to enhance contrast and permit real-time decision making with the data-acquisition sensor is expected to be beneficial in many areas of remote sensing, particularly in the remote detection and analysis of life on other planets and in permitting agricultural economists to obtain timely information on crop species, maturity, vigor and, possibly, yield, thereby helping to improve management of food resources. The spectral region used with this technique covers from 0.32 to 14 μ. Optical-mechanical scanners constitute the primary airborne data-acquisition sensors. Whenever possible, aerial photographic coverage is obtained with black and white panchromatic, black and white infrared aerographic, color ektachrome, and infrared ektachrome film. The photographic data are obtained at the same time and in the same aircraft as the multispectral data and are used for reference and "ground truth" purposes. Spectrometers and meteorological ground instrumentation are also used to support the investigations.

Between 1 June 1964 and 1 October 1964, five missions were flown at the Purdue Agronomy Farm, and airborne scanner imagery in four spectral regions, along with extensive ground-truth data, was collected. Both day and night flights were made. Some of the data were processed for computer analysis, but, as originally anticipated, further funding was needed to complete the analysis. References 1, 2, and 3 provide a description of the results obtained from the 1964 work.

An amendment to the original grant provided an extension of time and funds for a study of how variations in altitude affect the multispectral signature of vegetation as determined from low-altitude data. Even if agricultural crops have a characteristic and useful spectral signature, their classification or identification from a spaceborne platform would be possible only if attenuation, scattering, and emission by the intervening atmosphere does not alter the signature in an unpredictable manner. Therefore, experiments were designed to determine how a spectral signature in the 0.3- to 14-μ region is affected by variations in altitude from 1000 ft to 15,000 ft. This limitation in altitude was set by the available instrumented aircraft. The flights for this investigation were delayed until the present grant period was funded, which was not until March 1966. Fortunately, during this delay a more complete multispectral sensor capability was established under another program at Willow Run Laboratories* and is now available for this program.

1.2. DEVELOPMENT OF THE SPECTRUM-MATCHING TECHNIQUE

The primary goal of efforts under the current amendment to the original grant is the development of an optimum technique for automatic recognition using calibrated multispectral sensors. To attain this objective, a new type of sensor, which we call the spectrum-matching imaging system (SMIS), has to be developed. Basically, this sensor collects energy from each resolution element of a scene simultaneously in many spectral bands. A decision is made, using pattern recognition techniques, on whether or not the spectral radiance of each scene point belongs to a set of radiances known to exist for a particular terrestrial feature at the time of overflight. The tones in the resulting graphic presentation can then be made to represent how well the spectral radiance or brightness of a given scene point corresponds to a reference or a known spectral radiance. A graphic presentation permits the data user to interpret the resulting image or pattern, but, in some applications, it is envisioned that the output can be numerical, e.g., the acreage planted in wheat or the percentage of vegetative ground cover. This represents a radically new sensing concept, since all current sensors (cameras, radars, electro-optical sensors, infrared sensors) observe and display the magnitude of the differences in radiance from each scene point in a given spectral interval. SMIS observes the spectral properties of each scene point, makes a decision as to whether these properties correspond to those being sought, and then graphically displays the results of this decision.

Optical-mechanical scanners are widely used to generate imagery in spectral regions where photographic or photoemissive detectors are not responsive. In most instances, these scanners use the sensitive area of a detector element as the scanning aperture. The operating principles of airborne optical-mechanical scanners have been discussed by Holter and Wolfe [4].

*Under Project MICHIGAN, Contract DA-28-043 AMC-00013(E).

When mounted in an aircraft or spacecraft, such systems contain a scanning mirror which sweeps the scanning aperture (instantaneous field of view) in lines perpendicular to the flight path, and the forward motion of the vehicle provides the advance of scan lines. With suitable processing and printing the resulting image is a strip map of the scene below, which is not unlike a television picture with an endless frame. Since the signals from the detectors in an optical-mechanical scanner are electrical, they are amenable to electronic processing in real time prior to display or the generation of imagery.

While most scanners use the detector (or a field stop in front of or imaged on the detector) to define the field of view, the entrance slit of a multichannel spectrometer can be used as the field stop, as shown schematically in figure 1. In such a system, each detector of the spectrometer observes the same resolution element of the scene, but in a different wavelength region. The output signal from each detector element is a video signal corresponding to the scene brightness in the particular wavelength region of the detector's operation. This video signal can be used to generate an image of the scene in the wavelength region defined by the position of the detector in the spectrometer. The output signals from multiple detectors can be combined to determine the spectral distribution of the radiation from each scene point, and this spectral information can then be used selectively to enhance or suppress the brightness of objects or materials in a scene on the basis of their spectral radiance. Thus, the multichannel video data can be fed to a signal processor designed to generate a single video signal the intensity of which, for example, might be proportional to the probability that the spectrum measured indicates the object or material being sought.

The possibility of material selection on the basis of the spectral distribution of its radiation is quite reasonable. Numerous investigators have made or are making spectral measurements of natural features in situ to optimize single-band imagery, but only a few are attempting to determine the feasibility of recognizing landscape features on the basis of their spectral reflectance [5-11]. These measurements are largely confined to the photographic region or are being made by nonimaging sensors. Only in recent programs has the idea of combining spectral and spatial information been considered [9, 11]. An optical-mechanical scanner is not limited to the photographic region and can operate in many bands between 0.33 and 13.5 μ, where reflected solar radiation and thermal emission predominate. The discrimination potential of a multispectral scanner is enormous. Assume for the moment that an object's tone can be determined to within one of ten gray levels in any given spectral interval. A multispectral scanner operating in 20 wavelength bands would be capable of distinguishing up to 10^{20} different states. Admittedly, this number of states does not exist: large spectral variations in reflectance and emittance do not occur over narrow spectral intervals in a random manner; variances can occur in a given class of objects; most materials exist as mixtures; and the spectral distribution of the scene

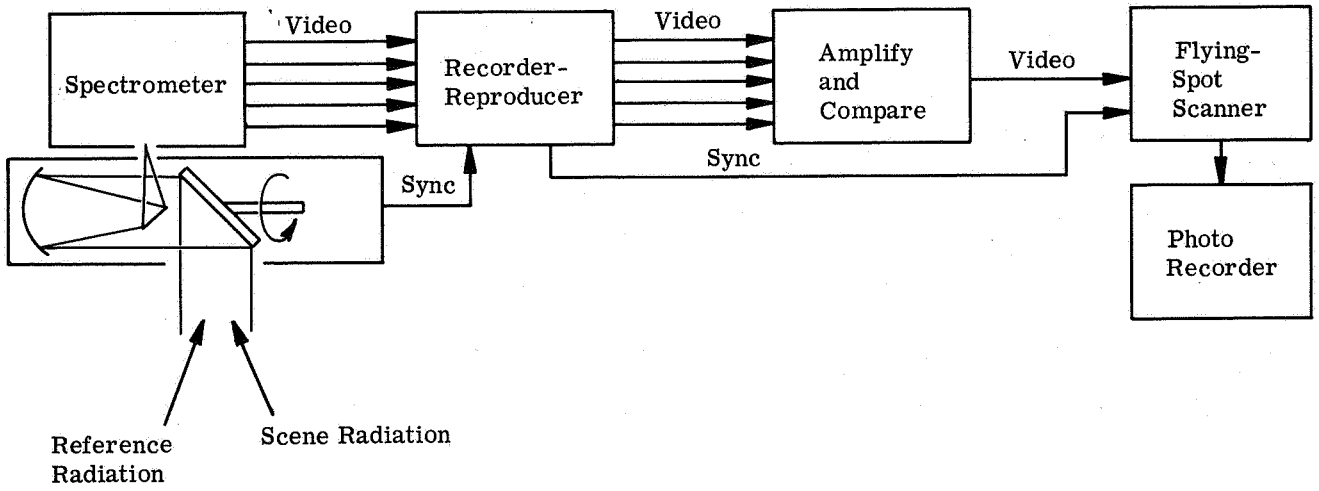

FIGURE 1. SCHEMATIC OF MULTISPECTRAL SCANNER AND DATA PROCESSOR

illuminance varies. Nonetheless, it is obvious that simultaneous observation in many wavelength bands permits one to distinguish between considerably more objects than does single-band operation. The number of channels of operation is a function of the detector signal-to-noise ratio and optical design configuration. Under normal illuminating conditions and ambient temperatures, the spectral interval of 0.33 to 13.5 μ can be split into more than 30 bands, each giving usable SNR. (The Infrared and Optical Sensor Laboratory has completed a design study for such a new sensor operating with up to 29 channels [12].)

The system designed in the above-mentioned study permits collection of data in both the visible and infrared regions from the same resolution element at the same time. This system would obviously be preferred in conducting the next step in the research into spectrum-matching techniques. The system available for use under this grant has been developed under Project MICHIGAN and is useful in laying the groundwork. This system is further described in section 3. A 12-channel spectrometer has been built which replaces a cooled, single-element detector in an airborne scanner. The 12 channels collect energy in the region between 0.4 and 1.0 μ from the same resolution element at the same time. The detailed description of this unit is given in section 3.1. Other data in the ultraviolet and infrared regions are collected at nearly the same time to give 18 channels of information between 0.32 and 15 μ. In order to effectively use the data from any of these multispectral sensors for obtaining spectral signatures, there must be channel-to-channel calibration. We have stated earlier that conventional sensors record only the variations in the radiation received over a scene. The new SMIS technique requires a knowledge of the actual radiation levels in each channel from each resolution element. Calibration of radiation levels for each scan line is provided by reference lamps that produce a voltage pedestal when they are scanned by the same optics that scan the terrain. By obtaining a signal that contains operator gain settings information (a black reference produces zero voltage while the standard lamp voltage is proportional to gain) as well as signal power calibration, the scanner output can be monitored for stability and a spectral brightness curve can be derived. The details of the calibration scheme's implementation in the system used in 1966 data-acquisition program is given in section 4.

The derived spectral-brightness curve is the spectrum that is to be matched to the spectrum of the object being surveyed. These spectra are proportional to the spectral energy emitted or reflected by the source under observation and carry the information such as the species of vegetation, level of maturity, and whether or not diseased sections are developing. Continuing studies are needed to establish the signatures of the many objects of interest and to study the influence of such factors as angle of view, sky condition, altitudes, row direction, soil type, and moisture on the uniqueness of the spectrum. The SMIS can be used to obtain the data needed to analyze the spectrum taken in real situations. For meeting the purposes of the research in 1966,

the outputs of the 12-channel spectrometer as well as the six spectral bands distributed in the ultraviolet and infrared regions are tape recorded. The tapes are then replayed, new digitized tapes are made, or the data are displayed on multichannel chart recorders to facilitate analysis. The electronic processing used to obtain signatures and to perform the spectrum-matching function is described in section 5. Some of the pictorial results obtained from initial experiments are shown in a classified supplement to this report.

The spectral data collected in 1964 and 1966 are being analyzed for the effects of angle of view, altitude, and instrumental effects. The results of the analysis to date are presented in section 6, where it is shown how the response from crops can vary as a function of different angles of view and with different row orientations. Section 6.4 describes how the 1966 data will be processed to determine altitude effects on the spectral signatures. As planned, the level of funding for the third amendment to the grant does not permit analysis of the 1966 data; this must be performed under follow-on contracts. The program for data collection under the 1966 contract is described in section 2.

2
DATA-ACQUISITION PROGRAM FOR 1966

To meet the objectives in the development of the spectrum-matching imaging system for agricultural uses, a series of controlled data-acquisition missions over a known agricultural site was needed to collect data to be used for studies of signatures at different states of maturity, as well as variances of spectra for crop species and varieties and the investigation of altitude effects on signatures. It was also desired to collect data over an extended flight path of a few miles so that tests of electronic spectral-matching techniques could be made later in a simulated operational sense.

The data collected will help answer many specific questions requiring research: How many wavelength channels of information are required for reliable identification? What wavelength resolution is adequate? What is an acceptable signal-to-noise ratio for a useful detection probability? What maximum ground resolution can be tolerated? What time of day is preferred for sensing? How do sky condition, soil moisture, and soil type influence spectral signatures? Does the spectral intensity from a particular field observed at angle θ_1 differ enough from another field observed at angle θ_2 to permit automatic recognition? What is the acceptable range for the angle of view of the receiver? What are the overall statistical variations on signatures? How should the spectrum matching be made?

The data-collection tests and their analysis form the main stream of a verification procedure whereby all inputs, such as spectral wavelength, sun angle (time of day), view angle, crop types and conditions, etc., are weighed to determine the major factors in successful identification from an airborne or spaceborne platform. It is expected that the research will identify the conditions and situations that lend themselves to space sensings in comparison to conditions under which ground equipment or airborne sensors can be used more profitably.

2.1. SITE SELECTION

The total agricultural experiment consists of airborne tests, ground-truth measurements and checks, ground calibration checks, data processing and analysis, and interpretation of results. To keep the data processing and handling less complex and permit easier interpretations, simple data-acquisition operations were planned. Fields were chosen in which the vegetation types of interest were arranged in a linear array so that a single aircraft pass covers the complete set of fields. The fields selected were large enough that, by either electronic sampling

or densitometry, an accurate estimate of the corresponding intensity in each spectral band can be made at any of the altitudes flown.

The number of crops sensed and the condition of the crops were selected on a priority basis. Such factors as the economic importance of the crop, the mean size of the fields, the effect of different types of soil, and the crop's maturation rate bear on whether the operational sensing will ultimately be done from orbital altitudes or from conventional aircraft altitudes.

The above factors were considered in the choice of the several flight lines at Lafayette, Indiana, and the locally flown passes in Michigan. Since only three 1-week missions to Lafayette were budgeted, flights were made in June, July, and September to sample the maturation states of wheat, corn, soybeans, and some of the less important crops.

2.2. DATA-ACQUISITION OPERATIONS

The three 1-week missions flown at Lafayette were organized to provide the following types of data for analysis (see table I):

(1) Altitude-variation data. A series of flights over a 3-mi path was made at increments of 2000 ft up to 10,000 ft.

(2) Source-angle and view-angle data. Morning and noon sun angles were chosen and a flight at an altitude of 700 ft was made so that the radiation from the selected fields could be sensed over most of the receiver's total scan angle. The morning sun provided forward scattered and backscattered light for flight lines oriented north and south. The noon sun provided left- and right-scattered light for the same flight orientation in addition to a different source elevation angle.

(3) Crop-signature data and simulated operational data for future analysis. Several passes were made at altitudes of 3500 ft and 2000 ft over the Agronomy Farm and over areas southwest of Lafayette to gather statistical data on different crops for signature analysis. Three relatively long flight lines at 10,000 ft provided wide-area coverage for general ground-truth orientation, and at least one of the flight lines provided data to test spectrum-matching technique development.

(4) Livestock data. Data-collection flights were made both day and night for comparison of livestock detection probabilities.

(5) Soil-moisture stress data. Data collected at the Sand Farms area north of Lafayette will be analyzed mainly by personnel at Purdue University.

TABLE I. 1966 DATA-ACQUISITION SUMMARY

Date	Mission Time	Areas and Altitudes* (K = Altitude × 1000 ft)																								Weather (c = cloudiness)
		Agronomy Farm								South of Wabash River							Sands Farm			Livestock			High Altitude 8 to 10K			
		West Run				East Run				C1	C2	C3	C4	C5		C6										
		0.7K	2K	3.5K	6K	0.7K	2K	3.5K	6K	3.5K	3.5K	3.5K	3.5K	0.7K	2K	2K	0.5K	1K	3.5K	1K	2K	3.5K	W	C	E	
5 May	1300			X				X		X	X	X	X						X			X				Clear, dry, 5%c
28 June	1152		X	2.6			X	2.6		2.6	2.6	2.6	2.6		X											Bright haze, 70%c at 4000 ft
29 June	1243	X	X				X							X	X	X	X	X	X							Hazy
29 June	2136		t.o.*				t.o.								t.o.					t.o.	t.o.			t.o.		Hazy, clear
30 June	0836	X	X				X							X	X	X							X	X	X	
30 June	1400	X	X	X		X	X	X		X	X	X	X	X	X	X				X	X					Hazy, 10%c at 6000 ft, 30% at 15,000 ft
26 July	1020			4K			X	4.0	X	X	X	X	X										X	X	X	Hazy, 20%c at 10,000 ft
26 July	2145		t.o.				t.o.								t.o.					t.o.	t.o.			t.o.		Hazy, 50%c at 10,000 ft
27 July	0840	X	X			X	X						X		X	X					X	X				Hazy, dull, 100%c at 8000 ft
28 July	1203	X	X			X	X								X	X	X	X	2K							Hazy, dull, 75% at 3000 ft
29 July	0802	X	X			X	X								X	X	X	X	X							Clear, bright, 10%c at 25,000 ft
15 Sept.	0745	X	X	4K	X	X	X						X				t.o.	X	t.o.				X	X	X	Wet from night before, 0%c
15 Sept.	1211	X	X	X			X	X		X	X	X	X				t.o.	X	t.o.	X	X					West from night before, 5%c at 5000 ft
15 Sept.	2030		t.o.				t.o.								t.o.					t.o.	t.o.		t.o.	t.o.	t.o.	Clear, 0%c

*t.o. = tape records only, no photographic coverage.

X = scanner plus photographic coverage.

3
NEW EQUIPMENT CONFIGURATION FOR 1966

The data-collection equipment available to the contract to accomplish the planned measurement program was not completely suited to the task without modification. Fortunately, the available equipment, developed under the Project MICHIGAN, was being modified to increase the scope of a Project MICHIGAN data-collection program in a manner quite similar to requirements of this project. Therefore, some of the required modifications to the data-collection system were developed under the army-funded contract while others were developed under this grant. The new capabilities include: (1) a 12-channel spectrometer configured to replace a detector in The University of Michigan modified AN/AAS-5 airborne scanner, (2) conversion of one of two 7-channel magnetic-tape recorders into a 14-channel machine, (3) purchase of new detectors and filters with better performance characteristics, (4) the reconfiguration of the C-47 instrumentation aircraft to incorporate 11 new scanner data channels, one new operator position with controls and displays, and radiometric calibration provisions for all 18 scanner data channels, and (5) the development of ground-based data-handling equipment to sample and serialize up to 12 data channels simultaneously.

3.1. 12-CHANNEL SPECTROMETER

Probably the most important new equipment development during this reporting period has been the spectrometer detector unit. This unit provides simultaneous multispectral information in the visible and near-infrared regions using off-the-shelf components.

A problem inherent in the design of a spatial scanner with a spectrometer detector system is illustrated by the system shown in figure 2. The single detector of a conventional spectrometer observes one spectral resolution element at any one time, and the system scans in time through the spectral region of interest. However, terrestrial scanners of the kind in which we are interested scan across one ground resolution element in times which are short compared with the scan time for the fastest scanning spectrometers. Therefore, the system must be designed to detect many spectral bands simultaneously and must use multiple detectors. The simultaneous spectral observation by an array of detectors imposes several severe requirements on the spectrometer optics. The same spectral dispersing element (the prism in fig. 2) must be capable of operating over the entire spectral range of interest, and its spectral dispersion should be reasonably matched to the spectral resolution desired in the region of interest. Finally, the optics selected for the spectrometer must be matched to the optics of the scanner and must handle the radiation without undue attenuation losses.

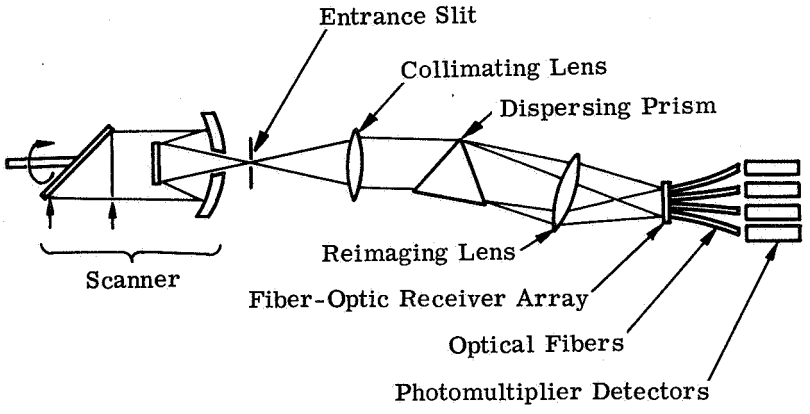

FIGURE 2. EXISTING DISPERSING MULTISPECTRAL SCANNER AND ASSOCIATED SYSTEM

Because spectral information in the region 0.4 to 1.0 μ would prove useful and because optical components for operation in this wavelength region were readily available as off-the-shelf items, it was decided to first develop a simple spectrometer for this region of the spectrum. Rapid completion and earlier collection of data were thus to be realized. In addition, a foundation of experience would be laid for expansion of similar techniques into the ultraviolet region and further into the infrared.

The design concept has been to produce a spectrometer which is readily interchangeable with any of the conventional single-element detectors usually associated with an airborne scanner. Its configuration is shown in figure 3. The detector is a prism-type spectrometer with its entrance slit located at the focal point of the scanner collecting optics (where the detector flake of a single-element detector would normally be located). The lenses and prism shown are all conventional components readily available from camera or spectrometer manufacturers. The spectrally separated radiation output of the spectrometer is picked up by an array of 16 fiber-optic bundles which distribute the energy to 12 photomultiplier detectors located in a ring around the top of the assembly. One to four fiber bundles can be grouped at each photomultiplier to establish the wavelength resolution of each channel. Thus, at any instant of scan, the identical ground resolution element is registered in 12 bands in the wavelength region of the photomultiplier response, 0.4 to 1.0 μ.

The instrument allows for latitude and versatility in selection of several channels. Already mentioned is the possibility of grouping any combination of fiber bundles. The whole fiber array may be positioned or shifted to any desired point along the dispersive spectrum by use of the focal-plane adjust screw illustrated in figure 3. Finally, the fiber-optic array and entrance slit may be completely replaced by any number of customized configurations for obtaining different resolutions or any desired optical bandpass within signal-to-noise limitations. To allow for flexibility in choosing wavelength assignments, interchangeable photomultipliers with either S-20 or S-1 sensitive photocathodes are used in the detector array. Two views of the spectrometer detector are shown in figure 4. Figure 5 shows the fiber-optic assembly prior to its incorporation into the system.

The 12-channel spectrometer detector has now been operated continuously on a relatively busy flying schedule since April 1966. Strip-map quality from the system has been at least as good as has ever been achieved with any of the former single-element infrared detectors. Of equal significance is the fact that it has never experienced an operational breakdown, not even a single failure of a photomultiplier tube.

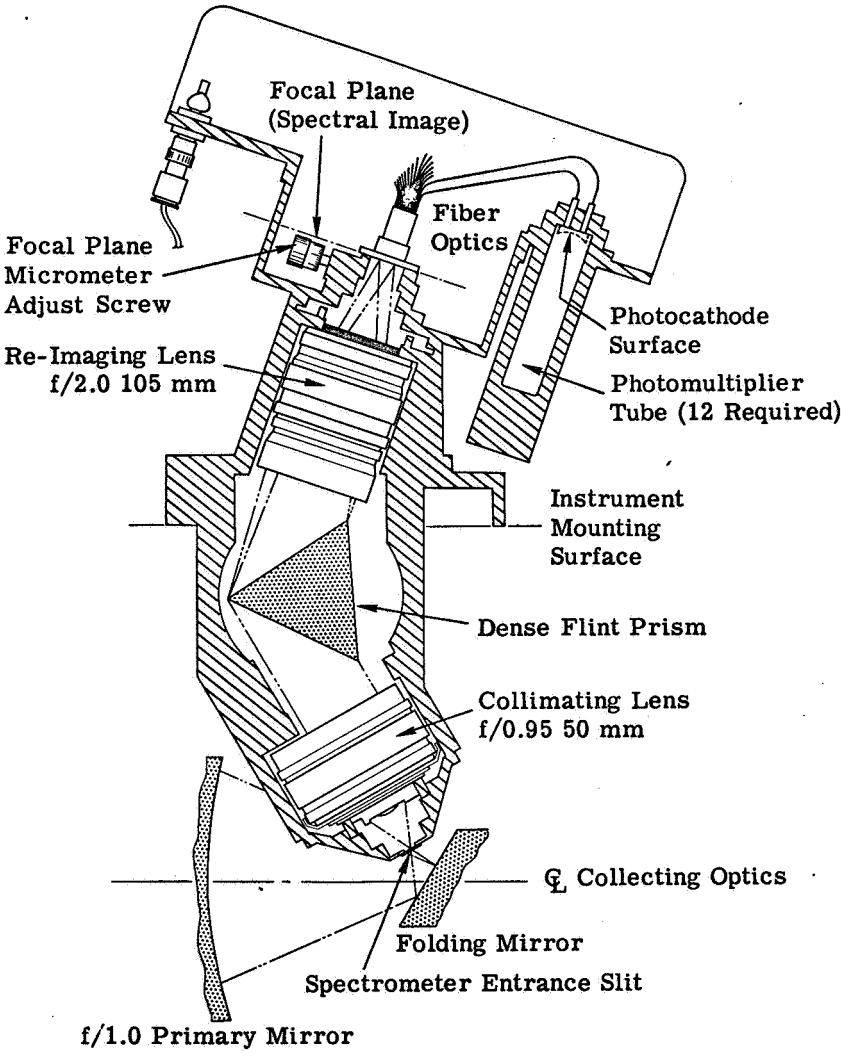

FIGURE 3. 12-CHANNEL SPECTROMETER (0.4 TO 1.0 μ)

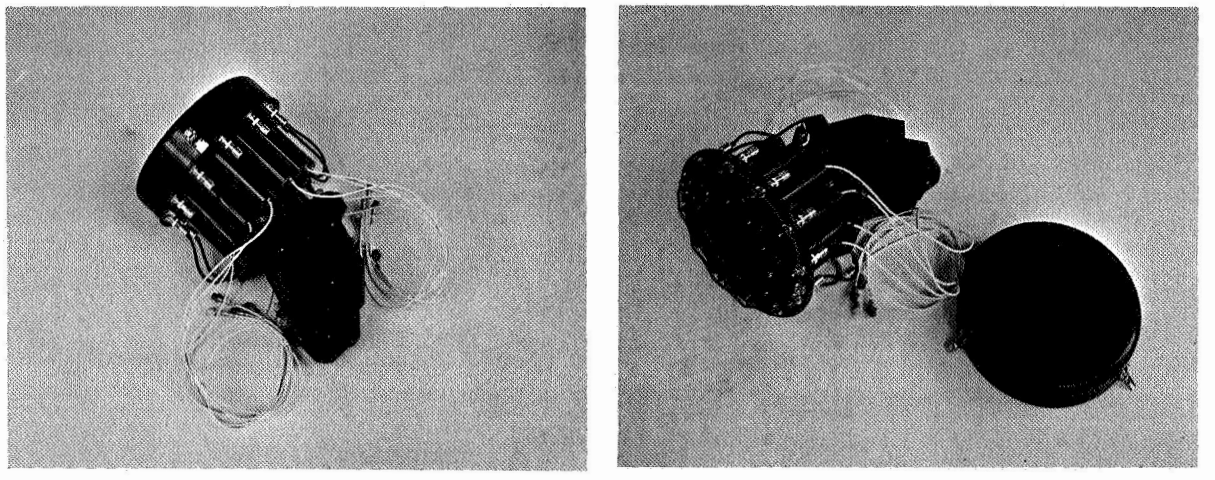

(a) Overall View

(b) With Cover Removed

FIGURE 4. SPECTROMETER-DETECTOR ASSEMBLY

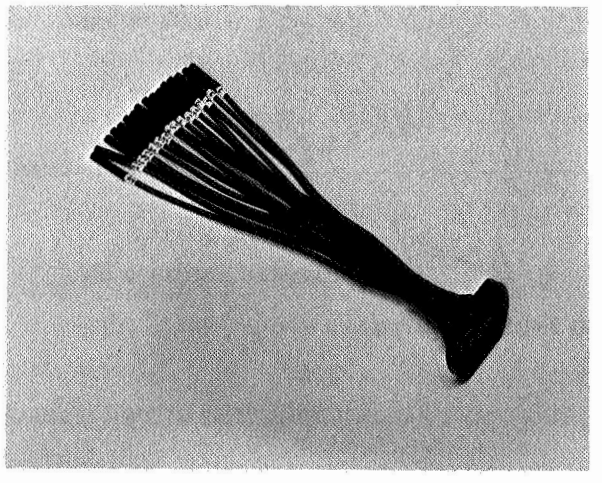

FIGURE 5. FIBER OPTICS OF SPECTROMETER-DETECTOR ASSEMBLY

3.2. CONVERSION OF TAPE RECORDER

The two 7-channel Ampex 1300 magnetic-tape recorders which were part of the original data-collection equipment assembled in 1964 lacked the capability of recording 12 simultaneous data channels on a single tape. Therefore, one of the two recorders was converted by Ampex field personnel to a 14-channel machine. The conversion was routine and involved replacing the recording head and adding the required electronic signal-handling units. An edge track for a voice channel was also added.

The 18 video channels from the two double-ended airborne scanners are recorded on tape in the data format given in table II. Opposite ends of each scanner are referred to as A and B ends. The data format places the sync in the center of each tape to minimize time displacement effects of tape skew. Odd- or even-numbered tape channels are grouped on the same tape head. Thus, to minimize channel-to-channel time displacement caused by tape flutter and stretch, the outputs of the four-element detector (B end of scanner no. 1) are placed on the same head.

3.3. NEW DETECTORS

Aside from the 12-channel spectrometer, no new detectors were developed for the airborne scanner. However, the configuration of the four-element InSb detectors was modified to incorporate more rugged mounting to improve reliability and more accurate wavelength filters to improve the data quality. Even with these improvements, the four-element detectors have not been reliable in operation and there is evidence of radiation leakage onto the detector elements from around the bandpass filters. The evaluation and investigation of replacements for this detector are continuing.

A Ge:Hg long-wavelength detector assembly, complete with helium dewar, was purchased as an operational spare to the one already in use. These detectors have performed well.

An evaluation of photomultiplier tubes which could be used in the spectrometer resulted in a selection of RCA types. Type 8645 with an S-20 cathode is used in the spectrometer channels between 0.40- and 0.72-μ wavelength, and type C70042CP1 with an S-1 cathode is used for wavelengths between 0.72 and 1.00 μ. These detectors provide optimum signal-to-noise characteristics under the operating conditions of this application. An Amperex 150 UVP with an S-13 cathode response is used for the photomultiplier detector in the 0.32- to 0.38-μ wavelength region.

3.4. C-47 INSTALLATION

The instrumentation configuration in the C-47 aircraft was modified to incorporate another operator position associated with the proper recording of the 12-channel spectrometer output.

TABLE II. DATA FORMAT

Mag.-Tape Channel No.	Scanner No. 1 on 1/2-in. Tape	Scanner No. 2 on 1-in. Tape
1	B: 1.5 to 1.8 μ	B: 0.32 to 0.38 μ
2	Illumination level	A: 0.40 to 0.44 μ
3	B: 2.0 to 2.6 μ	A: 0.44 to 0.46 μ
4	Sync No. 1	A: 0.46 to 0.48 μ
5	B: 3.0 to 4.1 μ	A: 0.48 to 0.50 μ
6	A: 8.0 to 14.0 μ	A: 0.50 to 0.52 μ
7	B: 4.5 to 5.5 μ	A: 0.52 to 0.55 μ
8		Sync No. 2
9		A: 0.55 to 0.58 μ
10		A: 0.58 to 0.62 μ
11		A: 0.62 to 0.66 μ
12		A: 0.66 to 0.72 μ
13		A: 0.72 to 0.80 μ
14		A: 0.80 to 1.00 μ

Radiometric calibration signals were introduced into all video data channels. Small-area, high-intensity radiation references were viewed in the reflective channels, and extended blackbody plates which filled the collection aperture were observed in the thermal channels. The dark illumination level and thermal radiation of the interior of the scanners were also registered in the video signals (see sec. 4).

The aircraft equipment configuration requires an instrumentation operating crew of three technicians and two engineers. One technician operates the four aerial cameras and the console used for photorecording two scanner channels directly on film during the flight. A second technician operates the 6-channel console and the 1/2-in.-tape recorder. The third technician operates the 12-channel console and the 1-in.-tape recorder. One engineer monitors the operation of the preset calibration references and notes all non-tape-recorded data. The second engineer directs the instrumentation and aircraft flight crews.

4
CALIBRATION OF DATA-ACQUISITION EQUIPMENT

The scanner output signals are a direct function of the viewed radiation. The scanner provides a voltage output for each resolution-element area on the ground which is proportional to the radiation received from each area, but the proportionality factor and the bias level (voltage output for zero radiation) are not known to the required accuracy. One way to improve this accuracy is to provide a constant reference radiation into the scanner which can be compared with the ground radiation. The constant reference radiance must then be either known (as in the present system for the 0.32- to 4.1-μ region) or compared with a known radiance from the ground. Ground panels of known reflectance are used as reference sources.

Two blackbody plates of known temperature are used as radiant reference sources for the 4.5- to 15-μ bands. The radiances of these reference sources are measured by the scanner and the apparent radiances of the ground sources are compared with these as necessary. The calibration sources must give a spectral radiance in each spectral band which is near that from the ground. Since no one source is available with the spectral distribution of the sunlit earth over the wide spectral interval from 0.3 to 14 μ, several sources of different temperatures and areas are used.

4.1. REFLECTION CHANNEL CALIBRATION

The dominant radiant energy from the scene in the 0.3- to 4.1-μ band is reflected sunlight. The source spectral characteristics therefore should match those of the sun. The sun's spectral energy as viewed through the atmosphere is approximately a 5800^{o}K graybody with some attenuation in the 0.4- to 0.5-μ region and more in the 0.3- to 0.4-μ region. Two quartz-iodine lamps are used as sources in the 0.3- to 1.0-μ band, which is the spectral region covered by one of the multispectral scanners. The two lamps have similar spectral radiance, but one is adjusted to be several times brighter than the other. The brighter lamp is the reference in the 0.3- to 0.6-μ part of the band, and the dimmer lamp is used for 0.6- to 1-μ channels. The dark interior of the scanner serves as the dark-level (zero-radiation) reference for each of the scanner data channels in the spectral band 0.3 to 1.0 μ.

Another multispectral scanner is used to provide the signals in the 1.5- to 14-μ band. Again a quartz-iodine lamp is used as a reference source for the detectors operating in the 1.5- to 4.1-μ spectral band. Since the thermal radiation from the area surrounding the lamp cannot be considered negligible in this band, the lamp is surrounded by an extended blackened

plate whose temperature is controllable and uniform. The radiance from the lamps is controlled by controlling the voltage from a regulated power supply.

Figure 6 shows the approximate spectral irradiance of the detector by sunlit earth and from the two quartz-iodine lamps, 45 W and 100 W, in the 0.3- to 1.0-μ region. A 45-W lamp is also used in the 1.5- to 4.1-μ band, but the lamp is normally operated at a lower current in this region. Figures 7a and 7b show the measured scanner output in each of the spectral bands given in table III.

The relative spectral radiation from the quartz-iodine bulb is shown in figure 8. Typical calibration pulses from both bulbs in the 0.3- to 1.0-μ band as a function of time are shown in figure 9. The central 250 μsec of the pulse is considered the calibration level. Data showing calibration signal levels in comparison with ground signals are shown in figure 10.

4.2. THERMAL CHANNEL CALIBRATION

The plate that provides a known background for the 1.5- to 4.1-μ band lamp and another plate, both with high emissivities and controllable temperatures, are used as reference radiation sources for the 4.5- to 14.0-μ band. Each of these plates is controlled to a fixed temperature which will result in a radiance comparable to the lowest and the highest ground radiances bracketing the targets of interest. Each plate is covered with a polyethylene window to reduce convective losses. The plates are grooved and painted dull black to reduce reflections. A uniform temperature is maintained by using a thick layer of copper for the plate. Heat is conducted to or away from the copper plate by thermoelectric modules coupled to a water-cooled heat sink. The water is cooled by a radiator in the air stream. The temperature of the plate is maintained constant by a closed-loop servo system using a thermistor sensor. The heating or cooling rate is about $0.2^{\circ}C$/sec. Measurements on the plate show the temperature to be uniform to $0.1^{\circ}C$ over the surface of the plate and controllable to $\pm 0.1^{\circ}C$ over the range of $0^{\circ}C$ to $60^{\circ}C$ with an ambient temperature change of $5^{\circ}C$ if (1) the temperature control is set for a higher temperature than the water and the mode switch is at heating or (2) the temperature control is set for a lower temperature than the water and the mode switch is at cooling. Two problems exist at the present time:

(1) If the desired plate temperature is near ambient, the operator doesn't know when to switch the mode switch to heat or cool. This is expected to be corrected soon with automatic mode switching.

(2) If the plate is below the dew-point temperature, either water or frost forms on the plate surface, causing an error in the expected radiation from the plate.

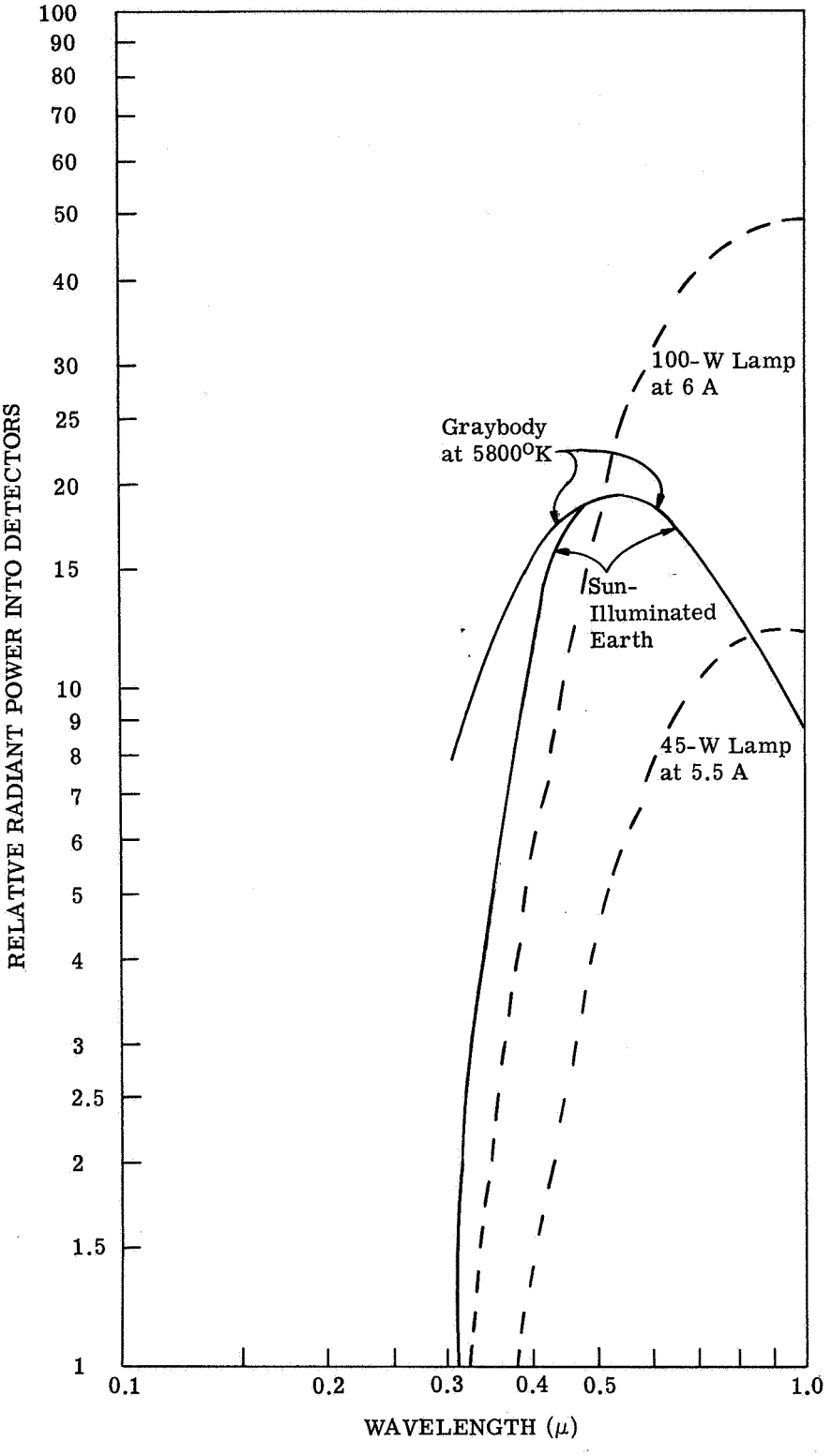

FIGURE 6. SPECTRAL CHARACTERISTICS

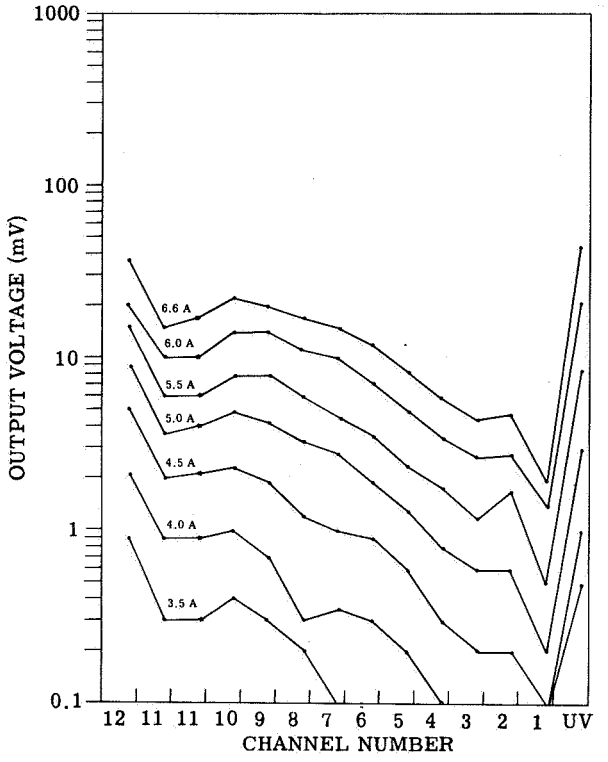

(a) 45-W Source

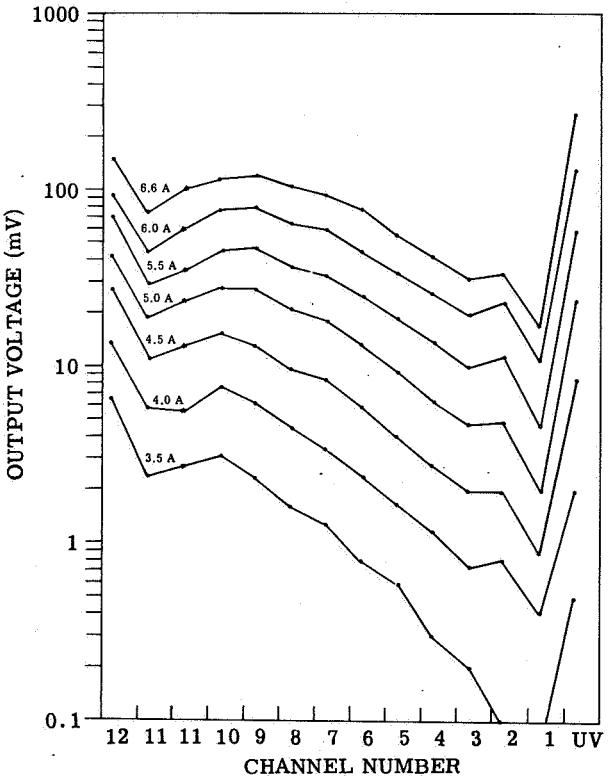

(b) 100-W Source

FIGURE 7. PHOTOMULTIPLIER OUTPUT. Operated at several bulb currents for 5-kΩ load.

TABLE III. SPECTRAL BANDWIDTHS FOR 12-CHANNEL SPECTROMETER

Channel	Fiber No.	Spectral Bands up to 15 April, 1966 (μ)	Spectral Bands After 15 April 1966 (μ)
UV	—	0.32 to 0.38	0.32 to 0.38
1	14, 15, 16	0.390 to 0.420	0.404 to 0.437
2	12, 13	0.420 to 0.442	0.437 to 0.464
3	11	0.442 to 0.455	0.464 to 0.482
4	10	0.455 to 0.470	0.482 to 0.502
5	9	0.470 to 0.480	0.502 to 0.524
6	8	0.488 to 0.509	0.524 to 0.549
7	7	0.509 to 0.532	0.549 to 0.580
8	6	0.532 to 0.559	0.580 to 0.617
9	5	0.559 to 0.594	0.617 to 0.659
10	4	0.594 to 0.630	0.659 to 0.719
11	3	0.630 to 0.682	0.719 to 0.799
12	1, 2	0.682 to 0.810	0.799 to 1.000

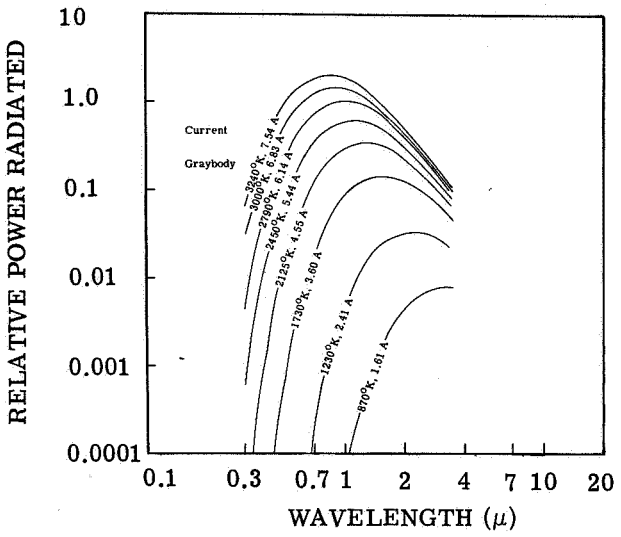

FIGURE 8. RELATIVE POWER OF QUARTZ-IODINE LAMP. Based on preliminary data. For $\lambda > 3.5\ \mu$, the tungsten emissivity decreases and the quartz envelope transmission decreases and reradiates.

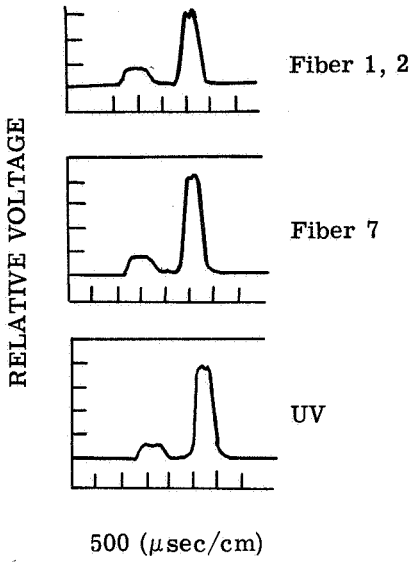

FIGURE 9. TYPICAL CALIBRATION PULSES

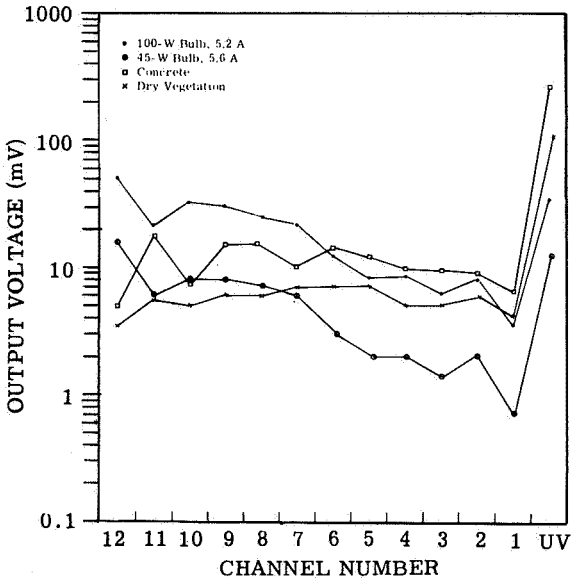

FIGURE 10. COMPARISON OF VOLTAGE LEVELS FOR GROUND SAMPLES AND CALIBRATION LAMPS

Thermistors calibrated to $\pm 0.05^{o}C$ every $11^{o}C$ by Fenwal are used for temperature monitoring in conjunction with a bridge circuit. Absolute accuracy has not been determined, but should be close to the thermistor limitation.

4.3. GROUND PANELS AS REFLECTANCE STANDARDS

The use of the internal calibration lamps provides a stable reference for monitoring the sensor detectivity as well as permitting any gain or dc bias adjustments to be automatically stored in the video signal since both a zero level and calibration signal are recorded. When the lamps are calibrated for power output, an instrument transfer function can be prepared. By using a set of ground panels of known percent reflectance, a way of converting the video signal to percent reflectance is obtained. A detailed analysis into the conditions for which this conversion is accurate is given in appendix I. The reflectance of the five-step gray panels used varies with wavelength as shown in figure 11a. Nominally, the wavelength percent reflectances for the panels are defined as 4, 8, 16, 32, 64; but as can be seen from the figures for a channel between 0.617 and 0.659 μ, the gray scales have values of 4.3, 6.7, 13.5, 27.1, and 58.6. Figures 11b and 11c show the percent reflection of the three-step set of black and white panels and of the red, green, and blue panels also used for calibration in 1966.

The motivation for conversion to percent reflectance can be seen from considerations of the sunlight variations on the fields during an overflight. Basically, one can consider spectral signatures of any object to be either the percent-reflectance curve or simply voltage vs. wavelength information existing in electrical signals from the object. When the clouds obscure the sun, the voltage, being proportional to power reflected from the object,is reduced and a multispectral signal processor may or may not be able to identify the sample. If the processor makes the decision on the basis of percent reflectance, then one might argue that this parameter is less susceptible to sunlight changes and a correct recognition may be made. The practical difficulty lies in the implementation of the conversion to percent reflection without introducing a significant error in the process. A standard on the ground is usable primarily on clear days since a sample taken at one location can be stored and used as a reference at later points in a flight line. For the present, the ground panels will be used to check system performance, to provide a standard object for both ground and airborne spectral measurements, and to aid in comparing spectral signatures on the basis of reflectance during the analysis phase. Essentially, they will be used to determine whether one must use reflectance rather than radiance for spectrum-matching decisions.

The total set of panels used during the 1966 missions consisted of a photographic-resolution bar chart, a set of three-color panels (red, green, and blue), and both a three-step gray scale and a five-step gray scale. The size of the color and gray-scale panels were generally 20×40 ft

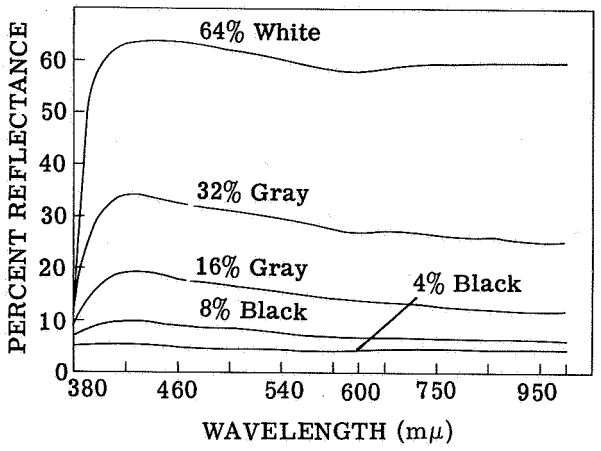

(a) 5-Step Gray-Level Set of Panels

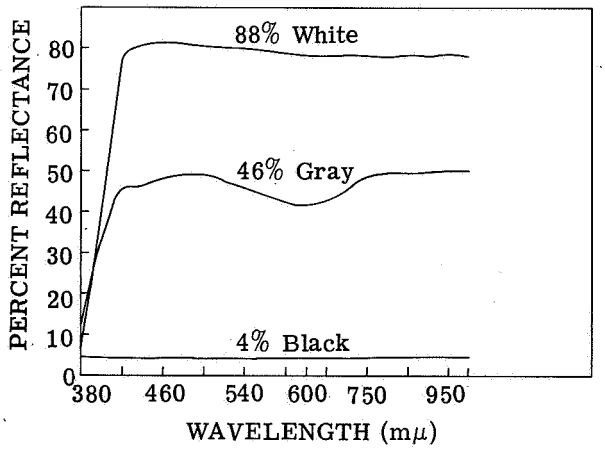

(b) 3-Step Gray-Level Set of Panels

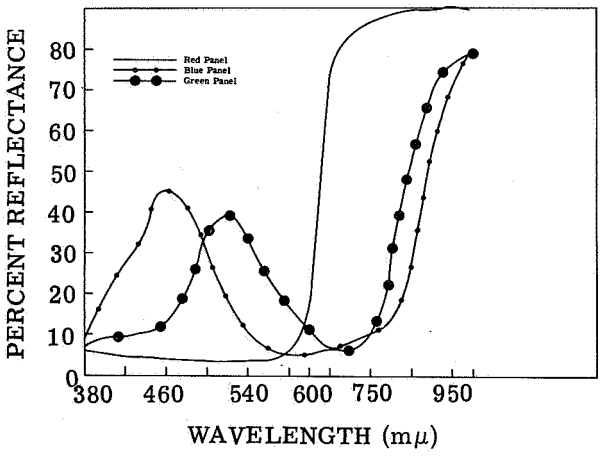

(c) Three-Color Set of Panels

FIGURE 11. PERCENT REFLECTANCE

for each level. Figure 12 shows the layout during the July mission at the Agronomy Farm near Lafayette. The panels were furnished and displayed under contract with Data Corporation, Dayton, Ohio.

4.4. PROGRAM FOR USE OF THE CALIBRATION PROCESS

Calibration sources are being used in the data-collection program so that spectral radiance can be measured on an absolute scale. This will help in determining the reflectivity of types of vegetation. In this way, such data may then be employed to recognize and map objects using standard spectral signatures developed from earlier measurements. In the past, it has not been possible to determine spectral signatures which could be used with data obtained on different flights. Only ordering of the reflectances for objects or crops was possible for data obtained at different times and in different places.

As shown earlier, the present program includes two basic calibration sources, ground-placed panels of known reflectivity and airborne thermal and luminous sources seen by the scanners during each revolution of the scan mirror. The calibration data from these sources are obtained in different ways. The panels located on the ground are seen by the airborne scanners for only a brief time, and it is therefore difficult to locate and to measure the signals corresponding to these sources directly (i.e., electrically). The use of cyclical scanning of the primary data tapes would allow such a measurement, but the necessary equipment is not available at present. Lacking such equipment, we have planned a less direct technique using photographic film as a transfer medium. An electrical step wedge signal of 11 gray scales will be inserted at the beginning and end of the strip maps created from the tapes. The internal calibration sources in the scanner will be recorded on the same film along the edge of the strip maps. The electrical signals may then be recovered by a densitometric measurement in which the film is required to function only as a medium for comparison. As a result, no particular care is required to calibrate the film; the only requirement is that the gray scales of interest be distinguishable.

In this manner the voltage equivalence of a scene point, the ground panels, and the internal calibration sources may be determined and the radiance or reflectance may be calculated for any scene point. Once the equivalence of the internal calibration sources to external standard reflectance panels has been determined, the reflectance of ground points for other areas may also be determined, provided the solar radiation is constant. If solar radiation varies because of clouding or haze, reflectivity cannot be determined unless the solar radiation can be measured under the various conditions encountered.

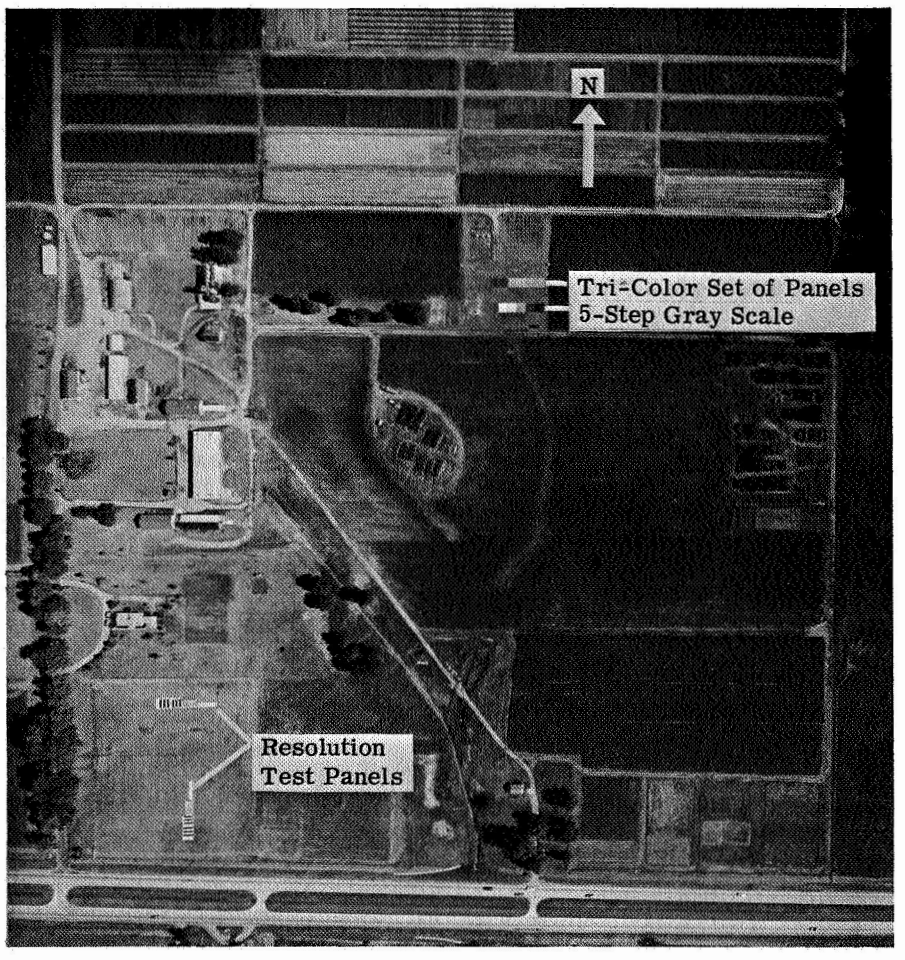

FIGURE 12. AERIAL PHOTOGRAPH SHOWING CALIBRATION PANEL DISPLAY AT PURDUE AGRONOMY FARM

Calibrated information will be generated for analytical work in three basic forms: film, serial analog video, and digital tape. The data will be of the same form in each case, that is, the relative locations of data in each record will be preserved.

In the case of film strip maps, each channel of data will be printed as a normal single-channel strip map, except that the calibration sources sampled during each scanner revolution will be relocated in time to appear at the edges of the strip map to form two bands of gray alongside the usual imagery. In addition, gray-scale step wedges generated from appropriate voltage waveforms will be inserted at the beginning and end of each film strip. This form of the data allows quantitative analysis by conventional densitometry and is preferred for some analyses.

In the second case, the data are first rearranged in the form of a sequentially presented (serialized) version of the 12-channel parallel data. These data can then be played back, digitized, and recorded in serial digitized form. A code is supplied to the tape channels to designate the kind of data present: signature, calibration, or zero reference. With these data, the radiance of the calibration sources may be read with the processing equipment. The variability of the instrumentation may be monitored from these data, also, since the calibration source is available during each scanner rotation and drift and gain variations may be determined.

More importantly, the statistical analysis of the data corresponding to particular classes of objects, e.g., corn or wheat fields, can be performed on a digital computer using these digitized, serialized tapes as a convenient input. The statistics can then be used as classification keys for processing future data.

5
SIGNATURE EXTRACTION AND SPECTRUM-MATCHING TECHNIQUES

5.1. SIGNATURE EXTRACTION

One of the principal objectives of the program is the extraction of signatures of crops from the scanner data. The scanner data, calibration data, and ground-truth information must all be accurately obtained and preserved to allow the signatures and their sources of variability to be determined. Not only must signatures of crops of interest be determined, but the similarity of the backgrounds to these crops must be examined to obtain a measure of the uniqueness of the signatures. Signature extraction then must consider the complete environment, the instrumental variability, and parameters such as the orientation of the scanner, its "look" angle, and the sun angles.

The primary means of extracting signatures and examining variability will be processing of scanner data on a digital computer. The digital computer data will be a tape containing a densely sampled version of the original analog tape data and will preserve the scanner look angles and roll information. It will also contain coding to define the data, whether it is the spectral radiance of a field of interest, of calibration data, or of useless information. With these data the statistics of a representative group of crop fields may be gathered and processed directly by computer program. The ground-truth information and calibration information can be merged with this tape or entered separately on cards. (A detailed description of this procedure is included in appendix II.) Since this record contains data not only from the field of interest but from other fields as well, samples of background signatures may be gathered from the same data and should allow the generation and testing of realistic covariance functions.

In addition to the extraction of signatures by digital computer, another means of signature extraction is available. The equipment necessary to prepare data for the computer may also be used to obtain spectral data about areas of interest. This equipment normally generates a sequential scan of the multispectral data in a continually cyclic form. This scan may be controlled, however, so that data are obtained only from a selected area. This serial scan may be photographed on an oscilloscope and a signature and the dispersion of the signature may be determined. Covariance properties of the signature are not retained with this technique, however.

This approach has been used to determine the signatures of several crops in the Lafayette area in order to evaluate the technique as a means of obtaining signatures quickly and as an independent means of signature extraction to serve as a check on the computer process.

Finally, an interesting means of analyzing spectral information in two bands has been used fairly extensively. Signals from two spectral channels may be supplied to the xy inputs of an oscilloscope and the complete distribution for some chosen scene can then be examined sequentially. The display may be calibrated and used to obtain signatures, but its principal usefulness lies in allowing a quick examination of the covariance of the signals for two selected wavelengths for every part of a completed scene. The discriminability of many targets using only two wavelengths can then be assessed by visual examination. This estimate or test of target discriminability is a useful one since it is pessimistic, i.e., if the desired target can be seen to have a distribution which does not overlap other distributions, the target may be discriminated and the false-alarm rate should be decreased when more spectral dimensions are employed.

An example of this form of presentation is given in the supplement to this report. Data were obtained on a flight over the ramp area of the Willow Run Airport beginning from an area including a lake and rural scene and proceeding north across the eastern edge of the airport. Several objects of interest have been identified in these photographs. Their recognition will be discussed in section 5.2.

5.2. SPECTRUM MATCHING

The objective of the program in spectrum matching is the recognition or enhancement of crops of interest or of important characteristics of these crops. Experiments have been conducted using two approaches so far. One is based on the use of the x-y display mentioned in section 5.1 and allows recognition of objects with separable x-y distributions. The other allows the simultaneous matching and recognition of 12-element sources by computing the instantaneous vector distance between an unknown signal and a signature and registering a match when the distance is within some arbitrary bound.

The first technique, christened the "x-y light pen," employs an x-y oscilloscope to present the two-color spectrum in an orthogonal manner and generates a display as shown in figure 13. If a detector is now located on the face of the CRT with an aperture properly sized to match the distribution of interest, the detector output will indicate that a target with the proper spectral coordinates has occurred and that it has occurred at a definite time. If a strip-map image is now generated employing the detector signal as the video signal in place of the original video, the map will indicate the location and shape of the targets within the aperture.

This has been done for the scene mentioned earlier (sec. 5.1), and four recognition strip maps have been generated. These are shown in the supplement, indicating the recognition of water, gravel-topped asphalt, concrete, and grass. These data were obtained on 21 March, and very little vegetation besides grass and winter wheat was evident. It was found to be possible to map some winter wheat under these conditions with the same spectral channels.

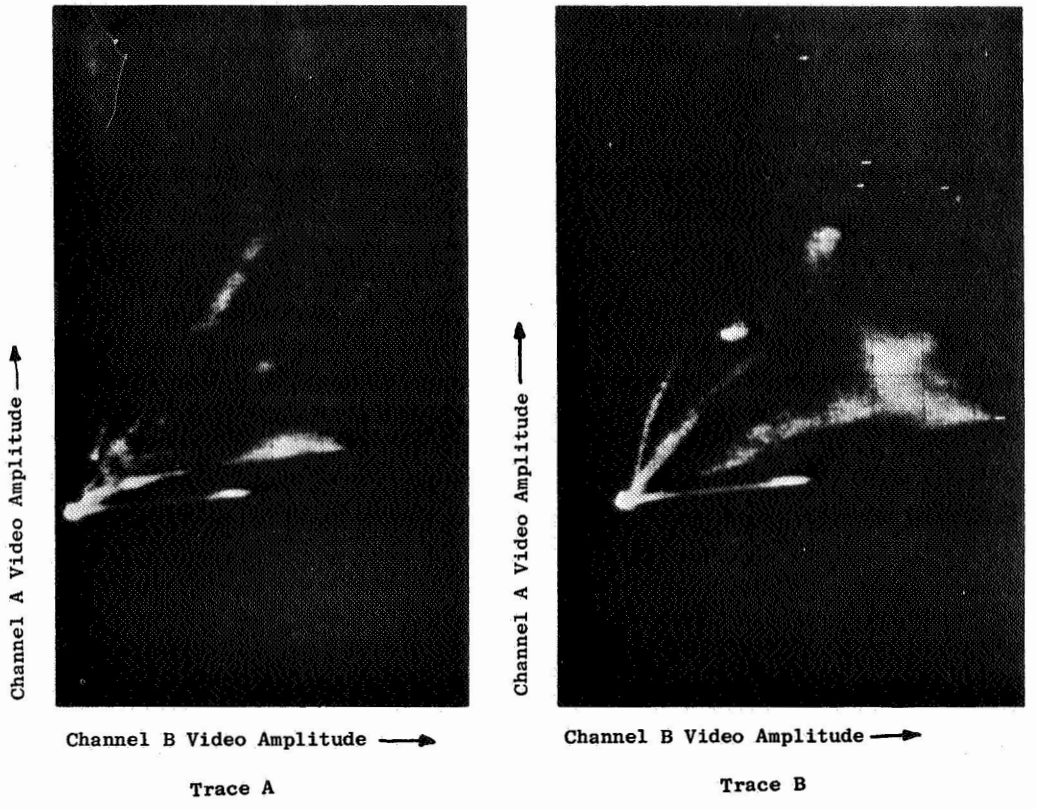

FIGURE 13. EXAMPLE OF x-y PLOT OF TWO-COLOR SPECTRA

Using equipment assembled for the serialization of the taped data, we were able to extract signatures readily from areas of interest and to determine the channels of the spectrometer which would allow the best discrimination of specific targets. This was done for some data obtained in a flight over the western portion of the Purdue Agronomy Farm on 20 July at 0800 hours. A particular question was raised concerning the possibility of discriminating corn and soybeans on that date since film-strip imagery of the spectral bands seemed identical. First attempts at recognition using the 0.46- to 0.48-μ and 0.66- to 0.72-μ bands were not conclusive, i.e., some corn and soybeans were confused. Investigation of the spectral signatures indicated that differences existed in channels 8 and 9 (0.58 to 0.61 μ and 0.61 to 0.65 μ) and, to a lesser extent, in channels 5, 6, and 7 (0.49 to 0.51 μ, 0.51 to 0.53 μ, and 0.53 to 0.56 μ). Additional tests performed as a result indicated that better discrimination of all corn and soybeans in the field of view could be found in channels 8 and 10 (0.58 to 0.61 μ and 0.66 to 0.72 μ).

Another application of the light-pen technique to data obtained on 28 June at 1200 hours in the Lafayette area illustrated both the practicability of using the data for identification and a typical difficulty in such simple processing. From data taken along a 2-mi run on that date, three different recognition pictures were made using spectrometer channels 3 and 10 (0.46 to 0.48 μ and 0.66 to 0.72 μ). In the first recognition picture, an attempt was made to recognize pasture lands. A comparison with ground-truth data reveals that the areas which are recognized are pasture land, alfalfa, and red clover. The false alarms which occurred were red clover, alfalfa, and one corn field (see fig. 6 in the supplement for the results).

Because it is impossible to tell precisely what the composition of the pasture was (it may have contained considerable alfalfa and clover), the only definite false alarm was the corn field. In the second recognition picture, an attempt was made to recognize corn, but soybeans were also recognized frequently as corn. Clover was also a false alarm. In the second picture, the sunlit part of the large soybean field in the center of the picture was recognized but the shadowed portion was not. In the third picture, an attempt was made to recognize wheat. Confusion resulted with the shadowed section of the large soybean field.

The confusion between corn and soybeans is particularly difficult to resolve. The confusion resulting when cloud shadows fill part of the field of view was expected in the absence of automatic gain and level controls in the video processing. Cloud shadows are a major problem in any discrimination technique (see fig. 7 in the supplement for an example).

This result indicates the need for a technique of gain control as a function of the actual irradiation of the surface. No clearly satisfactory solution to the problem of determining the surface irradiation is apparent yet; however, a form of automatic gain control based on a wide-area sensor may be useful. It is also possible that sensing of shadowed areas may be accomplished

by noting the difference between blue and red spectral bands, since the blue bands are less sensitive to shadowing because of the larger amount of scattered blue illumination of the scene. Another measure of illumination, but one which is very liable to error, is the sensing of illumination incident on the aircraft. Only under certain geometries of sun, cloud, and aircraft can this be considered useful in shadow correction.

An experiment has also been performed using the 12-channel processor for discrimination of crops. This equipment consists of a wideband analog computer equipped with a set of special-purpose plug-in modules to allow the video signals to be sampled and standardized prior to serialization for digital-computer tape preparation. Sufficient operational amplifiers are incorporated to allow the continuous computation of a parameter related to how closely the 12-channel signal matches a given crop signature. Once a signature has been obtained, it may be immediately set into the computer and the data may be matched in real time. If the match is within a certain bound preset on a voltage comparator, the comparator indicates the existence of a match and its output signal is used as a video signal to generate a strip map showing the location and shape of the area matched.

The same experiment described above, discriminating corn and soybeans, was performed with this computer. In this case the spectral signatures of corn and soybeans were obtained with the serializer and compared. These spectra are shown in figure 14. Measurement of these spectra indicated that differences are greatest in channels 5, 6, 7, 8, and 9. Therefore, only these channels were used in the recognition process. A test was made with two different threshold levels. The desired discrimination of the corn and soybeans was obtained for the fields chosen; however, some corn crops appear identical to the soybeans chosen for a reference. In this test the detection operation was not completely correct, insofar as the significances of differences in signatures were not properly weighted in the operation. It was found that the fields recognized are not uniform and, furthermore, there is some dependence of the process upon the angular position of the scanner (see fig. 8 in the supplement for the results).

These experiments with the light pen and 12-channel processor are preliminary in nature and are, properly speaking, only initial investigations of some techniques which appear useful in the recognition process. The results appear promising and indicate that these techniques should be useful both directly and in conjunction with the digital-computer analysis. Using imagery in the form referred to above allows the detection of variability in crop signatures and thereby helps to direct the investigation of the sources of variability. For this reason it appears that these techniques will be used extensively in the analysis of the data gathered during this reporting period.

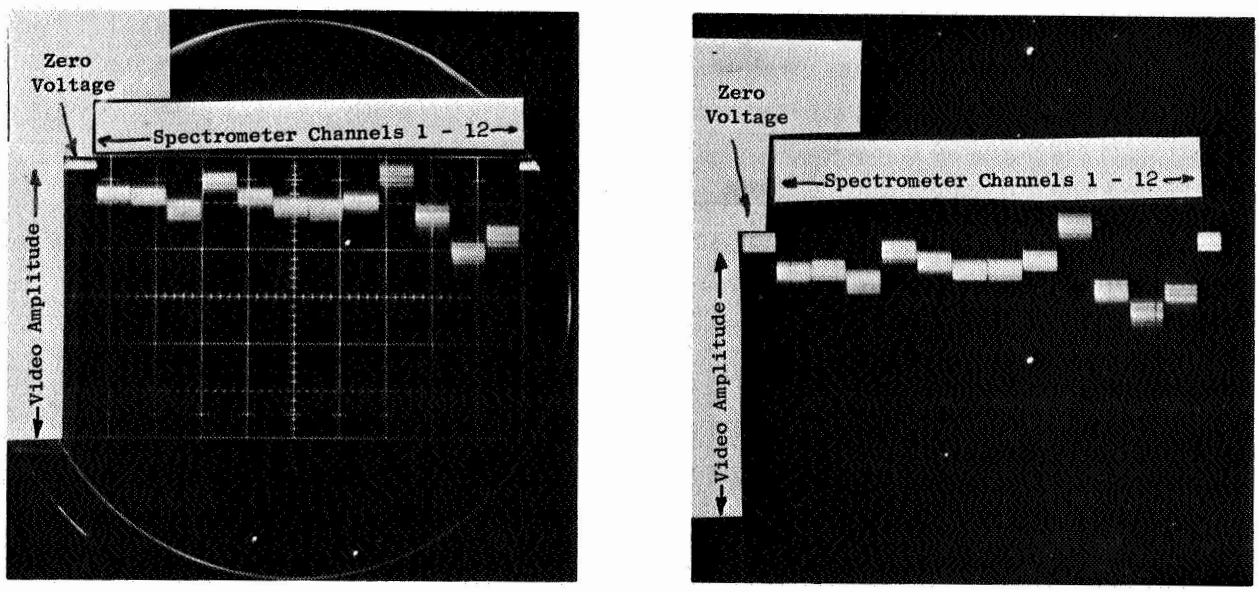

(a) Corn

(b) Soybeans

FIGURE 14. SPECTRAL SIGNATURES OF CORN AND SOYBEANS

5.3. PLANS FOR FUTURE WORK

5.3.1. IMPLEMENTATION OF TECHNIQUE FOR ELECTRONIC SIGNATURE EXTRACTION. During this reporting period the equipment needed to perform extraction of signatures has been fabricated and tested on typical data. The ability to extract signatures in the form of photographs of the spectrum from specific areas of fields has been demonstrated and allows some limited processing.

The equipment is ready to begin the preparation of tapes suitable for use on a digital computer and the selection of data for such analysis is now being made. Regular work on preparation of digital tapes should be underway in October.

A principal difficulty in the extraction of signatures arises when the areas to be examined are only a small part of the field of view of the scanner. The presently planned method of extraction in this case is to use film as a transfer medium and calculate the electrical equivalents of particular gray scales. A much more powerful and convenient method, the use of a cyclic storage device to allow repeated and regular representation of the data from a given number of scan lines, has been considered in the past. Such devices could be built from endless-tape loops, rotary-head tape scanners, digital core memories, and digital drums or discs. Their limited flexibility or their high cost were major disadvantages in all of these devices.

The solution which now appears very attractive involves the use of a digital storage device, a drum memory, to store analog data in the form of PFM. If the data stored on FM tape are simply transferred without demodulation, 12 channels at a time to a drum in such a manner that 12 tracks of the drum are filled with the next scan lines, a complete history of all 12 channels may be gathered on the drum in sequence as the tape is examined. Once a target has been found, the process may be stopped and the spectral characteristics are located within the drum storage capacity.

The drum may now be used to cyclically replay the data through demodulators and this replay may be limited to only those scanner lines of interest under digital control of the drum-track selection. The serializer may then be used to obtain spectral information from any arbitrarily small area or object in the data.

It is planned to test this technique as soon as possible with an available drum which is reasonably well suited to this operation.

5.3.2. INVESTIGATION OF SPECTRUM-MATCHING TECHNIQUES. The experimental investigation of electronic spectrum-matching or recognition techniques will be continued more intensively during the next period. Particular attention will be paid to determining the effects of experimental equipment, environment, and scene geometry on the recognition process. Both

the light pen and the 12-channel processor will be used for this purpose. Analog and digital techniques that use the full potential of the statistical properties (e.g., correlations between spectral channels) of the signatures will also be investigated. Determination and cataloguing of recognizable crops will be pursued, as will cataloguing of recognizable objects for other possible applications.

Another area of interest, which has an unknown potential as yet, is that of contrast enhancement. Although the function of contrast enhancement may be thought of as an intermediate step in the recognition process, it may be that in some cases it will help image interpreters to perform better than a mechanized recognition technique. Some possible applications of contrast enhancement have already been noticed in the discrimination of live from dead or diseased vegetation and in increasing contrast of man-made objects with respect to their surroundings.

6
ANALYSIS OF 1964 DATA

During the time that the 1964 multispectral data were obtained and during the year that followed, relatively little quantitative analysis was performed on these data, but a fair amount of qualitative analysis was performed [2]. For the main quantitative effort, transmittance readings on image transparencies were made at Willow Run Laboratories (WRL) with a film densitometer on approximately 50 points of interest, and a statistical analysis of some of these indicated that distinguishable multispectral signatures do exist [7].

It was proposed under the present grant extension that additional densitometer readings would be made and that the earlier quantitative analysis would be expanded and continued. Prior to this, however, it was deemed essential to investigate both (1) the extent to which the data-gathering instruments and the subsequent data-processing equipment might have affected the densitometer readings and their interpretation, and (2) the possibility of calibrating the 1964 data "after the fact" by self-calibration methods. The results of these investigations, as discussed in detail below (secs. 6.1 and 6.2, respectively), are such that the making of additional densitometer readings for the purpose of signature studies was deemed unadvisable since (1) it is not possible to quantitatively evaluate and reliably correct the readings for the chief deleterious instrumental effects and (2) the average quality of the imagery is poorer than that which is now attainable. The need for calibration in the data and for corrections of certain instrument errors has prompted various modifications and improvements in the data-gathering instrumentation for the 1966 season, as discussed in sections 3 and 4.

Another important parameter in the production of imagery and multispectral data by remote sensors is the geometry of observation and illumination. There can be marked changes in the observed radiation from a given crop or combination of crops dependent upon the angle of observation [13] and (in spectral channels in which reflected light predominates) upon the position of the sun and the distribution of clouds. Such angle-dependent variations were and are being studied both experimentally from photographs and theoretically from models of reflectance geometry (see sec. 6.3).

6.1. INVESTIGATION OF INSTRUMENT EFFECTS

Multispectral data are obtained with two types of instruments, optical-mechanical scanners and photographic cameras. Each type exhibits its own variations caused by the angle of observation (measured from the nadir); in the imagery they are superimposed on any angle-dependent

variations of the crop reflectances. Furthermore, the film processes that were used to record the images introduce added variations and uncertainties.

6.1.1. SCANNERS. Optical and electronic effects in the scanners produced changes in the detector signals as the field of view was scanned across the scene. It has been learned that the filters on the four-element array of infrared detectors did not provide uniform filtering for all observation angles and consequently there were angle-dependent variations caused by changes (as yet not thoroughly documented) in the spectral response of the four channels. Much less serious angle-dependent variations caused by the optics of the other scanners were probably present. In many strip maps, instrument noise degraded the image quality.

The electrical outputs of the detectors used in the scanners were ac coupled into the amplifier stages. At the scanning frequency used (e.g., ~60 scans/sec), one can consider the simplified output of one detector to be a rectangular wave with one-quarter of a cycle (~80^{O}) corresponding to the desired signal from the scene and the remainder of the cycle corresponding to the signal from the inside of the scanner (see fig. 15a). The absence of dc coupling causes the amplified version of the rectangular wave to exhibit a droop (fig. 15b). This droop is partially explained by the low-frequency cutoff of the coupling circuit, that is, the lower the cutoff frequency, the less the droop. Measurements made on the scanner electronics after the conclusion of the 1964 missions show that the maximum droop would have been approximately 15% of the peak-to-peak value of the square wave. Two facts preclude the correction of the data for the droop effect: (1) the peak-to-peak value of the square wave and therefore a percentage of this value (i.e., the droop) depend upon the relative radiances of the scene and the inside of the scanner (in certain spectral bands, the inside of the scanner may be as radiant as or more radiant than the scene), and (2) the signals generated by the inside of the scanner were not preserved during the tape-recording process in the airplane (i.e., they were gated out) and the playback gains were adjusted to obtain "best" images.

The final step, that of recording tape-recorded scanner signals on film, introduces a third potential source of angle-dependent variations in the output imagery. In this process, the amplified detector output signals are used to modulate the intensity of a cathode-ray tube (CRT) which is imaged on the recording film and is swept across it in correspondence with the motion of the scanning mirror across the scene; the film is slowly moved perpendicular to the CRT trace to provide the second dimension for the imagery. There are three factors affecting the densities which one might read from a transparency so produced. First, there is the nonlinear relationship between density and exposure for the film; the procedures used to expose and process the film were not documented and thus there is no reference from which to extract this information. Second, when a constant input voltage is applied to the CRT, the amount of exposure

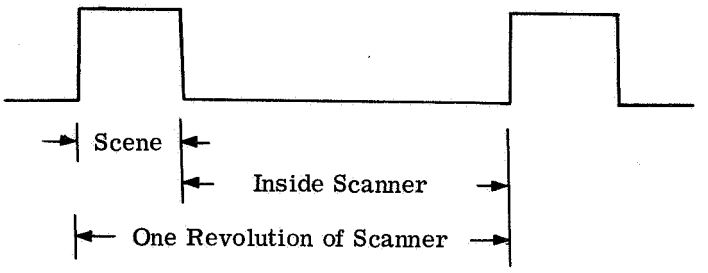

(a) dc Coupling

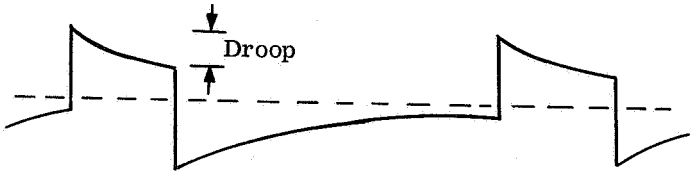

(b) ac Coupling

FIGURE 15. SIMPLIFIED SCANNER OUTPUT VOLTAGES

across a scan line varies, i.e., there is more exposure at the center of the line than at the edges; in addition, nonuniformities in the CRT phosphor produce other irregularities in the film traces. Figure 16, a plot of relative density vs. position across a film in a direction parallel to the scan line as measured with a long narrow aperture that spanned several scan lines, illustrates these effects; note that the traces deviate more and more from the ideal horizontal lines as the intensity (and therefore the density) increases.* Third, there were variations in the motion of the film past the CRT so that underlap and overlap occurred between adjacent scan lines; these variations increase the variability of densitometer readings. The above factors contributed in large part to the decision to analyze the 1966 detector output voltages directly without first transferring them onto film.

The scanners used to obtain data in 1964 were uncalibrated, as were all operational infrared and optical scanners at that time; section 4 describes the calibrations which have been added to the WRL scanners to make the 1966 data more useful.

6.1.2. CAMERAS. With uncompensated cameras, there is a falloff of illumination in the film plane from a uniform diffuse radiator. From a simple geometrical point of view, this falloff is proportional to the fourth power of the cosine of the angle from the center of the field of view. Such effects are discussed in reference 27. For imagery obtained in 1964 with the 73.7°-field of view (FOV) K-17 cameras (i.e., in both the 0.4- to 0.7-μ and 0.7- to 0.9-μ regions), a K-star filter which has a spatially variable transmittance was used near the objective lens to compensate for this falloff; the extent to which the compensation was successful has not been measured quantitatively, but to the eye there is a very noticeable improvement even though there does remain some falloff at the edges of the pictures. The smaller FOV nine-lens camera on the other hand was not corrected and a falloff of at least $\cos^4$ is estimated for its pictures. Figure 17 illustrates the magnitude of a $\cos^4$ falloff vs. off-axis viewing angle.

The other major factor that affects the densities produced on film is the generally nonlinear relationship between the actual exposure E and the density D produced. There probably are variations of a few percent in the shutter speed and therefore in the actual exposure values. The well-known curve of D vs. log E is illustrated in figure 18. The slope of the linear part of the curve is the development factor γ. As its name implies, γ depends upon, among others, the developer used for the particular film and on the development time; a long development time produces a large γ. The photographic data obtained during 1964 were not initially intended for quantitative analysis, so the development time was varied from roll to roll to obtain the best looking pictures, and the development parameters were not recorded. Consequently, new

*Some of the noise on the traces is caused by scratches on the test film strip.

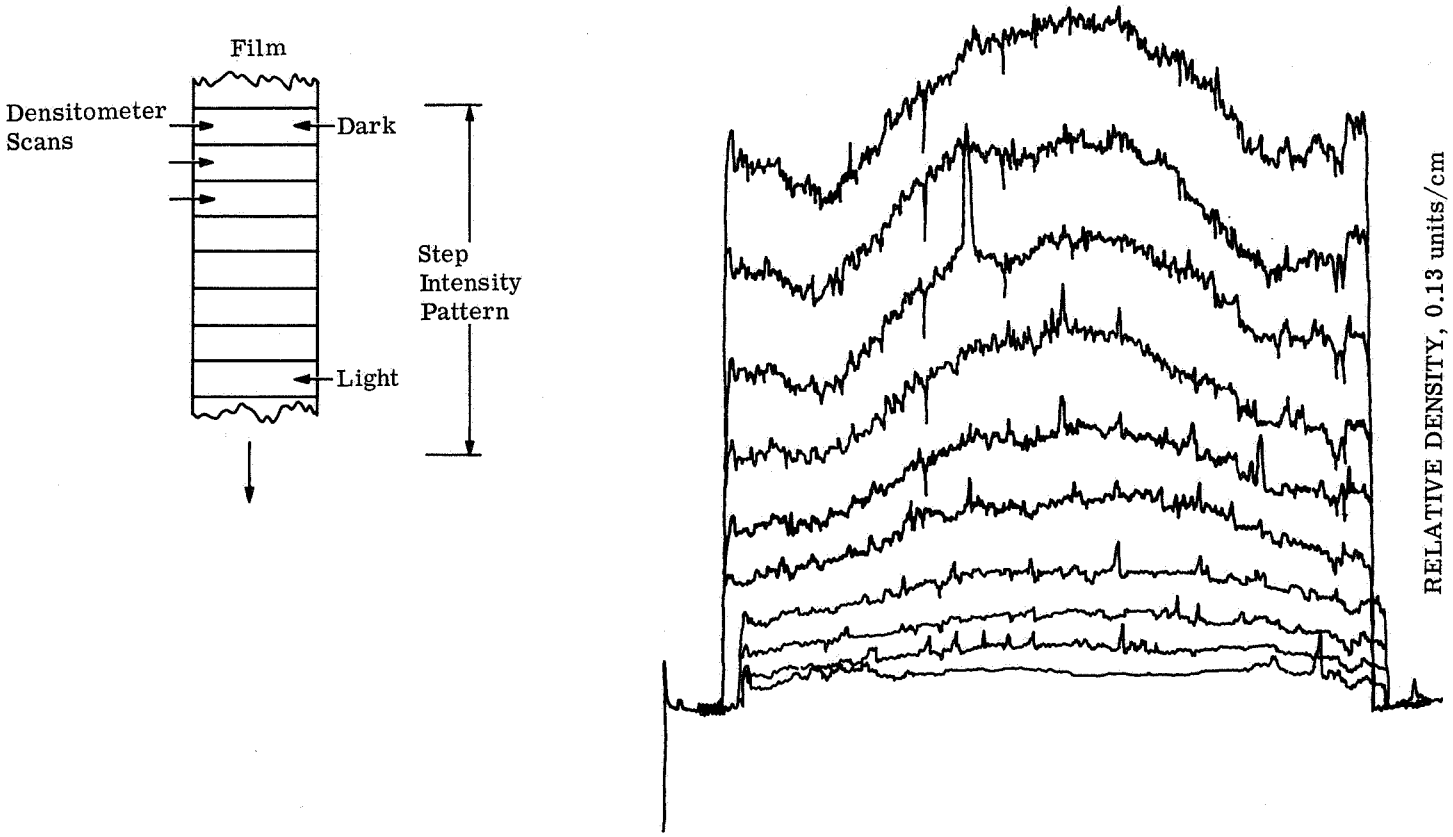

FIGURE 16. DENSITOMETER SCANS OVER STEP-INTENSITY PATTERN

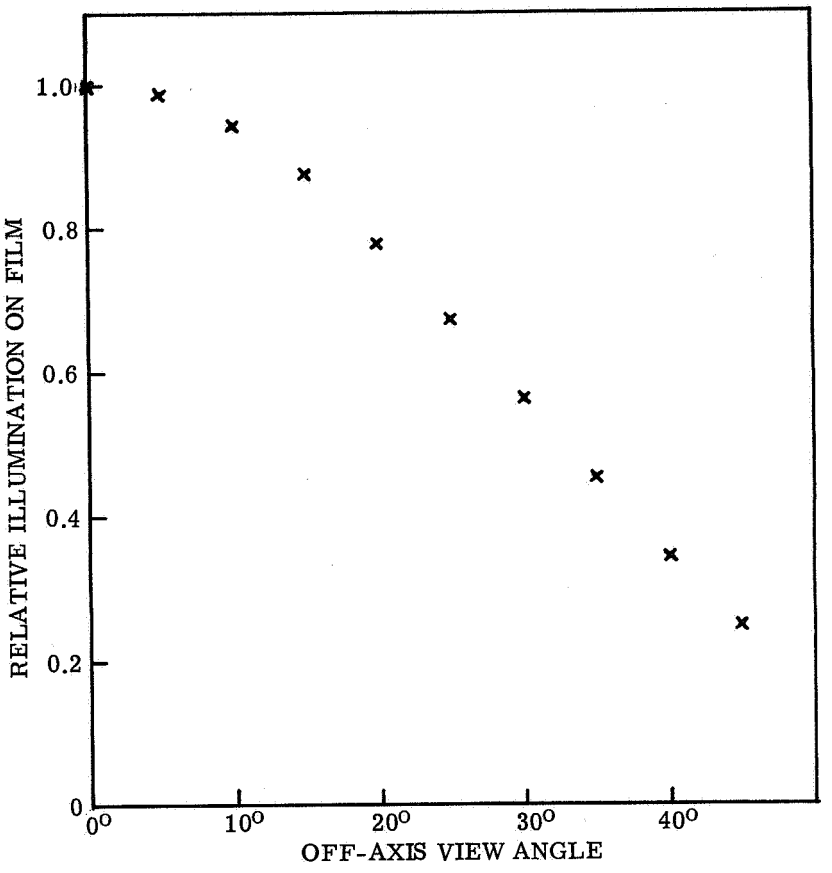

FIGURE 17. COS^4 FALLOFF, IDEALIZED CAMERA

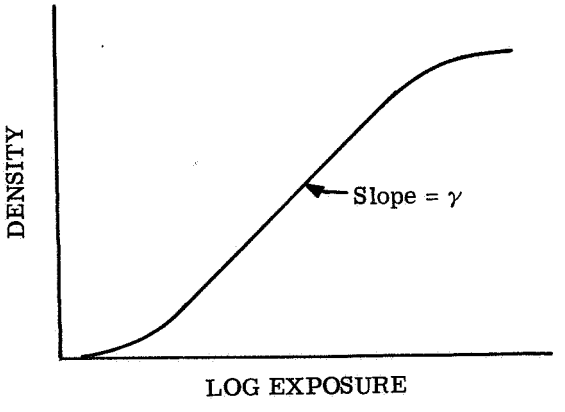

FIGURE 18. ILLUSTRATIVE CHARACTERISTIC CURVE FOR FILM

procedures were developed for processing the photographic data obtained on the 1966 flights. They involve standardized gray scales which are placed periodically throughout each roll along the margins of the film prior to development and the documentation of the development parameters; the illuminating source for the gray scales is spectrally filtered to represent the sun's energy distribution, and is further filtered by filters similar to those used in the cameras during their respective data-collection missions.

6.2. SELF-CALIBRATION ATTEMPTS

To obtain definitive quantitative data from imagery and compare sets of data obtained at different times and under different conditions, the data must be calibrated. Since the 1964 data were uncalibrated (sec. 6.1.2), self-calibration methods were investigated (in parallel with the investigation of instrumental effects) for both scanner and nine-lens imagery.

The technique investigated in both of the self-calibration methods involves the selection of one or more standard objects in the scene for which radiance values (or quantities related to radiance, such as temperatures) can be and are estimated on the basis of other data on conditions at the time the data were collected. These radiance or temperature estimates are then to be related to the measured densities of the standards in the imagery, and from these relationships corresponding values for other objects are to be estimated from their respective densities.

To be most useful, a standard object should be uniform in composition and be located in each of the several flight passes which were required to cover the Agronomy Farm; roads were the only objects meeting this requirement, so they were selected for the standards.

6.2.1. THERMAL INFRARED SCANNER IMAGERY. Two roads were selected as standards for the thermal infrared scanner channels, the concrete divided highway US 52 and the grass roads which subdivide many of the larger plots on the Agronomy Farm. Another essential requirement of a standard thermal object is that its temperature be calculable as a function of time throughout the data-gathering period, and such calculations were possible for the roads by using an existing digital-computer program at WRL which was adapted for the calculation of the temperatures of the two roads.

Two types of input data were required for the computations of surface temperatures: material properties and meteorological conditions. The material properties include the thermal conductivity and the thermal diffusivity as functions of depth, the albedo (fraction of solar radiation that is reflected), the total mean hemispheric emissivity, and an aerodynamic roughness of the surface for convective calculations. Purdue provided data on the amount of soil moisture near the surface and a qualitative description of the soil profile. It was necessary to apply and extrapolate data obtained from the literature [14] to complete the description of the soil

properties beneath the grass road and beneath the base of the concrete road. An energy-weighted average albedo was obtained for grass from pyranometer measurements made by Purdue on one 1964 mission, and emissivity and aerodynamic-roughness values were obtained from reference 15. The concrete road and its base were assumed to have properties similar to those of the east ramp of Willow Run Airport for which estimates were available.

The time-dependent meteorological parameters needed as inputs to the program include solar-radiation intensity, air temperature, relative humidity, wind velocity, and cloud cover. The first three of these were measured at the Agronomy Farm and for the most part were sufficiently accurate and continuous for the purpose, although interpolations through data gaps were necessary. The wind velocity and cloud cover were not measured at the site, but data from the U. S. Weather Bureau station at Purdue Airport were available and were used without extrapolation.

It was also necessary to account for the evapotranspiration from the grassy areas. The only data available with which to estimate this factor were the total daily amounts of evaporation from a standard water pan at the site. An estimate of the total daily evapotranspiration of the grass was then made by using very crude values [15] for the ratio of vegetation evapotranspiration to pan evaporation. This daily total was then assumed to be distributed throughout the day in direct proportion to the solar-radiation intensity.

The results of the calculations for the mission of 2-4 June 1964 are presented in figure 19. As can be seen, there is a considerable difference between the temperatures of the two roads throughout each 24-hr period. It was decided to obtain some knowledge of the possible error or uncertainty in the computed values of surface temperature. Because of the nature of the calculations involved, the uncertainty in surface-temperature calculation caused by the uncertainty in a single input is not independent of the other inputs. Consequently, since there are as many as 11 input parameters (5 material, 5 meteorological, and evaporation), each with two possible values (the error being describable by an upper and lower bound to the parameter), a full error analysis requires 2^{11} combinations of input for each case calculated, each combination leading to a different calculated surface-temperature variation. Since such an analysis was entirely out of the question, it was decided to find the calculation error produced by only the most uncertain input. For the grass field, the greatest uncertainty was in the magnitude of the evapotranspiration. Consequently, the grass temperature was computed for assumed errors of ±20% in the value of evapotranspiration. These results are also shown in the figure. For the concrete, no one input stood out as being most uncertain; consequently, no such error analysis was made.

Densitometer readings were made on the 4.5- to 5.5-μ strip maps that were produced throughout the day on 3 June 1964. In all cases, as predicted, the concrete road was more

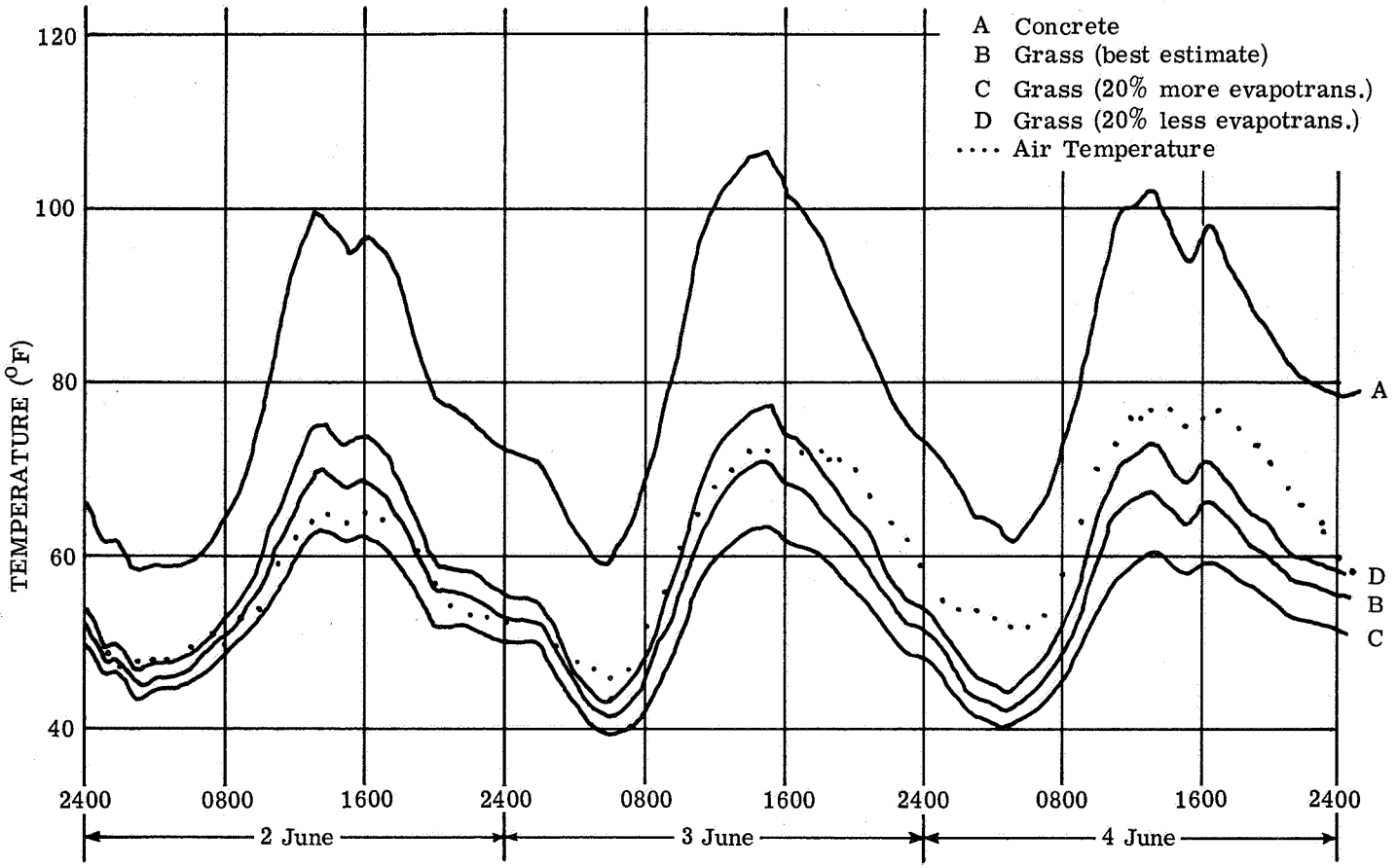

FIGURE 19. TEMPERATURE VS. TIME FOR CONCRETE AND GRASS

responsive (had lower film transmittance) than the grass road (see table IV). Among the four or five passes made on any one flight, one can observe a considerable variation in the average transmittances measured for the two roads;* these variations point out the uncertainties involved in making densitometer measurements on uncalibrated infrared strip maps of nonuniform quality. Upon comparing the transmittances measured for fields of oats, wheat, alfalfa, and grass with those of the two roads, one sees that the majority of the crop transmittance values are greater than those of the grass road, which means that they are less responsive than either of the roads (see table V for a description of the crops measured). The reason for this condition is not known; it may be that (1) the emittances of the grass road and the crops differ because of natural differences or because of the compacting caused by vehicles, (2) the actual effective surface temperatures of the crops are lower, or (3) a combination of both. Therefore, despite the fact that the calculated difference in road temperatures was at least $20^{\circ}F$ and as much as $33^{\circ}F$ in one case, the crops' apparent temperatures (and transmittances) lie outside this span.** Consequently, one cannot reliably estimate the apparent temperatures of the crops by extrapolation because the curve of D vs. log E of the film is not known.

From the experience gained in attempting to predict the temperatures of the roads during 1964, suggestions were made and forwarded to Purdue University for obtaining meteorological data and crop data for the 1966 flights so as to improve the reliability of the input data for similar calculations at a later date. An uncertainty about the adequacy of data remains, since there was no way to check the calculations made for 1964. With good ground truth and an improved, calibrated infrared scanner, the outcome of similar studies on the 1966 data is much more promising.

6.2.2. NINE-LENS CAMERA IMAGERY. The essential items for a quantitative analysis of crop densities on the nine-lens photographic plates are the applicable curves of density vs. log exposure. These items are not known directly for the 1964 flights because the parameters used during the development of the plates were not recorded; consequently, the curves can be determined only indirectly. The most desirable approach would have been to have placed a sensitometric step-intensity wedge (gray scale) on each nine-lens plate at the time of original exposure or at least before development. If the development conditions had been recorded, one might determine D-log E curves for similar plates under similar exposure and development

*The transmittances were measured along the same sections of the film as were the fields of interest; each value presented is an average of three or more readings.

**Densities read for the grass field (point 74) and the clipped bromegrass-alfalfa pasture (point 58) are most like those read for the road and are considerably different from alfalfa in bloom (points 77, 78, and 79). Also note the differences between Knox wheat (point 102) and Purdue 4930 wheat (point 115).

TABLE IV. TRANSMITTANCES MEASURED ON 4.5- TO 5.5-μ NEGATIVE STRIP MAPS, 3 JUNE 1964

Flight Time	Predicted Road Transmittances (°F)		Pass Number	Measured Road Transmittances (%)		Measured Crop Transmittances (%)							
	Concrete	Grass		Concrete	Grass	Oats	(Densitometer Point)	Wheat	(Densitometer Point)	Alfalfa	(Densitometer Point)	Grass	(Densitometer Point)
0715	65	44	03	28.7	44.3	51	(47)			49	(77, 78)		
			04	28.0	43.5			55 59	(102) (115)			41	(74)
			05	35.0	41.0			47	(20, 110)				
			06	36.0	41.0	46	(19)	47	(110)				
1000	88	58	02	23.3	31.3	41.6	(22)	42.4	(43)	29.6	(58)		
			03	22.3	33.7	44.6	(47)			51.2	(79)		
			04	24.3	34.0			52.0 53.4	(102) (115)				
			05	24.3	32.3			46.6	(20, 110)			34	(74)
			06	25.0	34.0	38.2	(19)	45.8	(110)				
1535	102	69	02	10.3	56.3	67	(22)	62.2	(43)	58	(58)		
			04	19.3	55.0	57	(48)	52 57.6	(102) (115)				
			05	19.0	46.3		(19)	50	(20, 110)			52	(74)
			06	12.7	55.7	46.8		60.2	(110)				
1800	95	65	03	11.3	40.7	52.6	(47)			58.4	(79)		
			04	9.3	73.5			62.6 74.2	(102) (115)				
			05	14.3	56.3			60	(20, 110)			65	(74)
			06	12.7	56.7	43.6	(19)	48.8	(110)				

TABLE V. DESCRIPTION OF CROPS IN TABLE IV

Densitometer Point	Crop	Variety	Planting Date	Height (in.)	Remarks
19	Oats	Goodfield	10 May 64	15 to 18	Fair uniformity
20	Wheat	Reed	20 Sept. 63	34 to 37	Heading
22	Oats	Tippecanoe	16 May		Poor uniformity
43	Wheat	Reed		37	
47	Oats			17	Preheading
48	Oats			24 to 26	Headed
57	Alfalfa			1 to 5	Bromegrass - alfalfa
58	Alfalfa			1 to 5	Clipped Pasture
74	Grass			3 to 5	Probably bluegrass and tall fescue sod
77	Alfalfa			20 to 30	3/4 bloom, variety tests
78	Alfalfa				Full bloom
79	Alfalfa				Full bloom
102	Wheat	Knox	Oct. 63	36	Headed
103	Wheat	Reed	Oct. 63	36	Headed
110	Wheat	5210 breeders	24 Sept. 63	30 to 36	Fully headed
115	Wheat	Purdue 4930	11 Oct. 63	38	Fully headed

conditions. The final recourse is to use the densities of one or more objects (self-calibration standards) in the scene to calibrate the film.

There are four steps to be followed in the self-calibration procedure. As with the thermal self-calibration method, one must first select objects whose spectral reflectances ρ_λ are known or can be reliably estimated. Second, one must estimate the spectral illumination I_λ on the objects at the time of exposure. Third, one must calculate both the relative values of effective irradiance H' of the objects in each spectral band of the camera and, by using the various aperture settings, the corresponding relative exposure values E' on the film. Finally, one plots in each spectral band the measured densities of the standards vs. the logarithm of the calculated relative exposure values. These plots are estimates of the characteristic curves of the film. If the plate was originally exposed on the linear part of its D-log E' curve, two points (or standards) will define the linear part in each spectral band; if, in addition, a single D-log E' curve is applicable for all spectral bands, a single standard object may suffice.

A nine-lens plate made near noon on 29 September 1964 was selected for the trial attempt at self-calibration. The zenith angle of the sun was about 43°, which corresponds to an optical path containing an air mass of 1.36 atm [16]. Interpolation was made between Gates' theoretical curves of global radiation [17] (i.e., the light scattered from a complete hemisphere of sky as well as that received directly from the sun) for air masses of 1.0 and 1.5 atm, and the result was used as an approximation to the spectral irradiance on the horizontal surfaces at the time the selected plate was exposed. The biggest uncertainty in this approximation lies in the transmittance of the atmosphere. The aerosol content of the air appears to have a greater effect on the atmosphere's transmittance in the visible than does water-vapor content [17], but there were no data collected during the 1964 (nor 1966) missions on aerosol content, although water-vapor content (relative humidity and temperature) records were kept.

The radiation that reaches the camera is not all equally effective in producing exposures in the various spectral bands; that is, the lens of the camera, any filters used, and the film plate itself all have spectrally dependent properties. The overall spectral response assumed for the calculations is the product of the relative spectral characteristics of lens, filters, and film as obtained from figures 20, 21, and 22, respectively. Spectral transmittance properties of the atmosphere between the object and the camera were not accounted for directly, but the solar illumination function used does incorporate average atmospheric transmittance effects.

The standard objects selected were the grass roads between various plots on the Agronomy Farm. To approximate their spectral reflectance, use was made of measurements made by the Photometry and Colorimetry Section, National Bureau of Standards, for The University of Michigan on a sample of sod obtained from a lane in an apple orchard (see fig. 23).

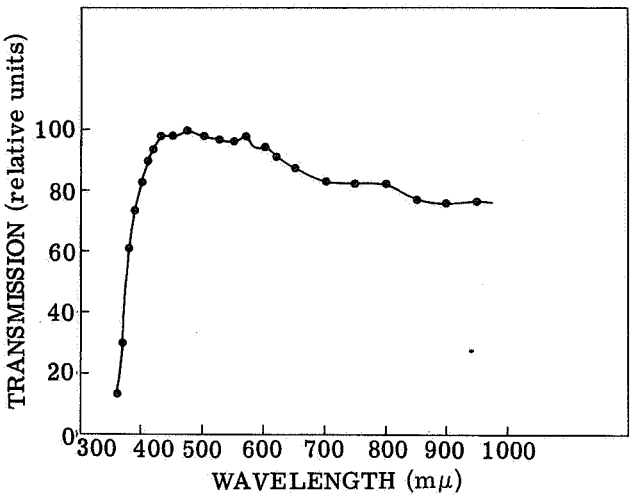

FIGURE 20. LENS TRANSMISSION FOR 9-LENS CAMERA

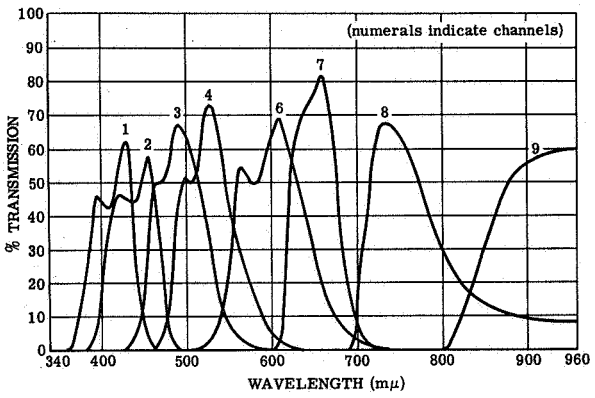

FIGURE 21. FILTER CURVES USED FOR THE 9-LENS CAMERA

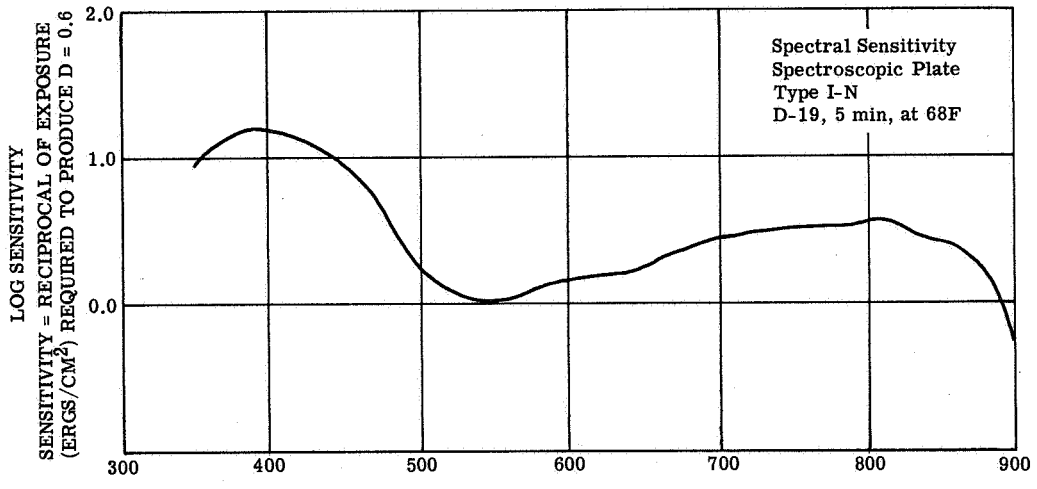

FIGURE 22. FILM CURVES USED FOR THE 9-LENS CAMERA GLASS PLATE

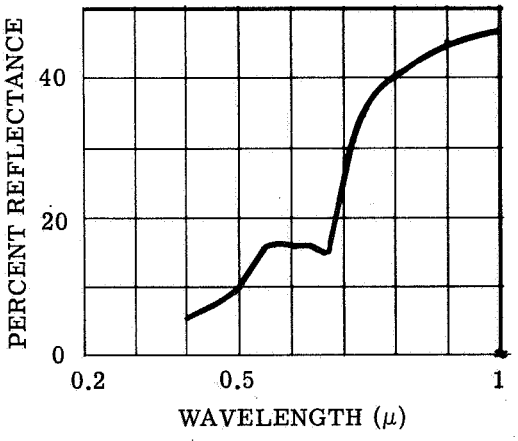

FIGURE 23. DIFFUSE SPECTRAL REFLECTANCE USED TO APPROXIMATE THAT OF GRASS ROADS

To calculate the relative exposure values for the film plate, the product of the spectral curves of illumination, sod reflectance, and camera response was integrated over each spectral band of the camera; for computational purposes, discrete values at intervals of 0.01 μ were used for each of the curves. The integrated values are related to the actual exposures that produced the film-plate densities by both a common constant of proportionality (that accounts for the normalizations of the spectral curves) and the individual aperture settings used for the nine lenses. The only record that could be found for the aperture settings during 1964 was made early in the summer, and there is no way to determine if and how they were changed during the season. The ratio obtained by dividing the collecting area of each spectral band (a function of its f-stop) by that of the band with the largest f-stop setting (see table VI) was used to obtain estimates of the actual relative exposures. These estimates were plotted against the densities measured on the selected nine-lens plate* for the grass road (see fig. 24). Note that all points except those for the bands 0.62 to 0.68 μ and 0.45 to 0.52 μ (marked with x's) lie close to a line with slope ~0.75; the point for 0.62 to 0.68 μ in particular is quite far removed. The locations of these two points may result from an aperture setting which was changed from the initial value assumed and thus produced an underexposure, an inaccurate estimate of the reflectance of the grass road, or some other reason. For the calculations here, it is assumed that a change of one f-stop setting was made in these bands on the camera (after the initial settings were recorded) so as to move the two points closer to the line and that, after the appropriate adjustments, the line ($\gamma \sim 0.75$) in figure 24 applies equally to all bands. The latter assumption in effect is equivalent to a modification in the assumed spectral reflectance of the grass road. Attempts were made to use a gravel road as a second standard to determine the film properties, but results with the available (poor) reflectance data were not satisfactory.**

From the camera's aperture factors for the various bands (table VI) and the assumed characteristic curve of figure 24, one can compute the estimated effective diffuse reflectances of other objects whose densities are read on the film plate.*** Densities were read for three fields of corn, two fields of orchard grass, one field of soybeans, and one field of alfalfa. The results of these computations are presented in figure 26; the reflectance estimates for each band are plotted at the center wavelength of the band. The corn and soybean reflectance estimates agree quite well with some laboratory leaf measurements; also, they seem to be very

*The image for the band 0.41 to 0.47 μ was noticeably distorted in the processing of the plate and therefore no readings in it are included here.

**There is some justification for using a single object to calculate the characteristic curve of the film. The gradient (and therefore probably the development factor) of the film plate used is, according to one set of Kodak data, within 5% of its average value for all wavelengths except those between ~0.43 and ~0.49 μ, at which it may depart by as much as 15% or slightly more (see fig. 25).

***Densities were actually read on 9× positive enlargements of the scene and were corrected for the transfer function of this intermediate photographic process.

TABLE VI. APERTURE FACTORS FOR 9-LENS CAMERA

F-Number Setting	Relative Aperture Factor
f/16	1.00
f/11	2.11
f/8	4.00
f/5.6	8.16
f/4.5	12.6
f/3.5	20.9

Wavelength Band (μ)	F-Number Setting	Relative Aperture Factor
0.38 to 0.44	f/11	2.11
0.45 to 0.52	f/5.6*	4.00
0.48 to 0.56	f/5.6	8.16
0.38 to 0.89	f/16	1.00
0.55 to 0.64	f/5.6	8.16
0.62 to 0.68	f/5.6**	4.00
0.71 to 0.79	f/5.6	8.16
0.85 to 0.89	f/3.5	20.9

*Revised by assumption from initial setting of f/8.

**Revised by assumption from initial setting of f/4.5.

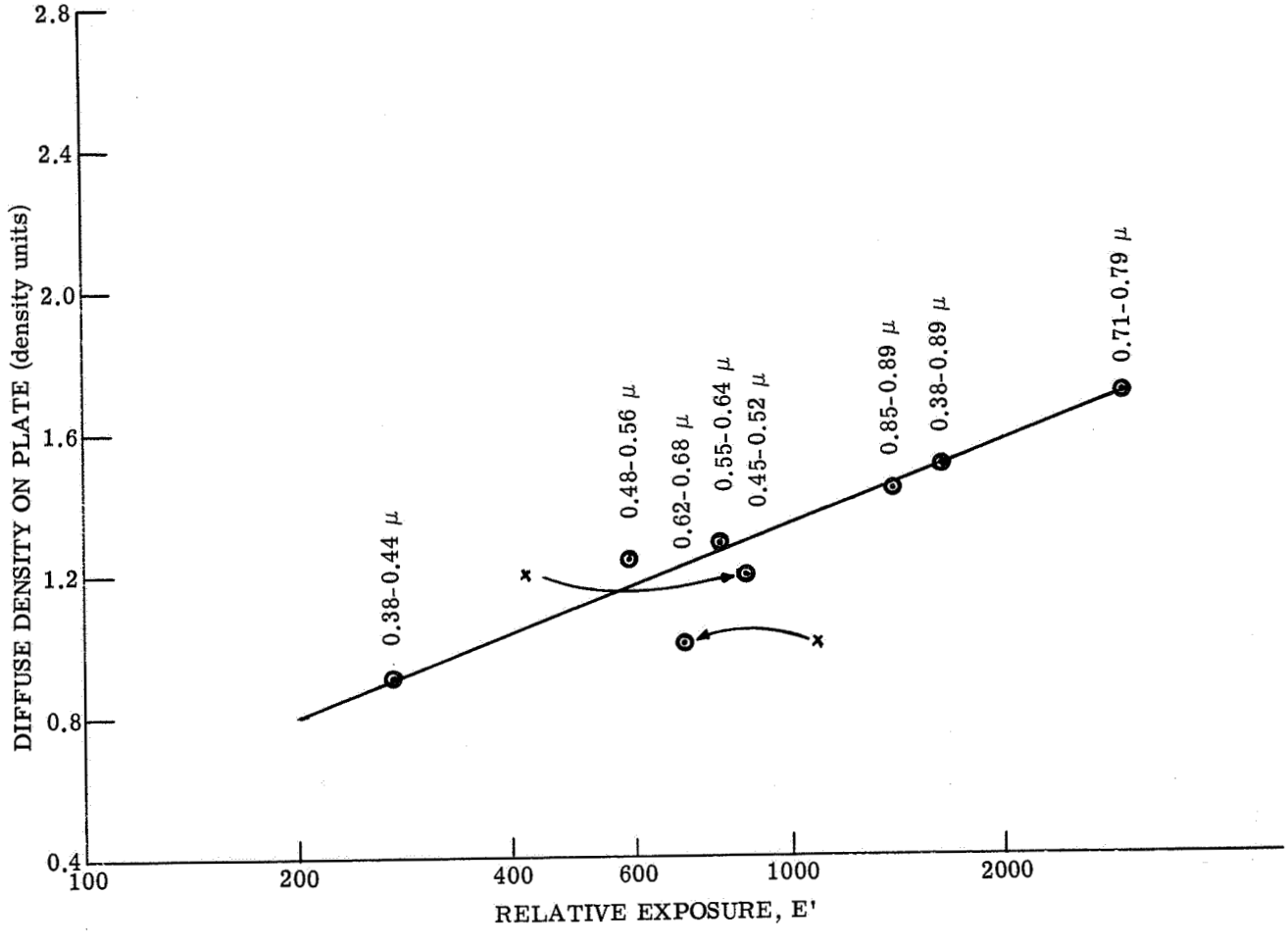

FIGURE 24. FILM CHARACTERISTIC AS DEDUCED FROM ESTIMATES FOR GRASS ROAD

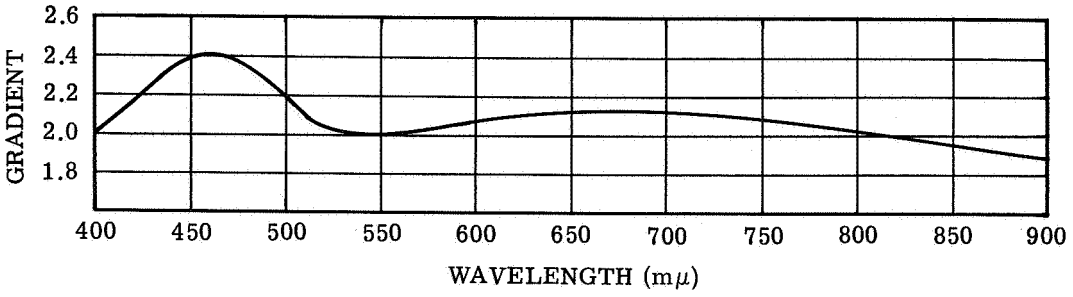

FIGURE 25. GRADIENT ($D_{1.0}$ - $D_{0.3}$) VS. WAVELENGTH

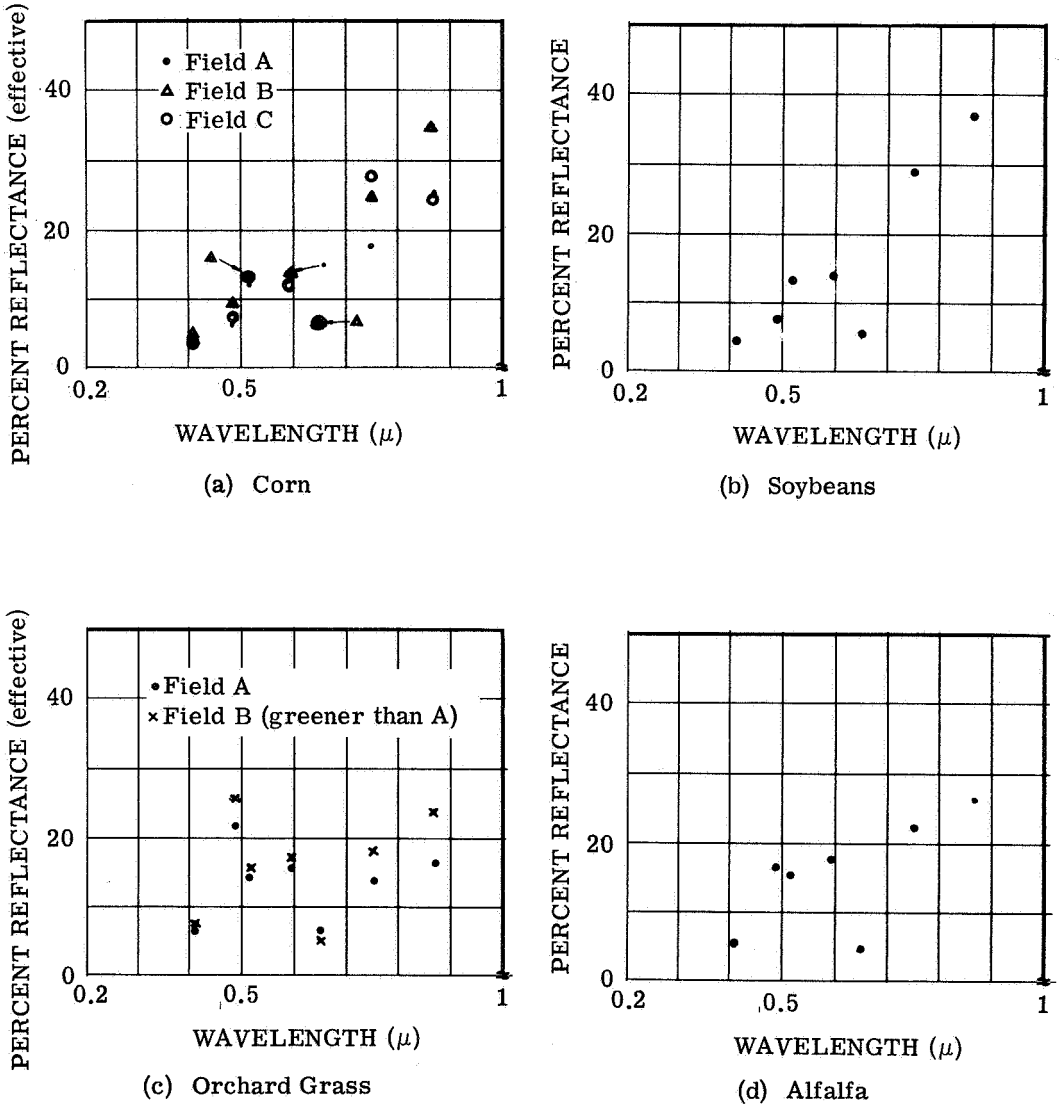

FIGURE 26. ESTIMATED EFFECTIVE DIFFUSE REFLECTANCE FROM 9-LENS CAMERA

similar except for a slightly higher reflectance that is observed for soybeans in the infrared bands. Alfalfa and orchard-grass estimates are also similar to each other except in the infrared, where the alfalfa is slightly higher. Note that orchard-grass field B exhibits a substantially greater difference in reflectance between the bands 0.55 to 0.64 μ and 0.62 to 0.68 μ than does field A, which was not as green. Upon comparing all four graphs, one notes that in the first four bands, starting at the short-wavelength end, the alfalfa and orchard grass have consistently higher reflectances than do the corn and soybeans; the reverse is true in the 0.62- to 0.68-μ band.

In summary, a technique has been demonstrated for self-calibrating multilens imagery to provide estimates of the spectral reflectances of objects; it would also be applicable to the setting of multilens camera apertures for field use. The uncertainties in the parameters used to record and process the 1964 film plates necessitated assumptions which reduced the confidence in the accuracy of the reflectance estimates enough to discourage an extensive use of the technique on the 1964 data. Nevertheless, comparisons made between the estimated spectral reflectances and laboratory curves show quite good agreement, and differences are noted between types of crops. Since the estimates can be no better than the standards, standard panels of known reflectance were deployed during the 1966 missions.

6.3. INVESTIGATION OF ANGLE-DEPENDENT EFFECTS

In spectral regions where reflected radiation is the major component of crop radiances (i.e., the ultraviolet through the near-infrared regions), the geometrical positions of both the illuminating sources and the observing sensor relative to the crop and its row structure (if any) have a strong bearing on the power observed. Two adjacent but different crops which are indistinguishable at one observation angle can sometimes be readily differentiated when observed from some other angle, as is shown for corn and wheat in figure 27.

There had been little quantitative effort to determine the extent and character of such angle-dependent variations from photographs of crops, so a study of this type was initiated. The photographs available from the 1964 missions had several faults (see sec. 6.3.2), but yet were felt to be good enough to give some useful clues that could be explored further in the 1966 flights.

To complement the experimental data, a theoretical model was developed and used to make estimates of the angle-dependent radiances of row crops such as corn and soybeans. These theoretical studies are discussed in section 6.3.2.3; comparisons are also made, where possible, between the experimental and the theoretical results.

6.3.1. POSITION OF THE SUN. The sun, when present, is the dominant source of the light that is reflected by the crops. Since it can be considered a point source, a simple relationship

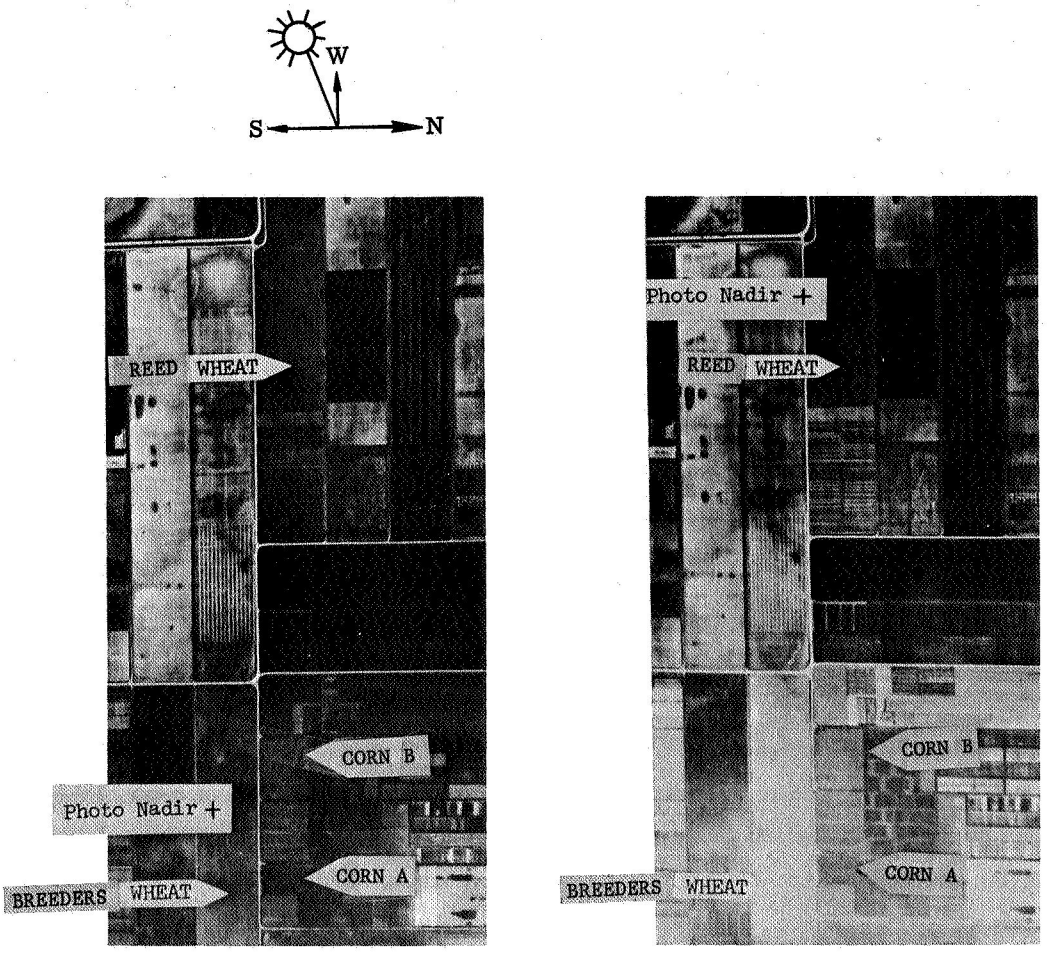

FIGURE 27. EFFECTS OF VIEWING GEOMETRY ON CORN AND WHEAT FIELDS 25 June 1964; 0.4- to 0.7-μ region; altitude 4500 ft; 1430 hours.

can be used to calculate the reflection geometries. The presence of clouds (which can be distributed throughout a hemisphere) greatly complicates the calculations and produces effects on photographs that are hard to differentiate from the clear sky and direct solar effects on crop irregularities. Consequently, the theoretical calculations were made with only the sun as a source, and attempts were made to find photographs for the experimental work that were made under conditions of little or no cloud cover.

The angular position of the sun varies in both azimuth and elevation throughout each day. There are also substantial variations with time of year and with latitude in the track that it makes across the sky over a given area. The approximate positions of the sun at Lafayette during the times of the 1964 flights were calculated from reference 18, and the results are presented in graphical form in figure 28. All sun-position data used in the analysis were taken from similar data.

6.3.2. PHOTOGRAPHIC STUDIES. Low-altitude photographs, high-altitude photographs, or both can be used to explore the two-dimensional bidirectional reflectances of crops.* Each type has advantages and disadvantages.

At a given time, all portions of a flat field are illuminated by the sun at a given angle, and the radiation is reflected by the crop into a hemisphere. Equal amounts of radiation are not, in general, reflected in all directions; therefore, the crop usually has a nonuniform bidirectional reflectance which one would like to measure.** For the given illumination condition, a single low-altitude photograph contains many portions of the field that are observed at a variety of angles relative to the vertical and azimuthal axes. To infer something about the bidirectional characteristics of the crop's reflectance from density measurements on the film, one must assume that each sample of the crop has the same reflection properties as its neighbors. When there are nonhomogeneities in the crop, they become confused with variations in the bidirectional reflectances of the crop. The analysis of low-altitude photographs taken in 1964 is discussed in section 6.3.2.1.

With high-altitude photographs, on the other hand, the field covers only a small portion of the frame and is observed at essentially a single angle, and the effects of nonhomogeneities can

*The distinction here between high- and low-altitude photographs is made according to the sizes of the images of the fields relative to the frame size of the camera. In a low-altitude photograph a field fills all or much of the frame, whereas the field fills only a small part of a high-altitude frame.

**With the available photographs one cannot directly measure the bidirectional reflectance because the illumination on the crops was not measured at the same time; one can only investigate the angle-dependent shapes of the reflectance distributions.

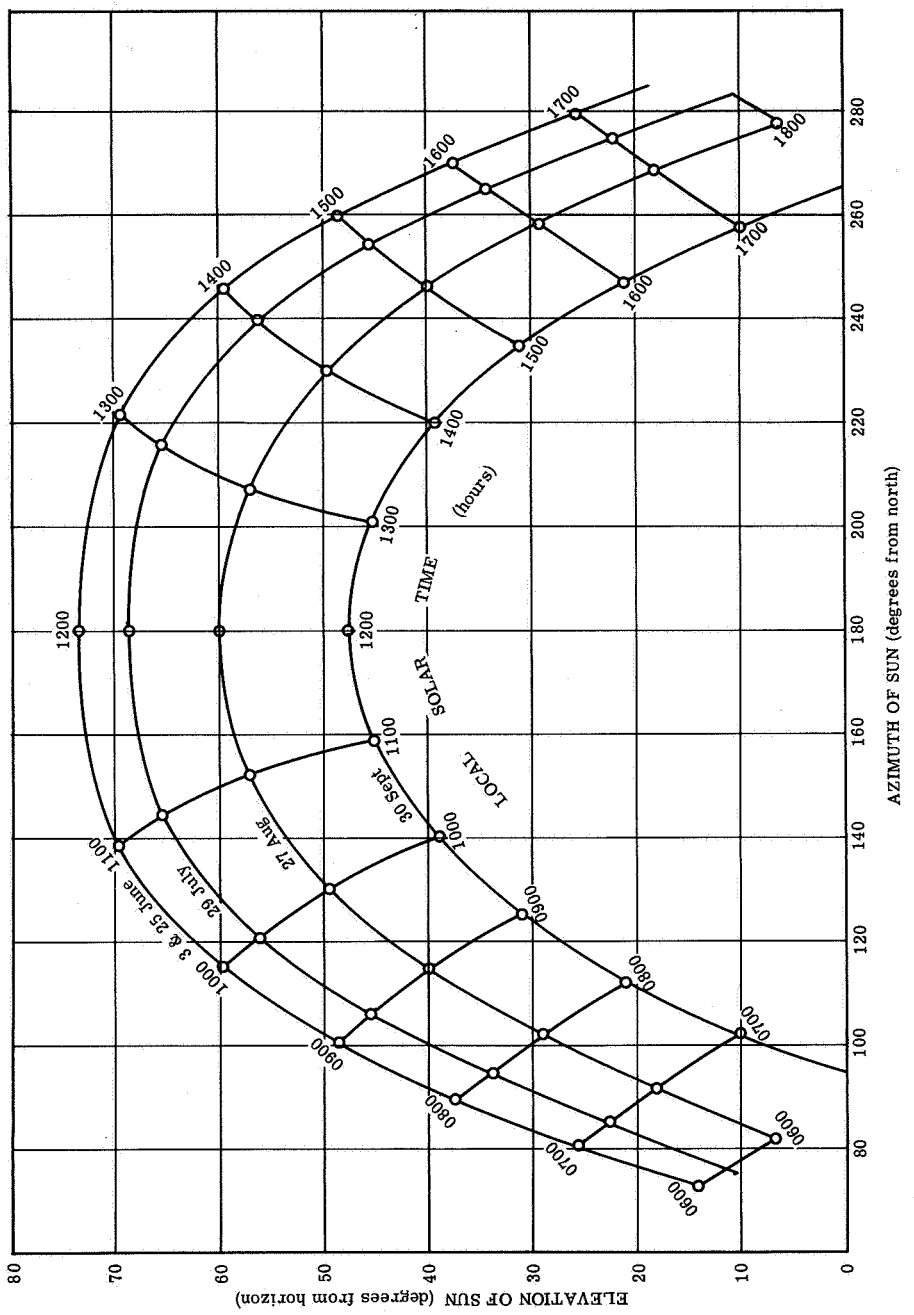

FIGURE 28. POSITION OF SUN AT PURDUE AGRONOMY FARM. 12:00 o'clock Central Daylight Time ≃ 11:00 o'clock Local Solar Time.

be minimized by averaging. One difficulty, however, is that many different frames at a variety of observation angles are needed to obtain information on the shape of the crop's bidirectional-reflectance distribution for the given illumination condition. Also, the effects of atmospheric absorption are more pronounced than for low-altitude photographs. Densities in photographic negatives from one high-altitude mission in 1964 and a series of high-altitude photographs that were made during a local 1966 test flight in Michigan were analyzed. The results of the analyses are discussed below; the 1966 photographs are included in this report because the analysis relates very well to the studies made on the 1964 photographs.

6.3.2.1. Low-Altitude Photographs. The small field sizes of the Purdue Agronomy Farm increased the difficulty of obtaining angle-dependent data from photographs. Only one crop (corn) was planted in a field large enough to fill a complete camera frame, even at an altitude of 500 ft. In order to obtain any usable data on other crops, such as wheat and soybeans, more than one frame had to be analyzed and combined to form a composite sample of the crop's reflection properties; even then, the composities are incomplete in many cases.

In analyzing the low-altitude photographic negatives, the first step was to locate and mark both the center of the frame and sixteen points equally spaced around its periphery (every 22.5^{o}). Radial traces were then made from the center outward in each direction by a line-scanning densitometer (see fig. 29a). The resultant curves were then smoothed and each was sampled at distances which correspond to off-nadir viewing angles of 2^{o}, 5^{o}, 10^{o}, 15^{o}, 20^{o}, 25^{o}, 30^{o}, and 35^{o} from the vertical. A curve was then plotted on polar graph paper from the set of points for each off-nadir angle; the radial scale indicates the measured density and the angle scale the azimuth direction in which the camera looked (see fig. 29b). To interpret traces such as those of figure 29b, it is helpful to consider a three-dimensional sketch of the geometry of the situation (fig. 29c). When one looks toward the direction of the sun, the light reaching the camera is reflected forward by the crop; when looking away from the sun's azimuth, the light is reflected back; in general, crops appear to be better back reflectors than forward reflectors at the off-nadir angles considered. The same density data were also used to plot linear graphs equivalent to the polar graphs of density vs. view azimuth (see fig. 29d). A different form of data presentation is discussed in section 6.3.3.2.

Approximately one hundred frames were so analyzed in total or in part. From these, three examples are presented in figures 20 through 32 for wheat, corn, and soybeans; parts a and b are the polar plots and parts c and d are linear plots for off-nadir angles of 2^{o} through 15^{o} and 20^{o} through 35^{o}, respectively; the numbers on the graphs indicate the elevation angles of the points as listed on the data sheets (part e of each figure). The reader is cautioned to avoid making comparisons between the density levels on these graphs because the photographs were

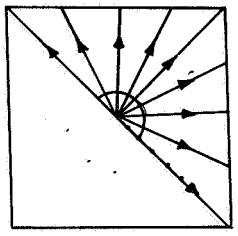

(a) Radial Density Traces on Film

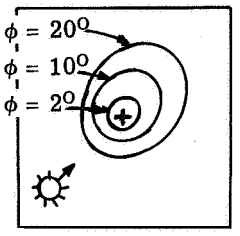

(b) Idealized Polar Plot of Measured Density vs. Viewing Azimuth Angle

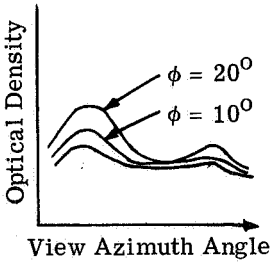

(c) Geometry of Illumination and Observation

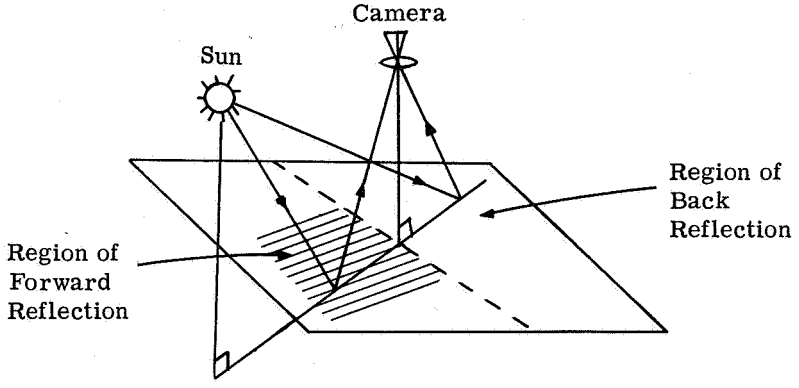

(d) Idealized Linear Plot Comparable to Polar Plot of Figure 29b

FIGURE 29. ILLUSTRATIONS TO EXPLAIN DENSITY PLOTS

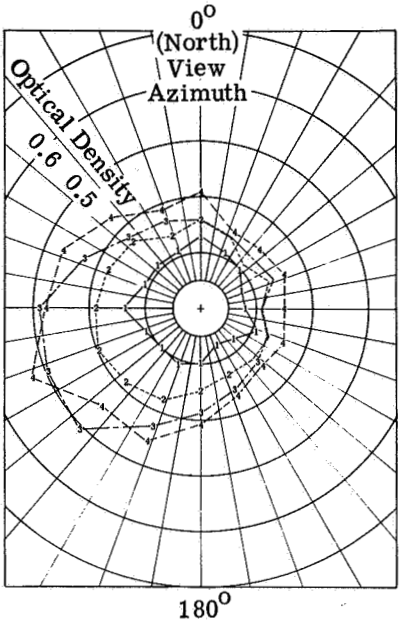

(a) Polar Plot, Off-Nadir Angles of 2° (1), 5° (2), 10° (3), and 15° (4)

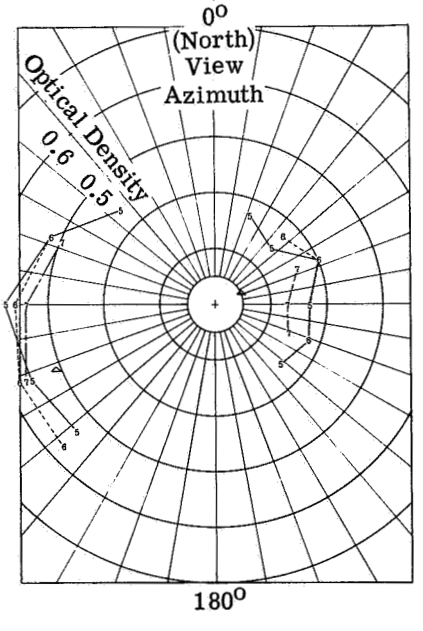

(b) Polar Plot, Off-Nadir Angles of 20° (5), 25° (6), 30° (7), and 35° (8)

FIGURE 30. SAMPLE PLOTS FOR WHEAT. 0700 hours, 3 June 1964.

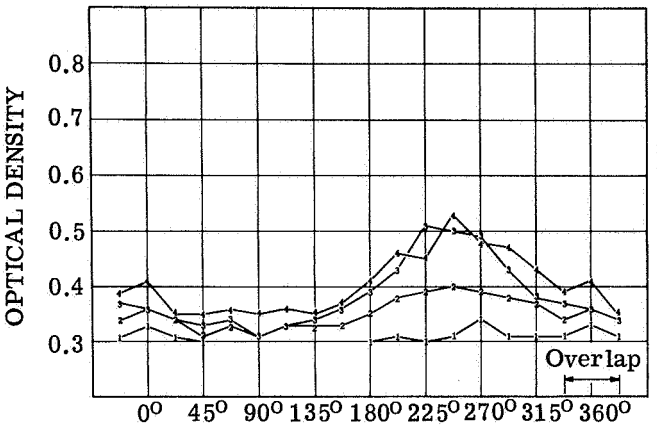

(c) Linear Plot, Off-Nadir Angles of 2° (1), 5° (2), 10° (3), and 15° (4)

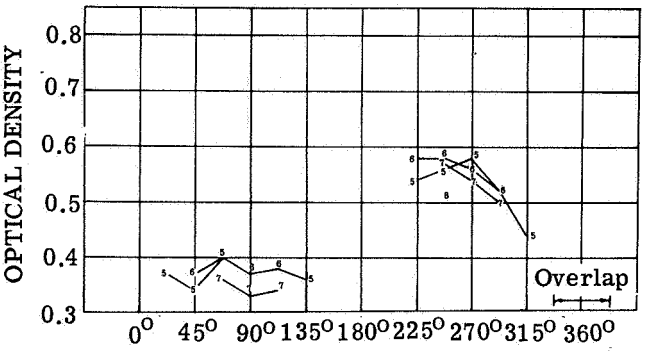

(d) Linear Plot, Off-Nadir Angles of 20° (5), 25° (6), 30° (7), and 35° (8)

DATE/TIME/TYPE OF PHOTO

640603/0700/V

FRAME NO. 75

SOLAR AZM. FROM N. 73°

SOLAR ALT. 14°

CAMERA DATA:

FILTER(S) K-2 Star

F STOP F 6.3

SHUTTER SPEED 1/200 sec.

FRAME RATE 3 sec.

WEATHER DATA:

VIS.= 10 miles

SKY COVER = 0

TOTAL OPAQUE SKY COVER = 0

AIR TEMP. 53 °F

DEW PT. 51 °F

WIND DIR. 280 °
SPEED 4 K

PRESSURE 992.3 mb

CROP DESCRIPTION:

TYPE Wheat

VARIETY 5210 Breeder

PLOT(S) 110

ROW AZM. FROM N. °

ROW SPACING FT.

PLANTING DATE 24 Sept. 63

HEIGHT 30 - 36"

SOILS 3398

STATE Fully Headed

LEGEND FOR CURVES:

1 = 2°
2 = 5°
3 = 10°
4 = 15°
5 = 20°
6 = 25°
7 = 30°
8 = 35°

VIEW ANGLES

(e) Data Sheet

FIGURE 30. SAMPLE PLOTS FOR WHEAT. 0700 hours, 3 June 1964. (Continued)

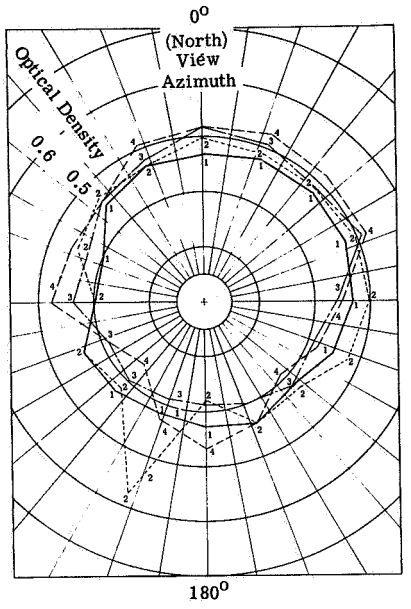

(a) Polar Plot, Off-Nadir Angles of 2° (1), 5° (2), 10° (3), and 15° (4)

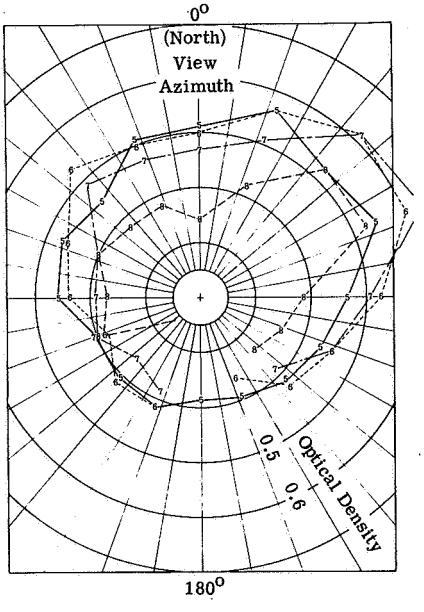

(b) Polar Plot, Off-Nadir Angles of 20° (5), 25° (6), 30° (7), 35° (8)

FIGURE 31. SAMPLE PLOTS FOR CORN. 1430 hours, 25 June 1964

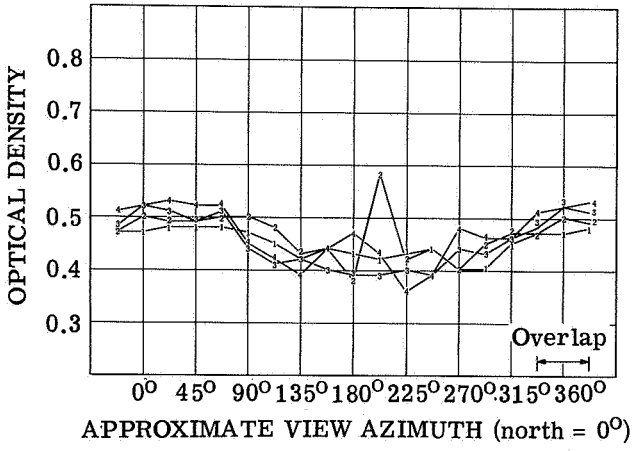

(c) Linear Plot, Off-Nadir Angles of 2° (1), 5° (2), 10° (3), and 15° (4)

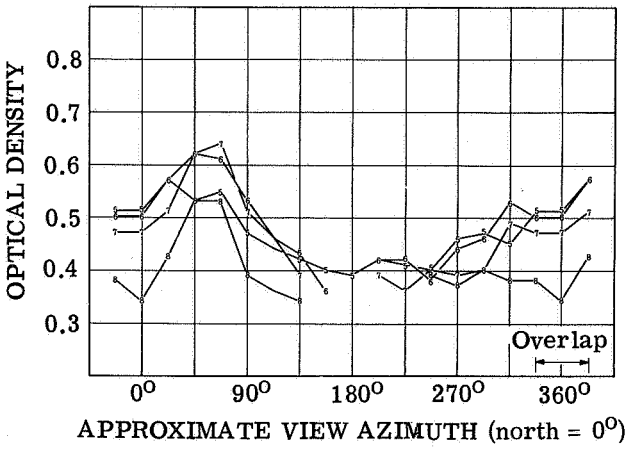

(d) Linear Plot, Off-Nadir Angles of 20° (5), 25° (6), 30° (7), and 35° (8)

DATE/TIME/TYPE OF PHOTO

640625/1430 V

FRAME NO. 7

SOLAR AZM. FROM N. 240

SOLAR ALT. 63

CAMERA DATA:

FILTER(S) K 2 Star

F STOP F 8

SHUTTER SPEED 1/200 sec.

FRAME RATE 3 sec.

WEATHER DATA:

VIS.= 12 miles

SKY COVER = 0

TOTAL OPAQUE SKY COVER = 0

AIR TEMP. 85°F

DEW PT. 61°F

WIND DIR. 270°
SPEED 6 K

PRESSURE 999.2 mb

CROP DESCRIPTION:

TYPE Corn

VARIETY Pfister SX29

PLOT(S) 128, 129

ROW AZM. FROM N. 93° o

ROW SPACING _____ FT.

PLANTING DATE

128 - 7 May 64

129 - 8 May 64

HEIGHT 38"

SOILS 128 - 3398

129 - 3398, 3399

STATE _____

Photo: uniform

LEGEND FOR CURVES:

1 = 2°
2 = 5°
3 = 10°
4 = 15°
5 = 20°
6 = 25°
7 = 30°
8 = 35°

VIEW ANGLES

(e) Data Sheet

FIGURE 31. SAMPLE PLOTS FOR CORN. 1430 hours, 25 June 1964. (Continued)

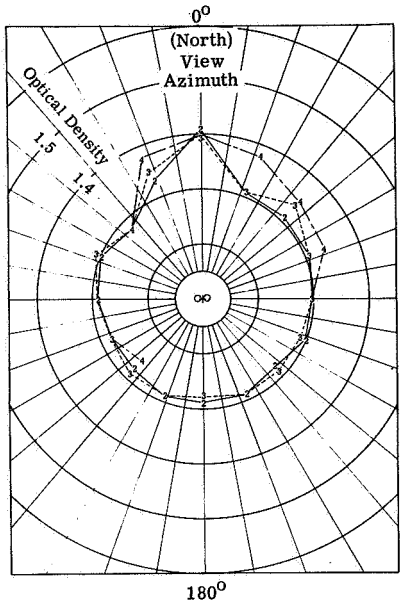

(a) Polar Plot, Off-Nadir Angles of 5° (2), 10° (3), and 15° (4)

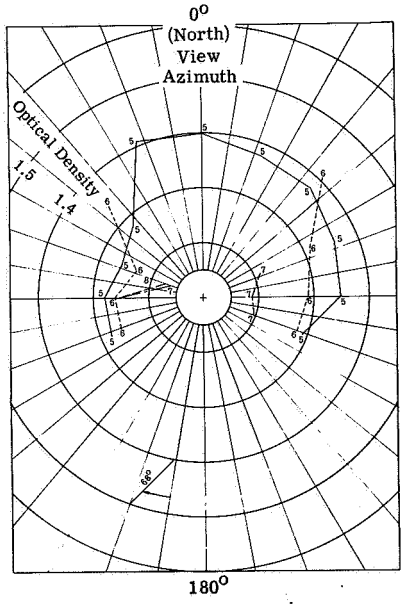

(b) Polar Plot, Off-Nadir Angles of 20° (5), 25° (6), 30° (7), and 35° (8)

FIGURE 32. SAMPLE PLOTS FOR SOYBEANS. 1315 hours, 29 July 1964.

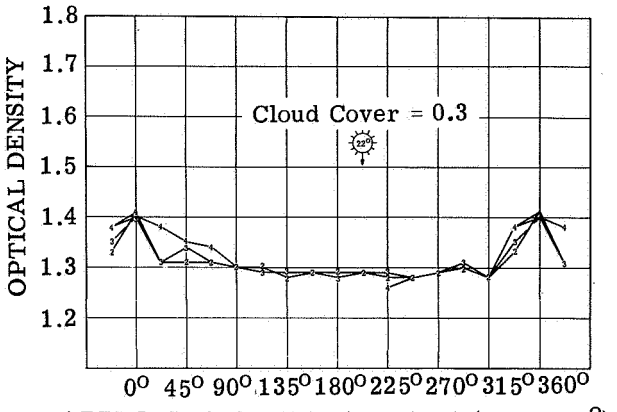

(c) Linear Plot, Off-Nadir Angles of 2° (1), 5° (2), 10° (3), and 15° (4)

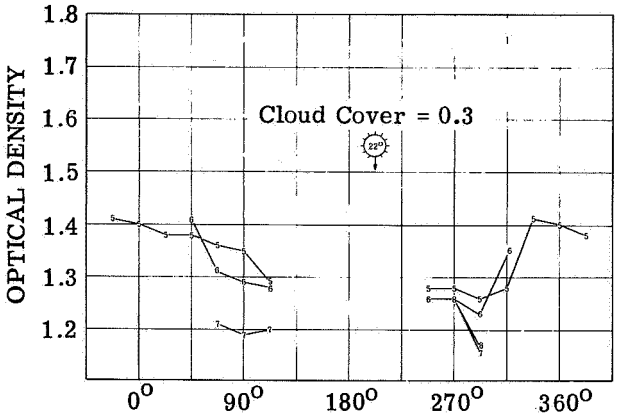

(d) Linear Plot, Off-Nadir Angles of 20° (5), 25° (6), 30° (7), and 35° (8)

DATE/TIME/TYPE OF PHOTO
640729/1315/IR

FRAME NO. 122

SOLAR AZM. FROM N. 190°

SOLAR ALT. 68°

CAMERA DATA:

FILTER(S) K2 + 87

F STOP F 8

SHUTTER SPEED 1/100 sec.

FRAME RATE 3 sec.

WEATHER DATA:

VIS.= 15 miles

SKY COVER = 0.3

TOTAL OPAQUE SKY COVER = 0.3

AIR TEMP. 83°F

DEW PT. 63°F

WIND DIR. 020°
SPEED 13 K

PRESSURE 1011.6 mb

CROP DESCRIPTION:

TYPE Soybeans

VARIETY Harosoy 63

PLOT(S) 106 & 107

ROW AZM. FROM N. 180°

ROW SPACING FT.

PLANTING DATE
21 May 1964

HEIGHT 40 ins

SOILS 106 - 3398
107 - 392

STATE Photo: uniform appearance

LEGEND FOR CURVES:

1 = 2°
2 = 5°
3 = 10°
4 = 15°
5 = 20°
6 = 25°
7 = 30°
8 = 35°

VIEW ANGLES

(e) Data Sheet

FIGURE 32. SAMPLE PLOTS FOR SOYBEANS. 1315 hours, 29 July 1964. (Continued)

made at different times of day and year and the exposure and development factors were not necessarily the same in each case; also, compensation was not made for any roll, pitch, or yaw of the aircraft. Therefore, in general, one can compare negatives obtained from the same roll of film only, and, even then, care must be exercised. For example, on one flight with a cloud cover of only 20%, one of the fields analyzed was in the shadow of a small cloud at the time it was photographed by one of the cameras and had a density level much lower than would be expected in comparison with the other fields photographed on the same flight. There might also be some variations in film response and processing throughout the roll of film which could make direct comparisons less accurate.

Two types of composite graphs of interest in discriminating between various types of crops can be made from such data as in figures 30-32. The first graph indicates, as a function of the off-nadir angle of view, the range of density values observed for each of several fields when data over all view azimuths are included.* Figures 33 through 35 compare the densities for Pfister corn, Reed wheat, and 5210 Breeders wheat (for more complete descriptions of the corn and Breeders wheat, see figs. 31e and 32e; the Reed wheat was 37 in. high) for mission times of 0630, 1030, and 1430** on 25 June 1964; part a of each figure is for the infrared film (0.7 to 0.9 μ) and part b is for the visible (panchromatic) film (0.4 to 0.7 μ). Note that complete data at all angles were not available to make the plots, and all observations made below are subject to this incompleteness. In the infrared (fig. 33a), there is almost complete overlay of the corn and the two types of wheat at all angles. From figure 33b, it can be seen that (1) corn in the visible is differentiable from both varieties of wheat at all off-nadir angles of view under the conditions of 0630 hours, and (2) there is much overlap between the two varieties of wheat. The same types of comparisons can be made at the other times of day. Note that the corn field in the 1030 infrared frame was in the shadow of a small cloud as mentioned earlier; therefore, the separation seen in figure 34a is not representative of the crops under identical illumination conditions; in the visible frame (fig. 34b), the corn field was completely out of the shadow, and, while the Reed-wheat field was out of the main shadow, there appears to be a slight reduction of response caused by a haze layer which extended past the cloud's edge. In the infrared at 1430 hours (fig. 35a) the corn has a considerably greater response than does the Breeders wheat. In the visible (fig. 35b) Reed wheat is more responsive than the others, and the Pfister corn has a lower response than does the Breeders wheat; the two wheats are quite similar for larger angles and also overlap with the corn.

*Note that the density readings were not corrected for the angle dependence of the camera; therefore, the falloff with large angles is probably caused by the camera rather than the crop. Furthermore, the ordinate quantity is density rather than exposure; the actual exposure changes cannot be obtained from the 1964 data.

**Mission times are approximate starting times of the flights; infrared and visible photographs were made from two different planes which followed similar paths but at slightly different times.

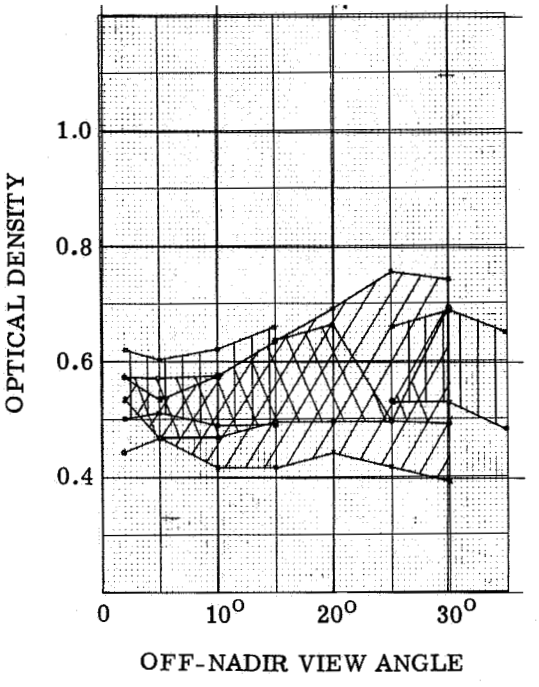

(a) Infrared Film (0.7 to 0.9 μ)

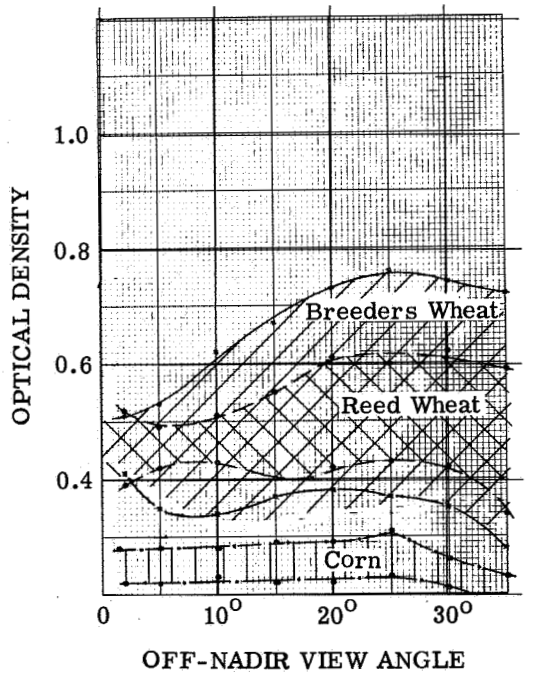

(b) Visible Film (0.4 to 0.7 μ)

FIGURE 33. COMPOSITE PLOTS OF DENSITY VS. OFF-NADIR VIEW ANGLE, 0630 HOURS. 25 June 1964. ▥: Pfister corn; ▨: 5210 Breeders wheat; ▧: Reed wheat.

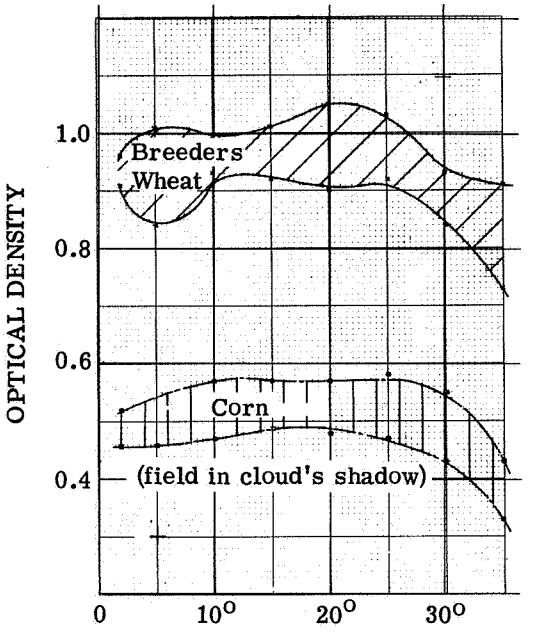

(a) Infrared Film (0.7 to 0.9 μ)

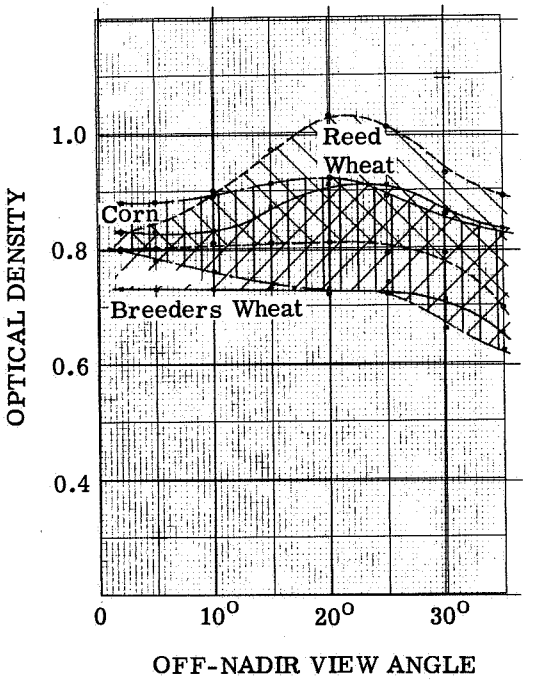

(b) Visible Film (0.4 to 0.7 μ)

FIGURE 34. COMPOSITE PLOTS OF DENSITY VS. OFF-NADIR VIEW ANGLE, 1030 HOURS. 25 June 1964. : Pfister corn; : 5210 Breeders wheat; : Reed wheat.

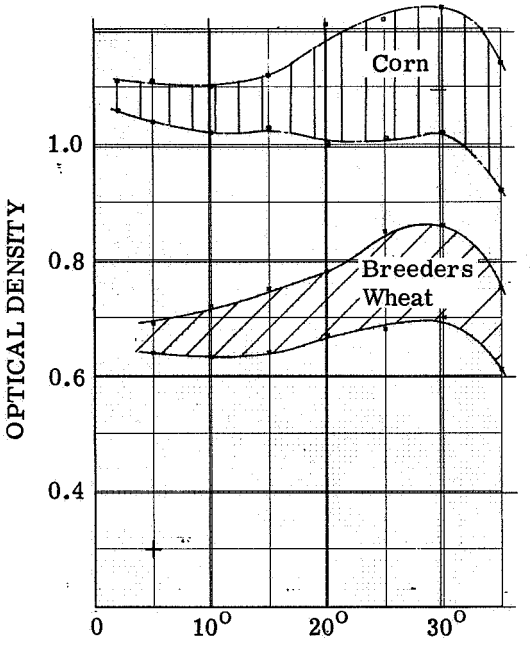

(a) Infrared Film (0.7 to 0.9 μ)

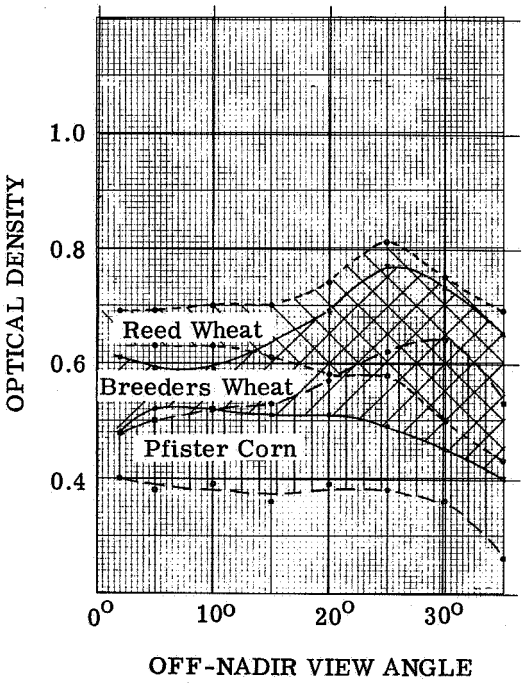

(b) Visible Film (0.4 to 0.7 μ)

FIGURE 35. COMPOSITE PLOTS OF DENSITY VS. OFF-NADIR VIEW ANGLE, 1430 HOURS. 25 June 1964. ▥: Pfister corn; ▨: 5210 Breeders wheat; ▧: Reed wheat.

The second type of composite graph helps to further define those geometries in which the crops become differentiable. It is a plot of density vs. azimuth angle in which the ranges of densities measured at all off-nadir angles from 2^{o} to 30^{o} or in the intervals 2^{o} to 15^{o} and 20^{o} to 30^{o} are indicated on the graph. When densities of two or more crops are placed on the same graph, one can determine those azimuth angles (if any) at which they are differentiable. Again, one can compare densities only on photographs that were obtained on the same flight, and, even then, care must be exercised. Several composite graphs of this second type are presented in figures 36 through 39; the crops included are tabulated in table VII, as are the fractions of cloud cover at the time of each flight. The direction of the sun is shown on each figure; the number in the sun is its angle as measured from the zenith; the fraction of cloud cover is also noted. It was not possible to obtain a full representation of crop types for each time of day and time of year because of the limitations in the photographic coverage.

The first graph (fig. 36a) shows infrared density values for 0630 hours on 25 June. From it one concludes that it is difficult to differentiate the corn from the wheat in the infrared under these conditions. At 0630 hours on 25 June in the visible (fig. 36b) it is noticed that corn was much less responsive than wheat and that the wheat types overlap considerably. Although the data are incomplete, there is a strong tendency toward backscattering in the wheat. Figure 36c is an attempt to provide an additional breakdown of the densities read at various off-nadir view angles. That is, each crop has two pairs of bounding curves, one for off-nadir angles of 2^{o} to 15^{o} and one for angles of 20^{o} to 30^{o}. Although the curves are rather difficult to read, the Breeders-wheat field here appears to be differentiable (slightly higher response) from the Reed-wheat field at viewing azimuths from 90^{o} to 200^{o} when the two ranges of off-nadir angles are compared separately.

At 1000 hours on 25 June in the infrared (fig. 37a) densities were read only for corn and Breeders wheat. As mentioned earlier, the corn field was in the shadow of a small cloud and thus has low density values. In the visible (fig. 37b) there is much overlap between corn and wheat, but oats are clearly more responsive. The Reed wheat in this instance appears to be slightly more responsive (angle for angle) than the Breeders wheat, even though it might have been illuminated less because of a haze layer as discussed earlier. Thus, one detects here a smaller change and apparent reversal in the relative responses of the two wheat fields in the visible in going from 0630 to 1000 hours.

At 1430 hours on 25 June in the infrared (fig. 38a), the one wheat field has a much lower response than did either corn or oats. The data on oats are less complete than on corn, but those available indicate that oats more often than not had a response greater than that of corn. In the visible (fig. 38b), Reed wheat is generally more responsive than either Breeders wheat or corn for azimuth angles from 90^{o} to 270^{o}. The corn is distinguishable from the wheat for the same angles but overlaps at other angles.

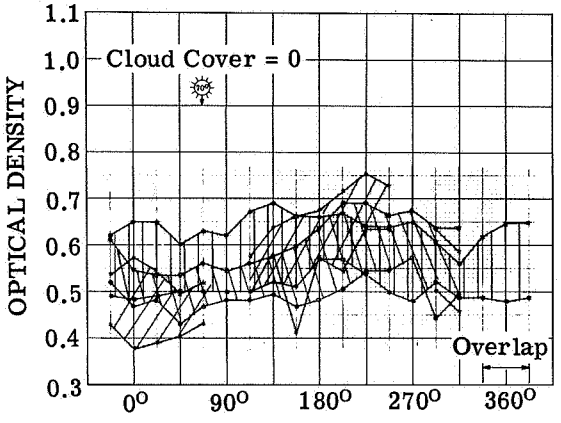

(a) Infrared Film (0.7 to 0.9 μ). Off-nadir angles 2° to 30°.

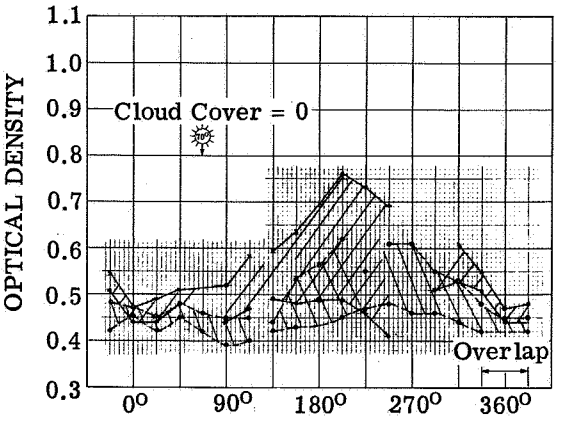

(b) Visible Film (0.4 to 0.7 μ). Off-nadir angles 2° to 30°.

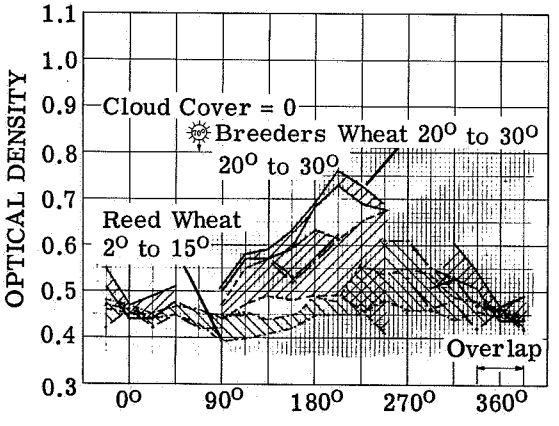

(c) Visible Film (0.4 to 0.7 μ). Off-nadir angles 2° to 15° and 20° to 30°.

FIGURE 36. COMPOSITE PLOTS OF DENSITY VS. AZIMUTH ANGLE, 0630 HOURS. 25 June 1964. : Pfister corn; : 5210 Breeders wheat; : Reed wheat. Nearly all values for corn lie between D = 0.2 and D = 0.3.

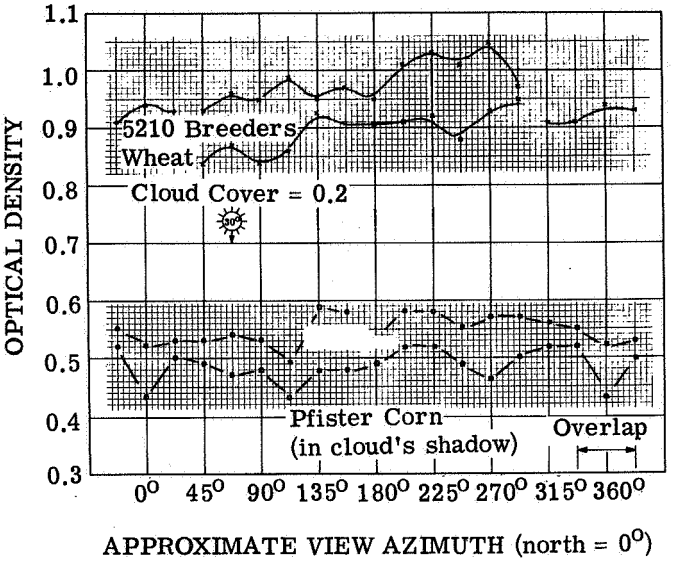

(a) Infrared Film (0.7 to 0.9 μ)

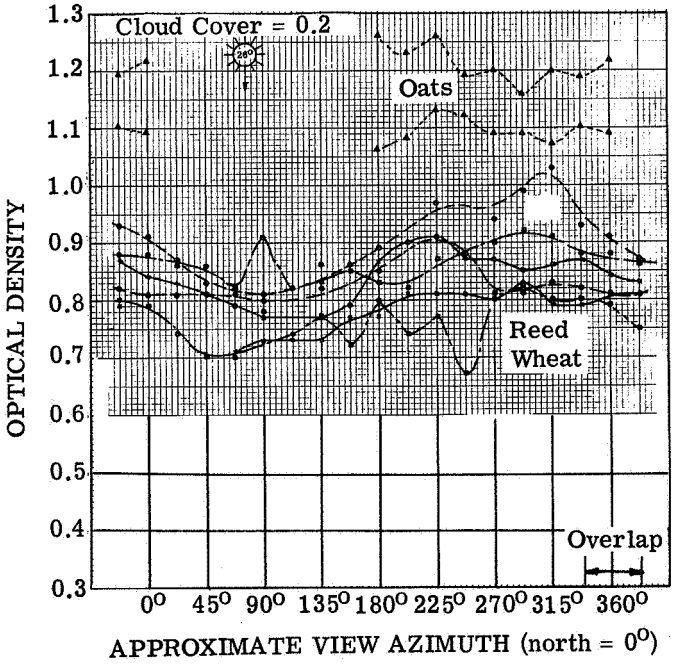

(b) Visible Film (0.4 to 0.7 μ)

FIGURE 37. COMPOSITE PLOTS OF DENSITY VS. AZIMUTH ANGLE, 1030 HOURS. 25 June 1964. ◘: Pfister corn; ×: 5210 Breeders wheat; O: Reed wheat; ▲: oats. Off-nadir angles 2^{o} to 30^{o}.

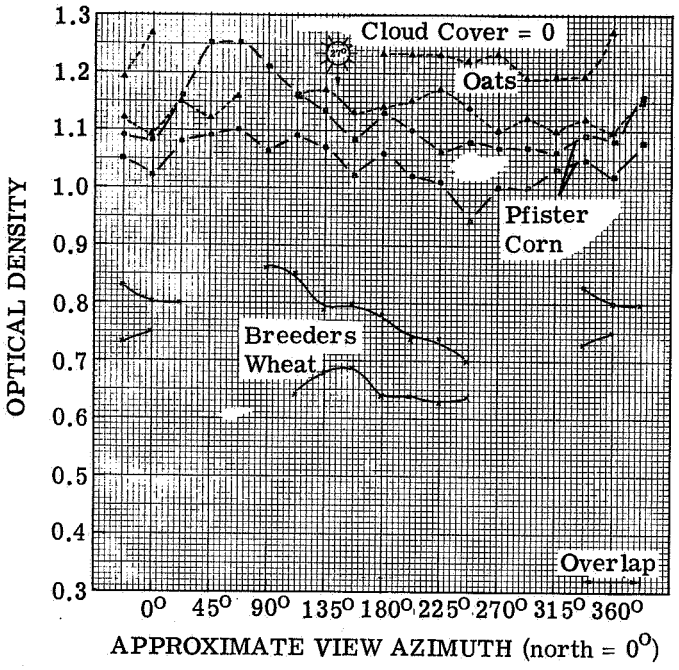

(a) Infrared Film (0.7 to 0.9 μ)

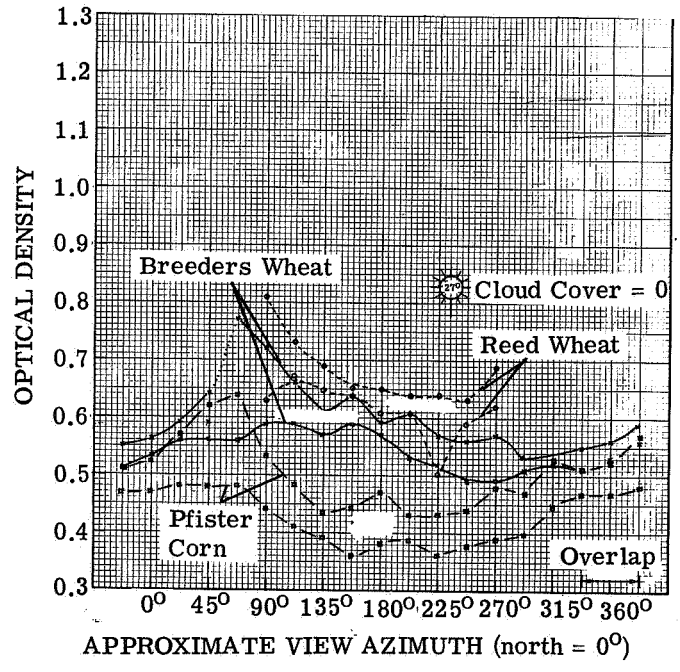

(b) Visible Film (0.4 to 0.7 μ)

FIGURE 38. COMPOSITE PLOTS OF DENSITY VS. AZIMUTH ANGLE, 1430 HOURS. 25 June 1964. ◘ : Pfister corn; ×: 5210 Breeders wheat; ○: Reed wheat; ▲: oats. Off-nadir angles 2^{o} to 30^{o}.

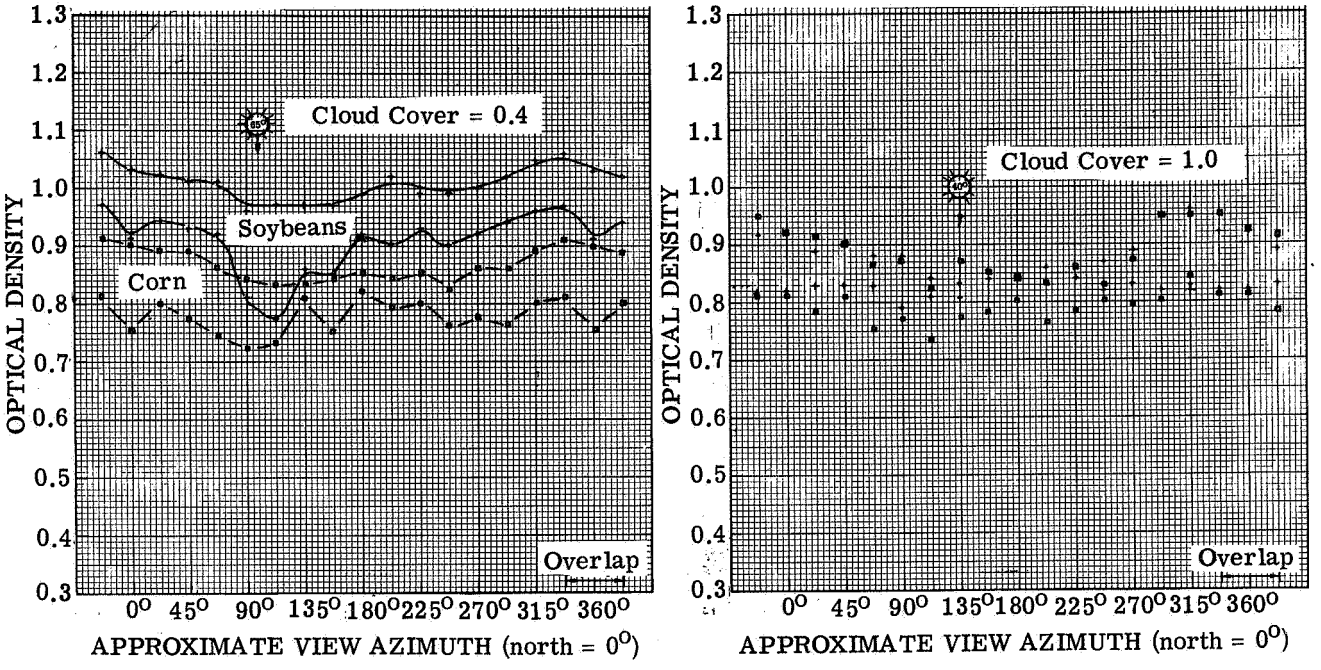

(a) 0825 Hours

(b) 1055 Hours

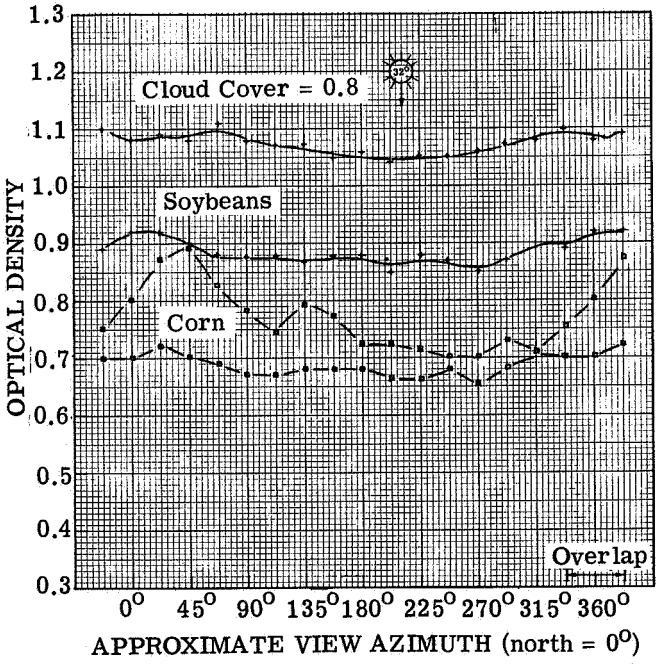

(c) 1400 Hours

FIGURE 39. COMPOSITE PLOTS OF DENSITY VS. AZIMUTH ANGLE, INFRARED FILM. 27 August 1964.

TABLE VII. DESCRIPTION OF DATA PRESENTED IN COMPOSITE GRAPHS OF DENSITY VS. AZIMUTH ANGLE

Figure No.	Date	Time	Fraction of Cloud Cover	Crops Included*			
				Wheat	Oats	Corn	Soybeans
35	6/25/64	0630	0	V, IR		V, IR	
36		1030	0.2	V, IR	IR	V, IR	
37		1430	0	V, IR	IR	V, IR	
38	7/29/64	1315	0.2			IR	IR
39	8/27/64	0825	0.4			IR	IR
40		1055	1.0			IR	IR
41		1400	0.8			IR	IR

*V denotes data from visible (panchromatic) film; IR denotes data from infrared film.

On 27 August, comparisons can be made between corn and soybeans on photographic infrared films at three times of day. At 0825 hours with 0.4 cloud cover (fig. 39a) the soybeans were with few exceptions more responsive than the corn. At 1055 hours with complete cloud cover (fig. 39b) the two crops were indistinguishable. At 1400 hours and with 0.8 cloud cover (fig. 39c), the soybeans were again more responsive. It is not known whether the changes in the relative responses of these crops can be attributed to temporal changes or angular dependences in the crops reflectances, to nonequal illuminations caused by the high fractions of cloud cover, or to a combination of the two.

The fields selected by no means exhibit all the differences and similarities that might be present in the real world. It is well known that differences in crop maturity resulting from different planting dates affect the responses of a given crop (one example is discussed in sec. 6.3.2.2). Figures 33, 34, and 35 illustrate the differences which an exist between varieties of the same crop (wheat) which have the same planting date. The most important facts that can be extracted from figures 35 through 39 are as follows. (1) There is a marked variation in crop reflectances when the angles of observation and/or illumination are changed. (2) The maximum responses occur at angles away from the nadir. In the negatives, the peak responses were usually found at off-nadir angles of 20^{o} to 30^{o} (beyond which the camera limited the response) and at view azimuth angles away from the sun. The amount of variation in response at a fixed off-nadir angle as one sweeps through all azimuth angles also tends to become greater as the off-nadir angle is increased. (3) There appear to be certain geometrical situations in which two crops become more differentiable than at other situations.

In the above study, only two relatively broad spectral bands were investigated, the photographic visible and the photographic infrared. Since two aircraft were used, the data in the two bands were not obtained simultaneously or under precisely identical conditions; also, one cannot convert from density to exposure values. One cannot therefore make meaningful comparisons of the results obtained from the two bands. The 1966 scanner data, which will consist of simultaneous imagery in twelve bands that cover the photographic region plus other nearly simultaneous data in other bands, should permit a meaningful analysis to be made of angular effects and their spectral dependence.

6.3.2.2. (U) High-Altitude Photographs. One series of high-altitude photographs was made during 1964 (i.e., visible film at 1430 hours on (25 June) for which it is possible to make limited comparisons with some of the preceding low-altitude data. The comparisons are limited because not enough individual frames were exposed at a variety of positions to permit the extraction of angle-dependent data for many of the angles of interest. The three crops studied are again Reed wheat, Breeders wheat, and Pfister corn (see fig. 27). The wheat fields are the same as were analyzed in the low-altitude studies, but the large corn field studied was not included in the

high-altitude photographs. Therefore, it was necessary to select other corn fields adjacent to the field of Breeders wheat. Two corn fields selected are of the same variety (Pfister SX29) as that of the low-altitude studies, but, while one (field A) had the same planting date, the other (field B) had a planting date 15 days later.

The photographic coverage was such that densities could be read only for crops viewed from the southern quartersphere toward the northern one. The polar plots for off-nadir angles of 0^{o} to 15^{o}, 16^{o} to 25^{o}, and $>25^{o}$ are given in figures 40a, 40b, and 40c, respectively; the corresponding linear plots are presented in figures 41a, 41b, and 41c. At those angles for which direct comparisons are possible, one sees that (1) Reed wheat is generally slightly more responsive than Breeders wheat, (2) corn field A (comparable to the field studied at low altitude) has the lowest response of all, (3) corn field B, the less mature corn (23-in. height as opposed to 38-in. for A), has a response which is somewhat greater than that of A and is comparable to and even slightly greater than that of Breeders wheat at certain angles, and (4) the crops again exhibit a tendency toward strong backreflection. Observations 1 and 2 agree very well with those made from the density readings on low-altitude photographs (see fig. 35), even though the azimuth-angle coverage is incomplete in each case. Observation 3 results from the greater amount of soil which is observed in the less mature corn (the reflectance of soil is greater than that of young corn leaves in the visible region). Observation 4 also agrees with those made earlier for both high- and low-altitude photographs from the 1964 missions.

A series of high-altitude infrared photographs were taken at WRL during a local test flight on 21 July 1966 at 1430 hours in order to investigate angle-dependent effects and check out the film calibration technique. On this particular flight, a ground point around which several crops of interest were located was selected as the target point for the data runs. The plan was to fly directly over the target point on several different headings while taking photographs with a large amount of overlap. Densities were to be read on each frame for a field of interest, with the density values then being used to produce curves for the field such as shown earlier from low-altitude photographs. The plan was followed except that the pilot found it difficult to fly directly over the target point on the various passes. Consequently, instead of having a single azimuthal direction for each reading on a given pass, each frame in the pass yielded a point with a different azimuth reading; the change was particularly noticeable for frames in which the target point was near the nadir. Another local flight has been planned in which there will be a different pattern flown with a higher frame rate so as to obtain better coverage of the fields.

Since the data collection is incomplete, it is not possible to construct curves as well defined as those shown earlier for the low-altitude photographs, but interesting observations are still made. Plots of the points obtained from the local flights are presented in figures 42a, 42b, and 42c for winter wheat and corn at off-nadir angles of 0^{o} to 15^{o}, 16^{o} to 25^{o}, and $>25^{o}$, respectively;

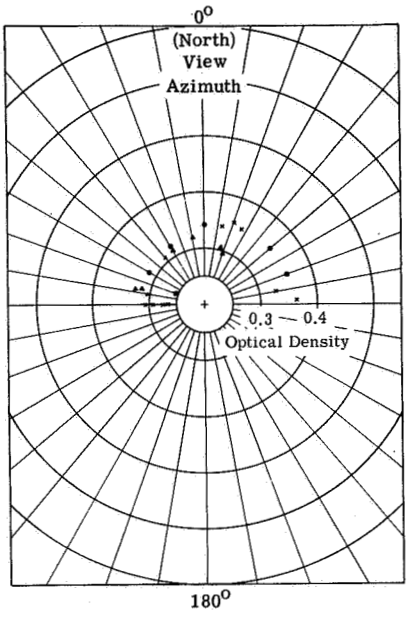

(a) Off-Nadir Angles 0° to 15°

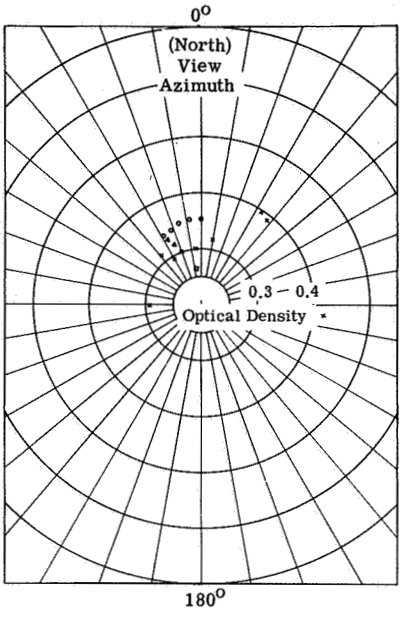

(b) Off-Nadir Angles 16° to 25°

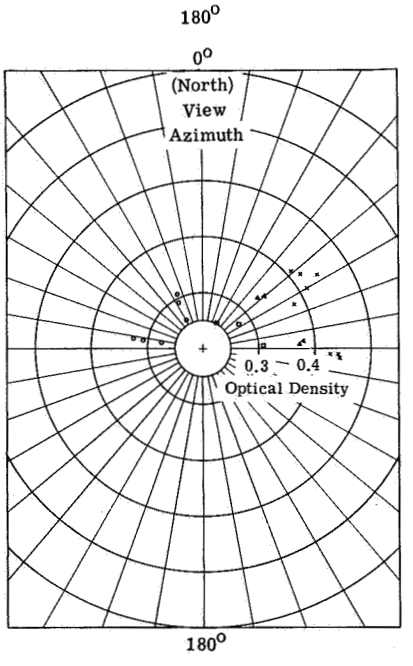

(c) Off-Nadir Angles >25°

FIGURE 40. POLAR PLOTS OF DENSITY FROM HIGH-ALTITUDE PHOTOGRAPHS. 1430 hours, 25 June 1964. × : 5210 Breeders wheat; ○: Reed wheat; □: Pfister corn (field A); ▲: Pfister corn (field B).

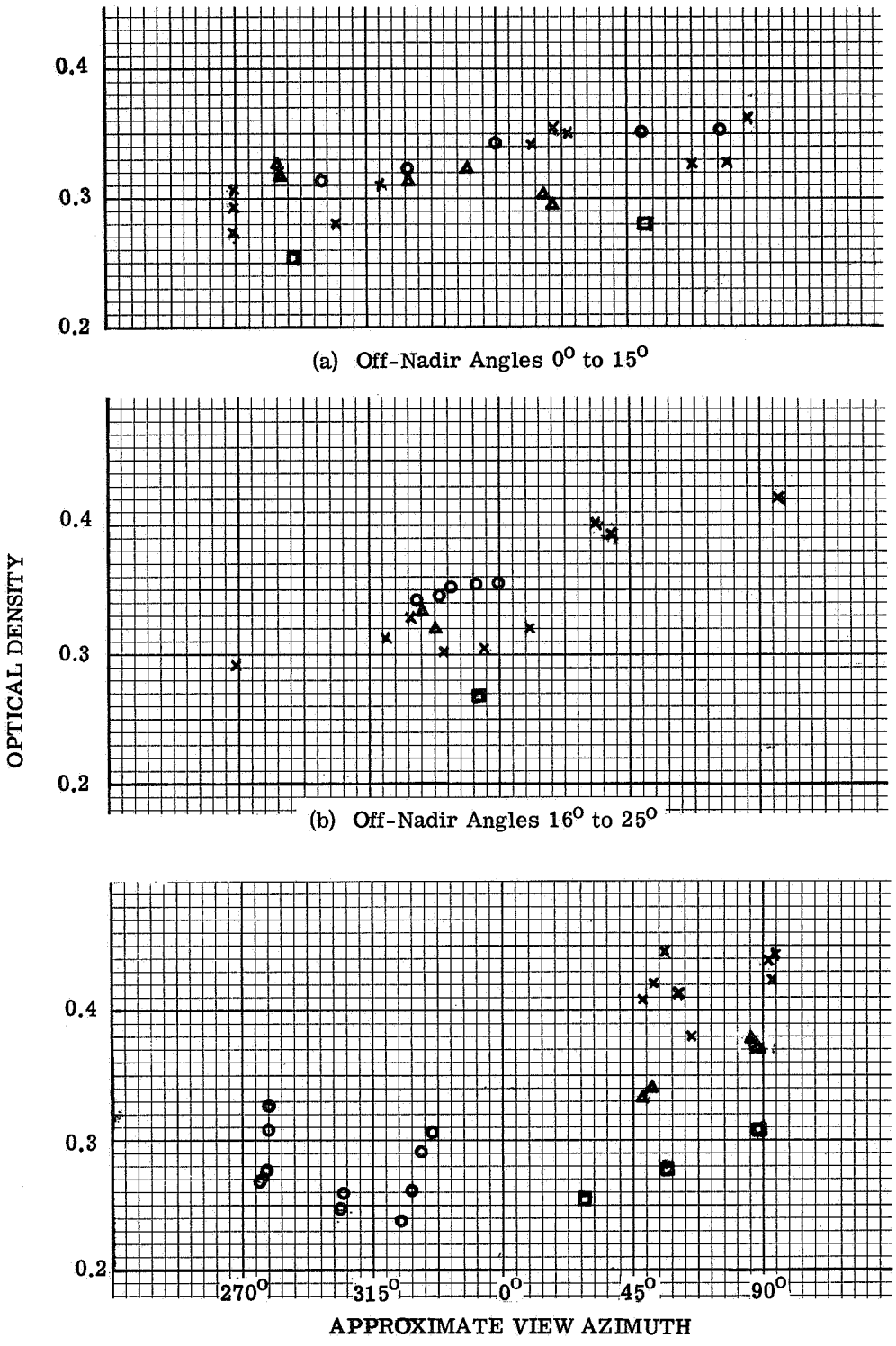

(a) Off-Nadir Angles 0° to 15°

(b) Off-Nadir Angles 16° to 25°

(c) Off-Nadir Angles > 25°

FIGURE 41. LINEAR PLOTS OF DENSITY FROM HIGH-ALTITUDE PHOTOGRAPHS. 1430 hours, 25 June 1964. □: 5210 Breeder wheat; ×: Reed wheat; ○: Pfister corn (field A); △: Pfister corn (field B).

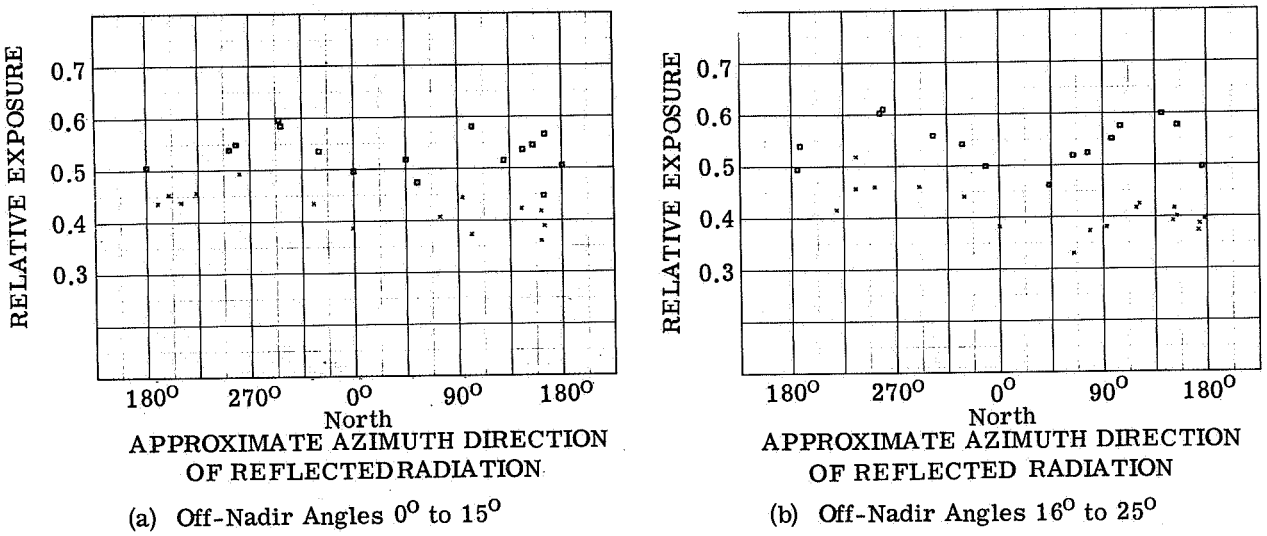

(a) Off-Nadir Angles 0^{o} to 15^{o}

(b) Off-Nadir Angles 16^{o} to 25^{o}

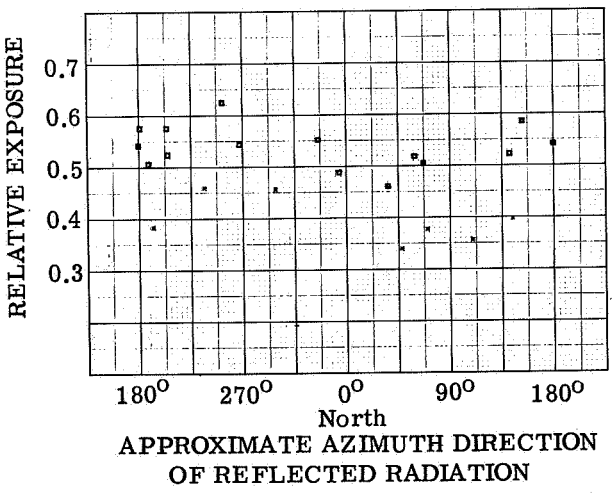

(c) Off-Nadir Angles $> 25^{o}$

FIGURE 42. LINEAR PLOTS OF RELATIVE EXPOSURE FROM LOCAL HIGH-ALTITUDE PHOTOGRAPHS, CORN AND WHEAT. 1430 hours, 21 July 1966. × : wheat; □: corn.

similar graphs for soybeans with two different row orientations are presented in figure 43. There are two differences between these high-altitude curves and the earlier low-altitude curves and the 1964 high-altitude curves. First, the ordinate has been corrected for the nonlinear response of the film emulsion and is proportional to the actual exposure or crop radiance except for any falloff with off-nadir angles caused by the camera; this correction was possible because of the standard gray scale which has been added along the margins of the films produced in 1966. Second, the abscissa scale is shifted 180^{o} from that used for the low-altitude plots. The abscissa was changed so that the data would be representative of the bidirectional reflectance patterns of the crops rather than being oriented toward the geometry of the measurement device as are the low-altitude graphs. The azimuth angle is here the direction in which the radiation is reflected rather than the direction in which the observer looks to see it. Consequently, the sun is shown at its true azimuth angle relative to the crop, and a back reflector is one which scatters most light back in the same direction as the sun. Also, the angle about the vertical axis is changed from off-nadir angle to zenith angle (which is measured relative to vertical).

From figures 42 and 43, one sees that for the conditions of the measurement (1) winter wheat is less responsive than either corn or soybeans, (2) corn and soybeans overlap considerably, with soybeans having slightly greater responses on the average, and (3) all three crops exhibit a tendency to scatter more radiation both back toward the sun (azimuth $\sim 240^{o}$) and in a direction symmetrically located about the north-south axis than is scattered in intermediate directions. The linear graphs of figure 43 allows one to compare the values obtained from east-west rows of soybeans with those from north-south rows. Because of the incompleteness of the data, it is difficult to see a meaningful difference. The only one is an apparent greater scatter of east-west rows at angles of $\sim 135^{o}$ (see fig. 43b).

6.3.2.3. Theoretical Studies. A theoretical prediction of the spectral radiances of crops (which depend on the crops' bidirectional-reflectance properties) was desired for comparisons with actual field data. To build a model to permit such predictions requires the use of data measured both in the laboratory and the infield together with an appropriate geometrical model of (1) the crop's surface, (2) the observer's direction, and (3) the illumination's characteristics. Laboratory spectral reflectances and a trapezoidal crop model were used to develop a first-order predictive model; the model can presently be applied only to certain row crops such as corn and soybeans because of limitations in the available data; the calculations are made on a digital computer.

Nearly all the applicable crop data are directional-reflectance measurements rather than bidirectional ones. That is, while a small source is used to illuminate the sample, the reflected

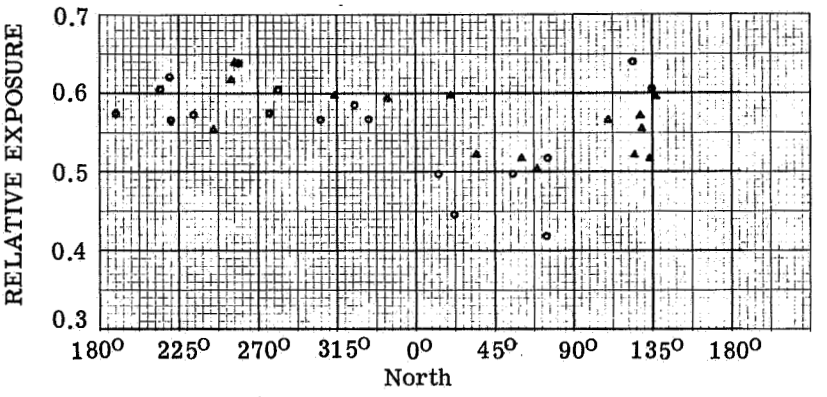

(a) Off-Nadir Angles 0° to 15°

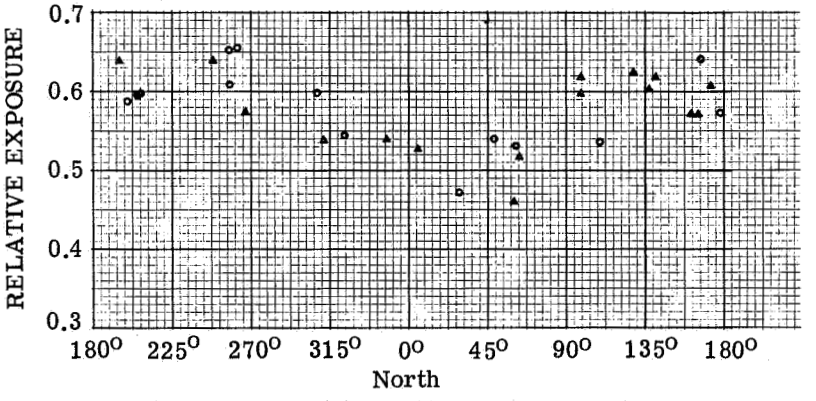

(b) Off-Nadir Angles 16° to 25°

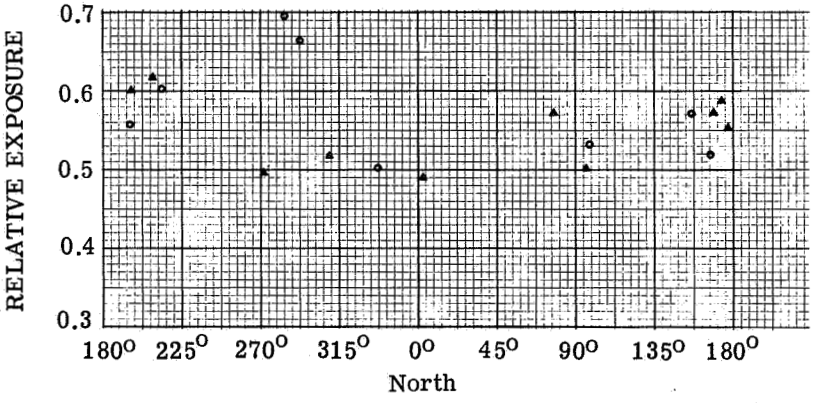

(c) Off-Nadir Angles >25°

FIGURE 43. LINEAR PLOTS OF RELATIVE EXPOSURE FROM LOCAL HIGH-ALTITUDE PHOTOGRAPHS, SOYBEANS. 1430 hours, 21 July 1966. O : soybeans, north-south rows; ▲ : soybeans, east-west rows.

radiation is collected (integrated) over an entire hemisphere. The only way that such data can be used in a model is to assume that the crop's surfaces are diffuse reflectors. While such an assumption may be appropriate in some instances, there are definitely situations in which specular characteristics have been observed. Most of the applicable spectral-reflectance data were measured by Purdue in 1964 and are primarily limited to the row crops, corn and soybeans; therefore, the first model was designed for these row crops.

The many corn and soybean data curves were sorted into several categories and the mean values were calculated with Target-Signatures Library* programs at WRL for each category for use in the model; two additional curves at ±1 standard deviation unit are also plotted with each mean-value spectral-reflectance curve as an indication of the variation in the data. The corn data were placed in four categories: (a) green leaves from the top of a plant, (b) green leaves from the center or base of a plant, (c) dry brown leaves, and (d) dry tassle. The four curves for corn are presented in figure 44. Curve a is assumed to apply for young plants.

There was a larger variety of colors for soybean leaves than there was for corn; therefore, the following six categorizations were made: (a) light green, (b) medium-light green, (c) dark green, (d) medium-dark green, (e) greenish yellow, and (f) yellow (see fig. 45). A curve for immature soybean pods (fig. 45g) was also plotted. For modeling, it is to be assumed that young soybean plants are dark green and that they progressively lighten and turn yellow as the plant matures.

The only spectral-reflectance data on wheat and oats in the Target-Signatures Library are bidirectional data obtained at Beltsville, Maryland, by personnel of the Department of Agriculture and the Army Engineer Research and Development Laboratory [19]. An artificial source was used to illuminate growing specimens of the crops at a fixed elevation angle (~75^{o}) and the reflected radiation was collected directly overhead. These data do not, therefore, contain enough variables to permit one to predict the angle-dependent properties of wheat and oat reflectances or to adapt the row-crop model to these crops.

In order to keep the first model as simple as possible, a trapezoidal shape was assumed for the cross section of a row (see fig. 46). The sides are assumed to be opaque so that from a rather simple geometry (extended to three dimensions) one can determine those portions of each surface that are both illuminated and observed. The model allows each surface to be composed of up to five subsurfaces, each of which in turn may have its own spectral-reflectance values. To make the model more representative of the angular orientations of the plant leaves, each subsurface is also allowed to have an effective tilt or effective rotation about an axis

*The Library is part of the Target Signature Analysis Center established at The University of Michigan and sponsored by the Air Force Avionics Laboratory.

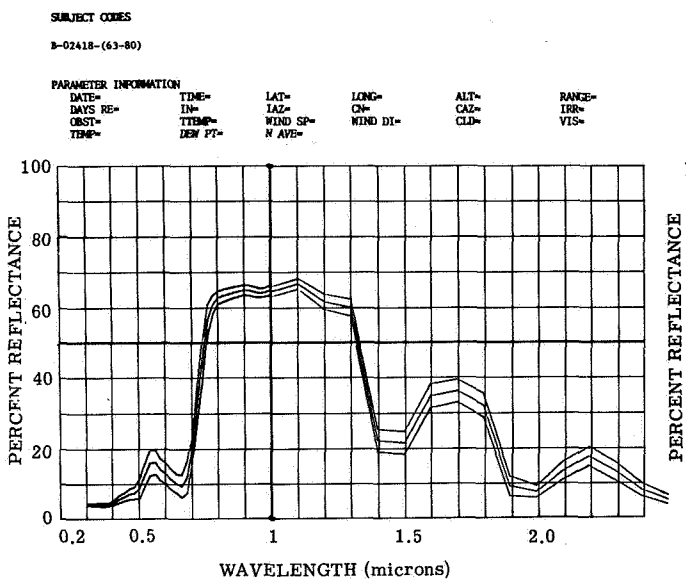

(a) Green Leaves from Top of Plant

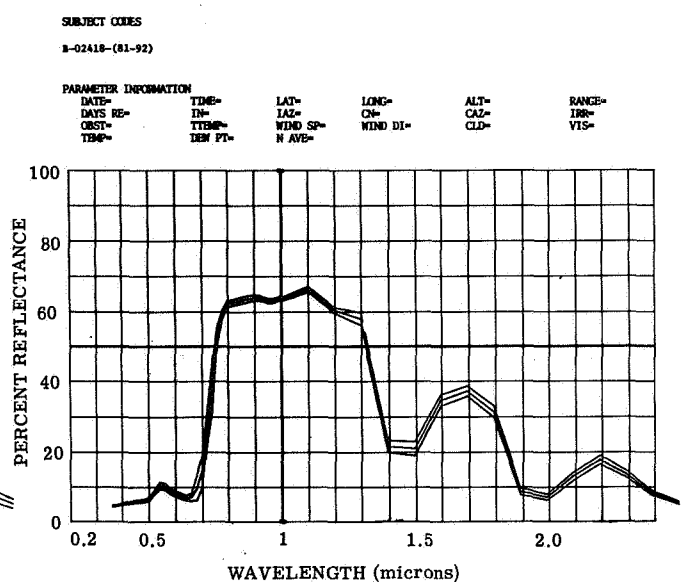

(b) Green Leaves from Center and Base of Plant

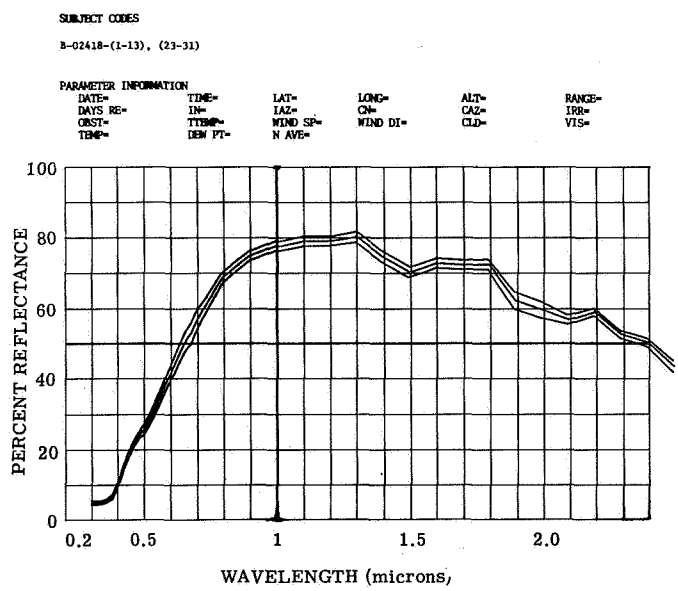

(c) Dry Brown Leaves

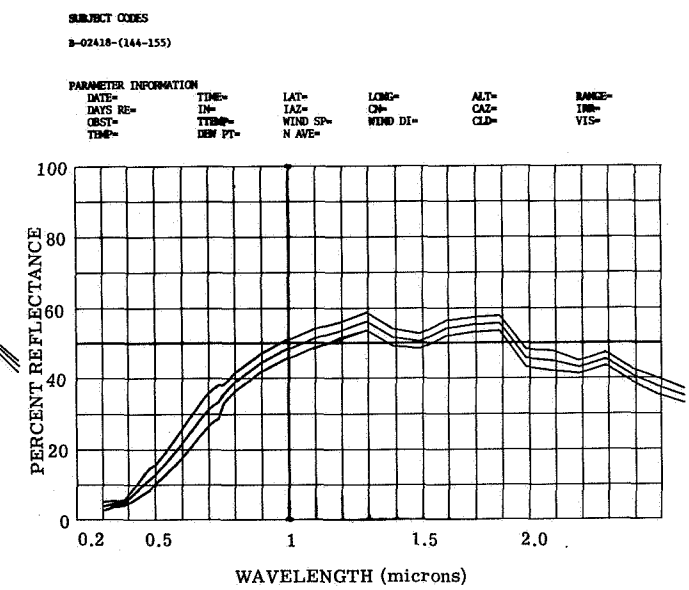

(d) Dry Tassle

FIGURE 44. SPECTRAL-REFLECTANCE CURVES FOR CORN

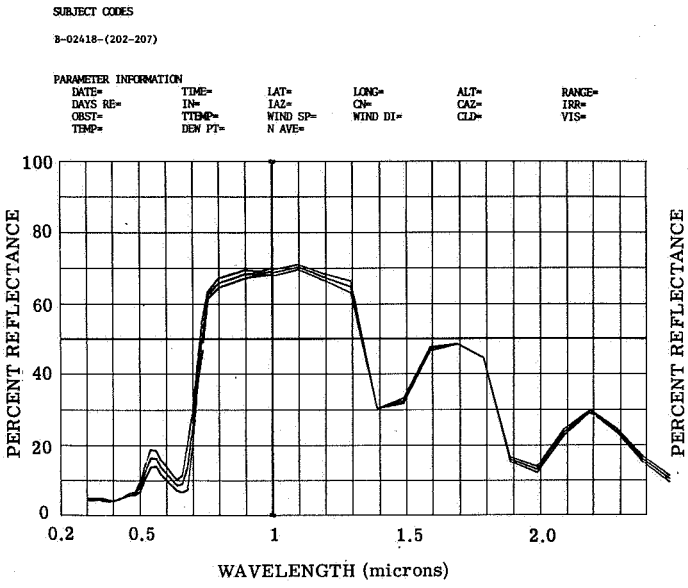

(a) Light-Green Leaves

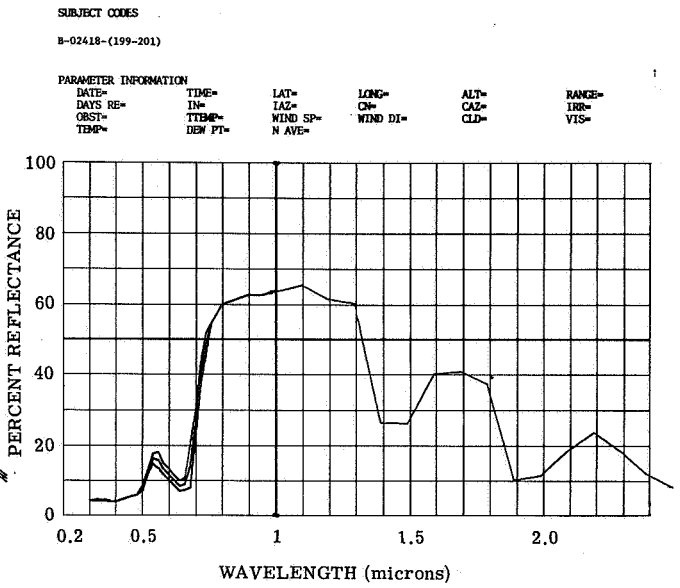

(b) Medium-Light-Green Leaves

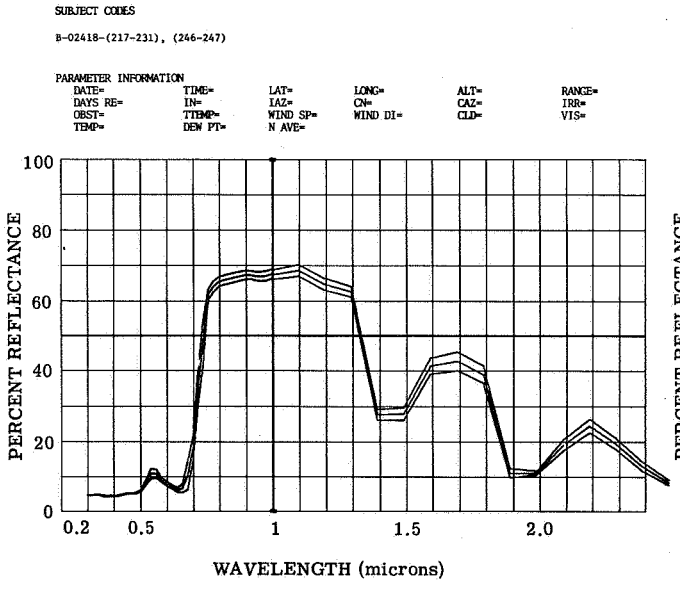

(c) Dark-Green Leaves

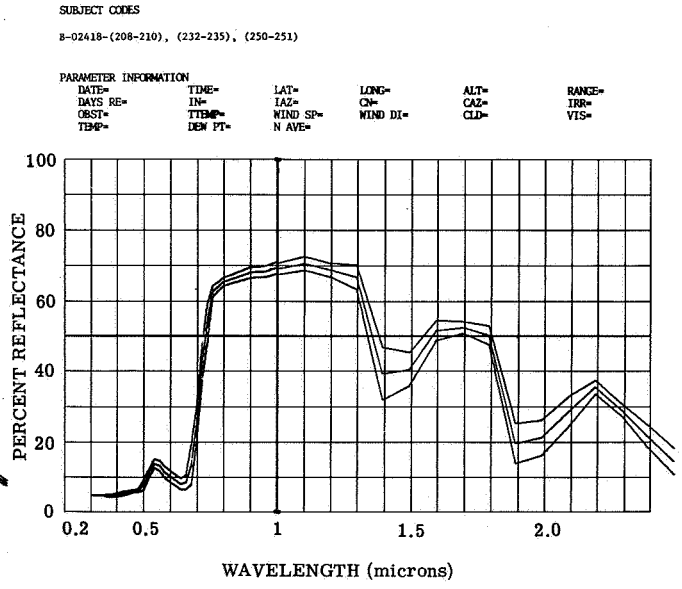

(d) Greenish-Yellow Leaves

FIGURE 45. SPECTRAL-REFLECTANCE CURVES FOR SOYBEANS

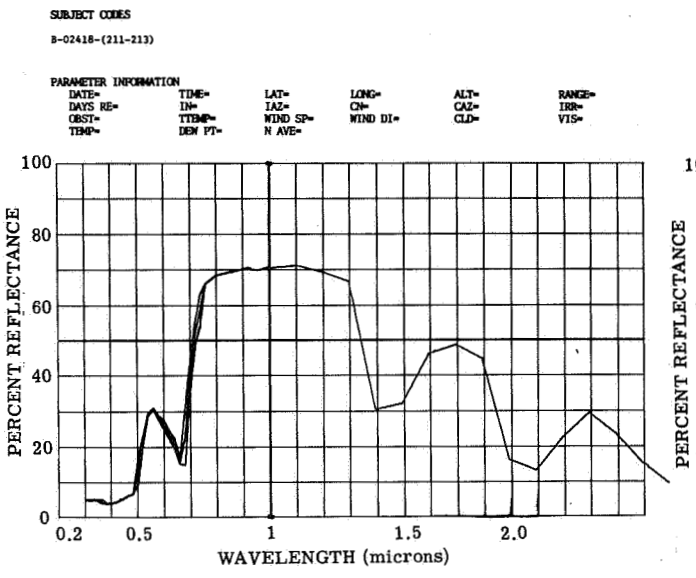

(e) Yellow Leaves

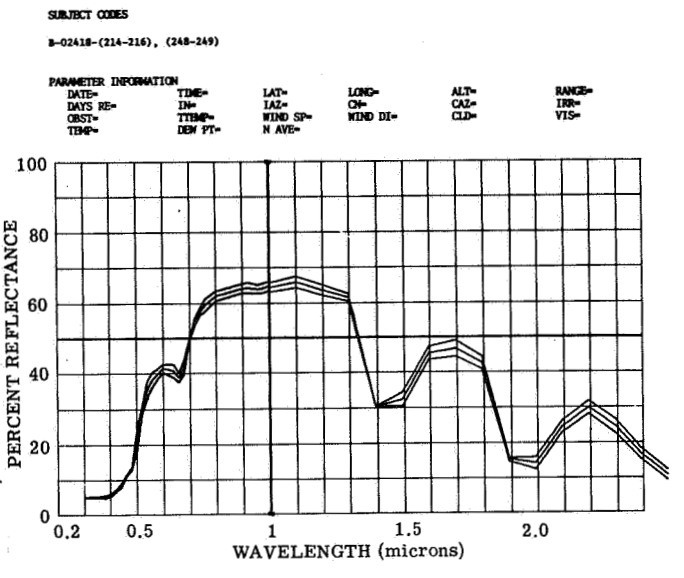

(f) Immature Pod

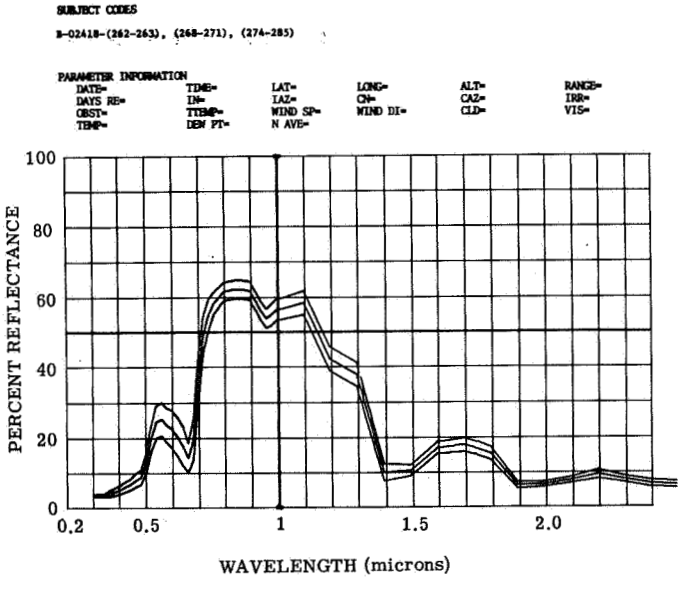

(g) Soybean Pod Immature

FIGURE 45. SPECTRAL-REFLECTANCE CURVES FOR SOYBEANS (Continued)

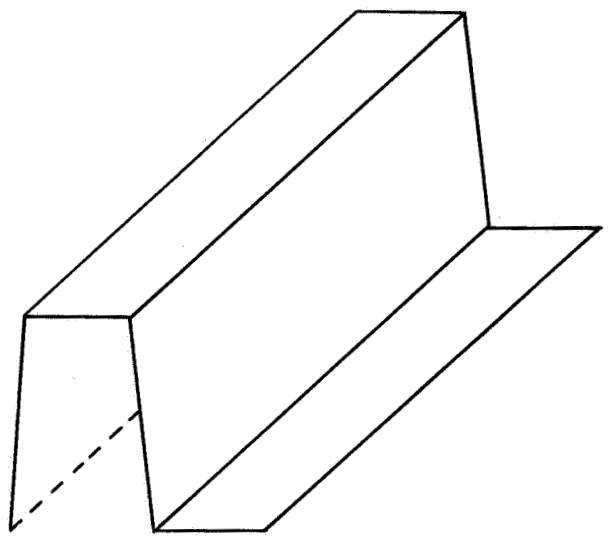

FIGURE 46. SIMPLE MODEL FOR ROW GEOMETRY

parallel to the row direction; the tilt rotates the reflection pattern of each surface and consequently changes the overall pattern from that of a nontilted model.

As discussed in section 6.3.1, the initial computer program included only the sun as the illumination source. This limitation was prompted by three facts: (1) the sun, when present, is the dominant source of short-wavelength radiation, (2) only limited data are available on the spectral-reflectance properties of clouds, and (3) the inclusion of clouds would greatly increase the complexity of the calculations. For all subsurfaces which are both illuminated and observed, the normal to the subsurface and the directional vectors of the source and illuminator are used to compute the spectral radiance of the subsurface in the direction of the observer; a summation over all subsurfaces gives the value for the crop.

If the crop were an ideal flat diffuse reflector, there would be no change in the amount of radiation observed by a fixed-FOV scanner as it is scanned across or around it; in other words, its radiance would be invariant with the angle of observation. Furthermore, the radiance retains none of the directional properties of the illumination. Thus, it can be seen that any angle-dependent properties of crops that are diffuse reflectors must result from their orientations relative to the observer and the illuminator.

Figure 47 illustrates the differences between computations based on a tilted crop model and those on a nontilted model. The crop characteristics were assumed to be typical of corn at Purdue during the last part of July and the time of day is about 1400 hours (solar zenith angle = 20° and azimuth angle = 200°). The calculated radiance distributions have symmetry about the normal to the crop row direction because of the nature of the crop model; consequently, the sun's azimuth has less effect than it might if tilts were also allowed in a direction perpendicular to the crop rows.

Calculations were made with the tilted crop model for the conditions which prevailed during the 1966 high-altitude test flights in Michigan; the results were normalized and are superimposed in figure 48 on the experimental data obtained for corn ($\phi \geqq 16^{\circ}$) from the high-altitude films. The curves for $\phi = 20^{\circ}$ and $\phi = 30^{\circ}$ fit the data quite well except for angles at which the shady side of the rows are observed (i.e., $270^{\circ} < \theta < 90^{\circ}$). Since the crop model is assumed to be opaque, the only surface which is both illuminated and observed from the angles mentioned is in the top, and tilting the top surface reduced the effective area even more; in reality, one would expect some illumination on the back side of the rows and thus a less severe dip in the radiance of the crop.

In searching for and using reflectance data for the crop models, we found certain deficiencies which decrease the usefulness of the data and thus restrict their value for general use in a library such as the Target-Signatures Library at WRL. It is therefore recommended that any future measurements be documented with the following information:

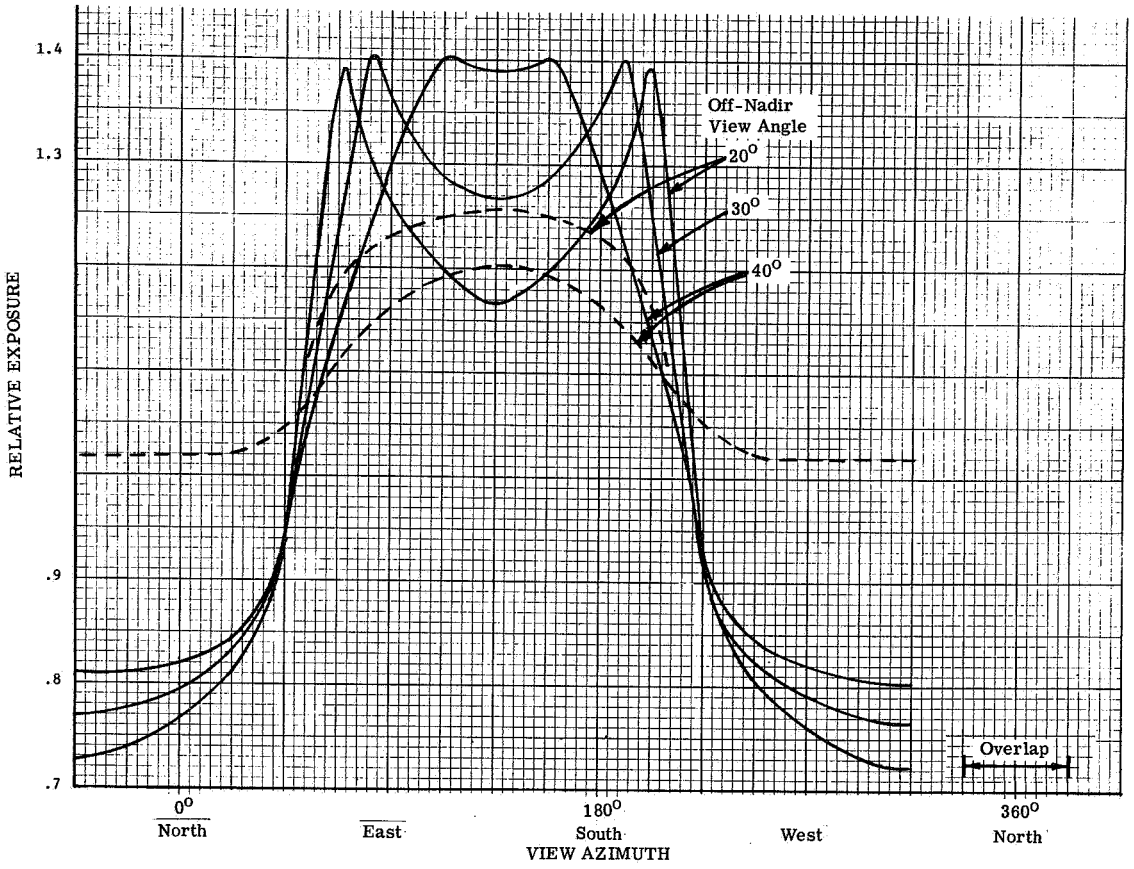

FIGURE 47. COMPARISON BETWEEN CALCULATIONS WITH TILTED AND WITH NONTILTED CROP MODELS. ——— Tilted - - - - Nontilted.

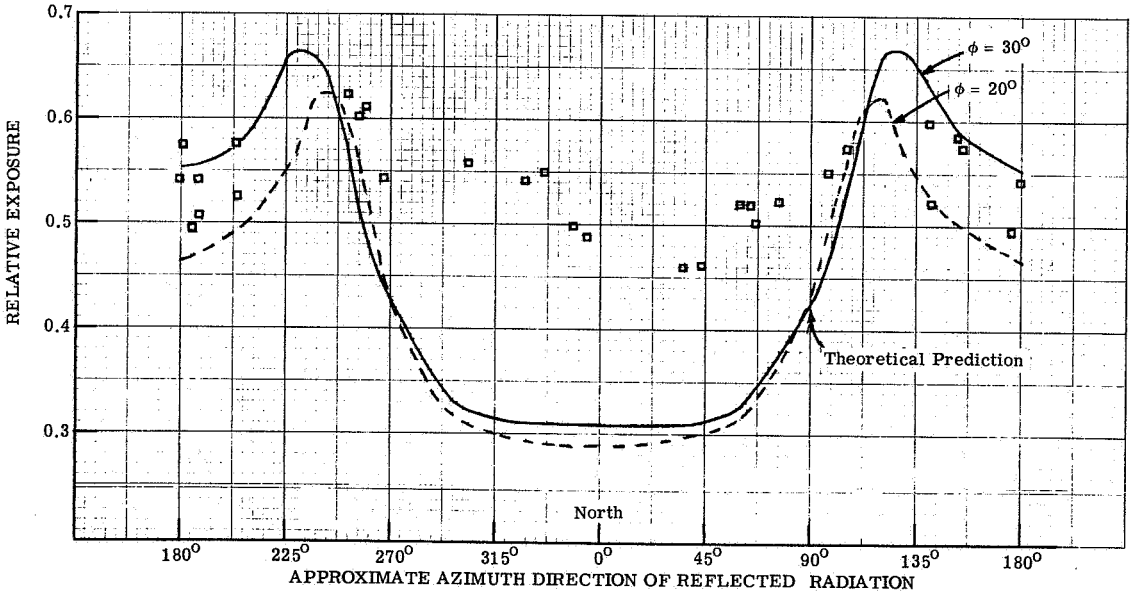

FIGURE 48. COMPARISON BETWEEN THEORETICAL PREDICTIONS AND ACTUAL MEASUREMENTS FOR CORN. 1430 hours, 21 July 1966.

(A) Vegetation measurements

(1) Species and variety

(2) Age of plant (planting date and the date of measurement)

(3) Stage of development: seedling, flowering, etc.

(4) The position on the plant from which the sample to be measured is taken (height from ground surface or number of leaves as counted from the base of the plant)

(5) Color of sample

It is suggested that a color standard be used such as the Munsell Color Chart for Vegetation.

(6) Any other information about a plant that might be useful, such as:

(a) Conditions under which the plant was grown, i.e., plant was grown under dry conditions or plant was grown in a highly fertile soil, etc.

(b) Condition of plant, i.e., healthy, diseased, etc.

(c) Type of soil in which the plant was grown

(7) A complete description of the method, procedures, and instruments used to make the measurements, including any changes made in the sample, intentionally, or unintentionally

(B) Soil measurements

(1) Geographical location from which sample was taken (county, township, section, 1/4 section)

(2) Color of soil as compared to a standard such as the Munsell Soil Color Chart

(3) Measurement of soil moisture content and description of method used in measuring it

(4) Description of the soil, including its type, texture, composition, etc.

(5) Description of the method used to collect the sample, including:

(a) The level at which the sample was taken

(b) The extent to which the soil has been changed from its natural state (soil moisture, surface geometry, etc.)

(6) A complete description of the method, procedures, and instruments used to make the measurements, including any changes made in the sample, intentionally, or unintentionally

6.4. ALTITUDE-VARIATION STUDIES

6.4.1. DEGRADATION OF MULTISPECTRAL IMAGERY. Multispectral imagery will be degraded in two distinct ways as the altitude at which the image is made is increased. First, the ground resolution will be degraded primarily by simple geometrical effects. Second, the

apparent spectral radiance of any part of the scene may be changed by spectrally selective or nonselective absorption, scattering, and emission effects occurring in the atmospheric path.

In either photographic or optical-mechanical scanner imagery, the spatial resolution set by the instrument generally has the form of constant angular resolution so that the linear resolution at the ground will be directly proportional to the altitude. This result can, of course, be altered by changing the focal length of the objective lens and making the appropriate changes to the equipment. This again, however, involves a simple geometrical relation and can readily be accounted for. What is more important here is to notice that there are other effects which may degrade resolution, but they are likely to become less important as altitude is increased or are likely to produce a constant degradation of the angular resolution (except perhaps under special circumstances.)

Thus, for instance, image degradation of the ground resolution due to scintillation caused by atmospheric turbulence (for a given atmospheric condition) will become less and less noticeable as the altitude is increased, while the geometrical ground resolution will fall off with altitude. In any case, turbulence effects are likely to be relatively insignificant except for oblique photography with very long focal length lenses with which we are not concerned in our aircraft measurements or satellite applications. If turbulence around the aircraft leads to significant scintillation, this would no longer be true, but such effects are believed to occur only in certain regimes of high-speed flight with which we need not be concerned at this time.

Again, vehicle vibration and instability may lead to image degradation resulting from motion of components of the imaging equipment during exposure. Usually such vehicular effects are reduced in magnitude as altitude is increased, so performance degradation with increasing altitude for this effect is unlikely. Particular vehicle operating conditions which lead to excessive vibration or instability should be avoided.

It is often supposed that haze can lead to spatial resolution degradation. However, it has been shown by Middleton [20] and others that this is not the case except perhaps under very special circumstances such as exist when a very thin layer of dense fog is almost in contact with the target. As shown by Middleton, the more general and more important effect of haze is to destroy the contrast in the image by the double action of scattering light out of the beam from the image and uniformly scattering light from any other source present into the beam.

6.4.2. SCATTERING AND ABSORPTION. For simplicity, we consider first a single narrow band of wavelengths and two uniform objects of spectral radiance $N_{1\lambda}$ and $N_{2\lambda}$. From some given altitude, both spectral radiances will appear to be attenuated equally by absorption and scattering by the factor ${}_{h}\tau_{\lambda}$, the transmission of the column of atmosphere of height h. This factor will be a function of the atmospheric conditions as well as of h and λ. At the same

time, the apparent radiances of both objects will appear to be increased by an amount ${}_h\Delta N_\lambda$, the radiance of the column of air of height h due to emission from and/or scattering by the gaseous and particulate matter in the column. Thus the apparent spectral radiances of the two objects have changed from $N_{1\lambda}$ and $N_{2\lambda}$ to

$$ {}_hN_{1\lambda} = {}_h\tau_\lambda N_{1\lambda} + {}_h\Delta N_\lambda \text{ and } {}_hN_{2\lambda} = {}_h\tau_\lambda N_2 + {}_h\Delta N_\lambda \tag{1} $$

In visibility and photographic work [21], it is usual to define contrast C by a ratio such as

$$ C = \frac{N_1 - N_2}{N_1 + N_2} \tag{2} $$

Thus, if ${}_oC_\lambda$ is the actual target contrast and ${}_nC_\lambda$ is the apparent contrast as observed from altitude h, for wavelength λ we find

$$ {}_oC_\lambda = \frac{N_{1\lambda} - N_{2\lambda}}{N_{1\lambda} + N_{2\lambda}} $$

and

$$ {}_hC_\lambda = \frac{{}_h\tau_\lambda(N_{1\lambda} - N_{2\lambda})}{{}_h\tau_\lambda(N_{1\lambda} + N_{2\lambda}) + 2{}_h\Delta N_\lambda} = \frac{{}_oC_\lambda}{1 + ({}_h\Delta N/{}_h\tau_\lambda)/\overline{N}_\lambda} $$

where $\overline{N}_\lambda$ is the mean radiance of the two targets. Thus, the factor ${}_h\Delta N_\lambda/{}_h\tau_\lambda$ is clearly important in photographic contrast determination. For our purposes, however, introduction of an arbitrary definition of contrast does not appear to be of value.

In this case, the path radiance ${}_h\Delta N_\lambda$ can be ignored and a knowledge of τ as a function of h, λ, and atmospheric conditions is all that is required to understand and predict the variation of spectral radiance differences with altitude. For radiation-noise-limited detectors, however, the detector noise level and responsivity will depend upon the total radiance, which must, therefore, be taken into account. Also, the term ${}_h\Delta N_\lambda$ will not in fact be constant as has been assumed above. The radiation scattered into the beams is predominately sunlight for wavelengths shorter than about 4 μ. At longer wavelengths, this radiance ${}_h\Delta N_\lambda$ is primarily the self-emission of the path with perhaps some thermal radiation from the earth and sky scattered into the beam. In all cases, ${}_h\Delta N_\lambda$ and τ_λ will depend upon the angle of inclination of the beam. In general, they will both become larger as the angle between the beam and the vertical increases.

Unless it is possible to work entirely at wavelengths at which atmospheric absorption and scattering effects are negligible, it will be necessary to correct multispectral imagery data using appropriate measured or theoretical values of ${}_h\tau_\lambda$ and ${}_h\Delta N_\lambda$.

It is interesting to notice that if a complete automatic system for data analysis and data processing of the type indicated in section 5 were available, consideration of such concepts as ${}_h\tau_\lambda$ and ${}_h\Delta N_\lambda$ would be unnecessary. The whole problem could be handled by including h and the view angle together with appropriate measures of the atmospheric conditions as components of the vector used to represent the measured spectra. This would be equivalent to using a separate library of target spectra for each condition of measurement (i.e., for every combination of h, view angle, and atmospheric condition). While this technique would probably be less efficient than a data-correction system, it might well be more practical. Automatic processing of this sort is unlikely to be available for some years; however, these considerations do make clear two problems of a general nature. The first is the rather obvious one of the very large amount of data that would have to be gathered to form a statistically valid basis for a definitive determination. The second is the difficulty of finding measures of atmospheric conditions which are both useful in this context and either measurable or predictable. For instance, while the total water-vapor content of the path would probably be useful in determining ${}_h\tau_\lambda$ in the wings of the water-vapor absorption bands, there is no way of obtaining a direct measure of this parameter under normal operating conditions. In fact, in this case, the measured spectra would probably contain the best available information on the water-vapor content. An ideal processing system would automatically take this information into account and neither extra vector components nor corrections to allow for water vapor would be required.

It is clear, however, that a study of ${}_h\tau_\lambda$ and ${}_h\Delta N_\lambda$ and an attempt to correlate these with measurable or predictable atmospheric parameters is desirable. In principle, a theoretical approach to the problem is possible, but the extreme complexity of molecular absorption and emission spectra and the equally great complexity of scattering theory make a purely theoretical approach impracticable.

A definitive experimental approach would be a major undertaking, so preliminary exploratory experiments designed to provide an understanding of the overall situations are indicated. If one measures the apparent radiance of two targets of different intrinsic radiance at one wavelength and from ground level and altitude h but otherwise under identical conditions, one will obtain corresponding measured values of $N_{1\lambda}$, $N_{2\lambda}$, ${}_hN_{1\lambda}$, and ${}_hN_{2\lambda}$. Then by inserting these values into equation 1 and solving the two simultaneous equations so formed, one obtains values for ${}_h\tau_\lambda$ and ${}_h\Delta N_\lambda$. While such experiments should undoubtedly be undertaken, the two difficulties mentioned above (the large number of measurements required and the difficulty of describing atmospheric conditions) are compounded by the difficulties of calibrating the measurement equipment. For instance, in the measurements just discussed, it would be necessary to make simultaneous measurements on the two targets from both ground level and the chosen

altitudes and to use spectroradiometers whose relative calibration was known to a high degree of accuracy and whose spectral bandwidths were essentially equal.

At the present time, all image interpretation, whether monotone or multiwavelength, is carried out by human interpreters. In view of this and of the magnitude of the sort of definitive experimental approach discussed above, it seems best to carry out preliminary survey experiments based in part on the skill of trained interpreters. A typical experiment would involve the collection of multispectral imagery of regions chosen for their intrinsic agricultural or other interest. Imagery would be made from as wide a range of altitudes as possible under as identical conditions as possible. (The latter condition might be approximated by having a single aircraft descending from the highest through the lowest altitude to keep the time between runs as low as possible and by doing this under stable weather conditions.) The lowest-altitude imagery would then be shown to an experienced interpreter who would be asked to note any interesting deductions he could make from the imagery. He would then select areas of specific interest. Data for the same areas taken from other altitudes would also be assembled. These data would then be analyzed in an attempt to answer the following questions:

(1) In what ways and how much do the measured spectra of ground targets of interest change with altitude?

(2) To what extent and in what way do these effects depend upon weather or other parameters?

(3) Do such changes seriously degrade the effectiveness of specific data-processing schemes?

(4) If such degradation does occur, can the original data be corrected for altitude and other measurable or known atmospheric conditions and can such degradation be made inconsequential by such techniques?

It will be seen that questions 3 and 4 cannot be properly answered except by reference to specific processing schemes. It should also be realized that the relevance of the answers to the first two questions also depends upon the specific processing scheme to be used, as this will determine the magnitude of spectral change which can be tolerated. In fact, no complete answers could be found for these questions until the nature of processing schemes to be used has been determined more explicitly than has been done so far. On the other hand, the value of a processing scheme will depend in turn upon the way in which altitude and other effects are handled. Thus, in fact, answers to these questions must be found concurrently with the development of processing schemes.

The specific data analysis experiments to be performed will no doubt be developed along with the data-processing and recognition schemes. However, there is no difficulty in inventing

experiments for analyzing the data gathered by the method discussed above; three experiments which appear particularly appropriate at the present time are described below.

(1) Higher altitude imagery should be compared with the corresponding low-level imagery by skilled interpreters. Such an experiment will not produce numerical results, but the interpreters may or may not find targets which they can identify on the basis of color effects in the low-altitude imagery but not in the corresponding higher altitude imagery. Perhaps the most important result of these experiments will be to find limited classes of targets and ranges of wavelengths and other parameters of importance. In this way, the data available for the other two experiments can be reduced to manageable proportions without greatly reducing their value.

(2) From such a reduced data bank calibrated values of spectral radiance for given targets and selected wavelengths should be plotted against altitude. The plotted points for each flight can then be joined or represented by smoothed curves as seems best. The result of this exercise will be a series of diagrams like that shown in figure 49. If these diagrams show serious divergence of behavior between flights, then an attempt should be made to determine whether particular types of behavior can be correlated with known or measurable atmospheric parameters. If it is desirable and possible to correct raw data for altitude effects, then these diagrams will contain the basic information needed to make such corrections.

(3) On the other hand, these experiments will not by themselves indicate whether or not data correction to allow for altitude effects is necessary. Ultimately this will be decided in the development of optimum spectral target-recognition processing techniques. In other words, while altitude effects will undoubtedly increase the variances of the spectra of various targets, the extent to which these increases will affect detection probabilities and false-alarm rates can be completely determined only when a statistically valid data bank of spectral signatures is available and optimum discrimination techniques have been developed.

In the mean time, however, it should be possible to obtain valuable indications of the magnitude of the problem by limited analysis. The technique of plotting two elements of the spectral signatures of a scene in an x-y oscilloscope display has already produced some interesting results. Such a plot, made using low-altitude data, could be overlaid by the corresponding plot for high-altitude data. It would then be possible to determine by inspection to what extent the increased variances of the combined data prevent discriminations possible with the low-altitude data.

Much useful information should emerge from these experiments on such factors as:

(1) How serious are altitude effects?

(2) At what, if any, wavelengths are such effects particularly serious or inconsequential?

(3) What kinds of meteorological parameters correlate with such effects?

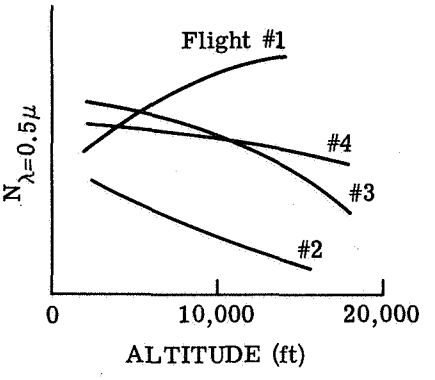

FIGURE 49. PROBABLE RADIANCE VARIATION AS A FUNCTION OF ALTITUDE

Thus, not only would the general characteristics of altitude effects be established in a way that would be of immediate value to both the planners of data-gathering flights and to the interpreters of data, but the results should be considered in planning more definitive altitude-effect measurement programs in the future. Perhaps most important, it will permit researchers to allow for such effects in the design and development of spectral recognition processing equipment.

From the summary of the data acquisitions for 1966 (table I, sec. 2), one can note the amount of data collected at various altitudes. These data have been tape recorded and will be used in the analysis for altitude effects on spectral signatures of crops. The most efficient way to conduct the analysis is to employ a cyclic display technique to obtain data from preferred small sections of the total video generated at each altitude and thereby work directly with digitized electronic signals. The analysis of the data will be delayed until this cyclic display capability has been implemented.

Appendix I
REFLECTANCE DERIVATION FROM SCANNER OUTPUTS

This appendix presents the relationship between the output voltage of an airborne radiation sensor and the reflectance of the earth. The system generates an output voltage for each sample on the earth that it sees; the voltage ratio for two samples is expressed as a function of the reflectance ratio of the two samples in the discussion that follows. An expression is derived first that relates the voltage ratio to the reflectance ratio for the general case; two special cases are then specified for which the voltage ratio equals the reflectance ratio.

The following assumptions are made. The incident and the reflected radiation are considered to be unpolarized. The attenuation of the atmosphere is neglected in this analysis. The ground resolution element contains a single substance that fills the field of view of the system. The reflectivity is constant across the narrow wavelength bands considered. The collecting optics of the scanning system subtend a small solid angle so that the radiation quantities and the cosine function do not change appreciably over the solid angle. Several definitions and equations are obtained from reference 1.

The following five conclusions are drawn:

(1) In the general case for which the sky contributes a significant amount to the total incident radiation and the samples observed are not Lambertian reflectors, the voltage ratio only approximately equals the reflectance ratio. The true relationship between the voltage ratio and the reflectance is given by equation 9 below.

(2) If the radiation from the sky can be neglected, the voltage ratio and reflectance ratio (between two samples on the earth) are equal for every kind of reflector.

(3) If the samples on the earth are Lambertian reflectors, the voltage ratio and the reflectance ratio are equal. The presence of sky radiation does not negate this conclusion.

(4) The percentage of the total incident radiation that is due to sky radiation decreases for increasing wavelengths and for decreasing polar angles of the sun. At approximately 1.0 μ the sky's contribution is negligible for all polar angles. At 0.5 μ the sky's contribution decreases to approximately 10% as the sun's polar angle decreases to zero (sun at zenith). On cloudy days, the sky's contribution is greater than that for a clear day.

(5) One cannot correctly say that all naturally occurring materials on earth are Lambertian reflectors.

The preceding conclusions, in summary, indicate that the voltage ratio only approximately equals the reflectance ratio. In certain special cases (conclusions 2 and 3) the two ratios are equal; however, these special cases do not always apply. The following sections verify these conclusions.

We first relate the system output voltage to the reflectance of the earth. The power P (in watts) at the collecting optics of the radiation sensor is

$$P = N_r A_o A_G R^{-2} \cos \theta_r \tag{3}$$

where $N_r = N_r(\theta_r \phi_r)$ = radiance ($W \cdot cm^{-2} \cdot sr^{-1}$) of the ground resolution element

θ_r = polar angle between the normal to the ground resolution element and the scanner (the polar angle is the complement of the elevation angle)

ϕ_r = azimuth angle of the ground resolution element

A_o = area (cm^2) of the collecting optics

A_G = area (cm^2) of the ground resolution element

R = range (cm) from the ground resolution element to the scanner

We next use the approximate relationship, $A_G = \sigma^2 R^2 \sec \theta_r$, ($\sigma^2$ = the field of view of the radiation sensor in steradians) in equation 3 to obtain

$$P = N_r A_o \sigma^2 \tag{4}$$

Since the system output voltage V is directly proportional to P, we obtain

$$\frac{V_1}{V_2} = \frac{N_{r1}}{N_{r2}} \tag{5}$$

The subscripts 1 and 2 denote the two ground resolution elements (the two samples) observed. The radiance N_r is a function of the angles θ_r and ϕ_r and is [22]

$$N_r = \int \rho' N_i \cos \theta_i \, d\Omega_i \tag{6}$$

where $\rho' = \rho'(\theta_i \phi_i, \theta_r \phi_r)$ = bidirectional reflectance (sr^{-1}) per unit projected solid angle of the received radiation

θ_i = polar angle between the normal to the surface and the incident radiation

ϕ_i = azimuth angle of the source radiation

$N_i = N_i(\theta_i \phi_i)$ = radiance ($W \cdot cm^{-2} \cdot sr^{-1}$) of the source radiation

$d\Omega_i = \sin \theta_i \, d\theta_i \, d\phi_i$ = elemental solid angle (sr) of the source

The bidirectional reflectance per steradian, ρ', is related to the bidirectional reflectance $\rho = \rho(\theta_i \phi_i, \theta_r \phi_r)$ by

$$\rho' = \frac{d\rho}{\cos \theta_r \, d\Omega_r}$$

where $d\Omega_r$ = the elemental solid angle subtended by the receiver.

The sun and the sky are the two sources of the incident radiation to be considered. The sky has a radiance N_i and equation 6 can be applied. The sun has an irradiance H ($W \cdot cm^{-2}$) related to N_i by $dH = N_i \, d\Omega_i$ so that

$$N_r = \int \rho' \cos \theta_i \, dH$$

Since ρ' and θ_i do not vary appreciably over the solid angle subtended by the sun, we can say that

$$N_r = \rho' H \cos \theta_i$$

In the preceding equation, θ_i and ϕ_i are evaluated at the position of the sun, $\theta_s \phi_s$, so that

$$N_r = \rho'_s H \cos \theta_s$$

where

$$\rho'_s = \rho'(\theta_s \phi_s, \, \theta_r \phi_r) \tag{7}$$

The total radiance at the collecting optics of the radiation sensor is obtained by adding the sky and sun contributions from equations 6 and 7 to obtain

$$N_r = \rho'_s H \cos \theta_s + \int \rho' N_i \cos \theta_i \, d\Omega_i \tag{8}$$

Using equation 8 in equation 5 yields

$$\frac{V_1}{V_2} = \frac{\rho'_{s1} H \cos \theta_s + \int \rho'_1 N_i \cos \theta_i \, d\Omega_i}{\rho'_{s2} H \cos \theta_s + \int \rho'_2 N_i \cos \theta_i \, d\Omega_i} \tag{9}$$

Equation 9 shows the relationship between the voltage ratio and the reflectance for the general case. We next look for simplifying assumptions to apply to equation 9 to make the voltage ratio equal the reflectance ratio.

The first simplifying assumption is to neglect the sky radiation and consider the sun as the only source. Equation 9 then reduces to

$$\frac{V_1}{V_2} = \frac{\rho'_{s1}}{\rho'_{s2}} \tag{10}$$

In this case the voltage ratio equals the ratio of the bidirectional reflectance per steradian between the two ground resolution elements. However, the limited available data show that the sky can contribute a significant amount to the total incident radiation. Measurements and calculations made for a clear blue sky were found in references 17 and 23-26. Figure 50 [17] shows the radiation from the sun + sky and from the sun alone as a function of wavelength for polar solar angles of 0^{o}, 48^{o}, 60^{o}, and 75^{o}. The contribution of the sky was calculated in reference 23. Figure 50 shows that for a polar angle of 75^{o} (elevation angle = 15^{o}), the contribution of the sky to the total radiation is 50% at 0.5 μ and 26% at 0.8 μ. When the polar angle decreases to 0^{o} (sun at the zenith), the sky's contribution to the total decreases to 10% at 0.5 μ and 3% at 0.8 μ. Percentages for other sun angles and wavelengths can be obtained from figure 50. Other measurements [23-26] recorded for polar angles of 20^{o} indicate a somewhat larger percentage for the sky's contribution. These data indicate that the sky contributes 15% at 0.5 μ and 13% at 0.8 μ.

From the preceding data we conclude that:

(1) The sky's contribution to the total incident radiation is particularly significant at short wavelengths (near 0.5 μ) and large polar angles (near 75^{o}).

(2) The sky's contribution decreases for increasing wavelengths and for decreasing polar angles. At wavelengths near 1.0 μ the sky's contribution is approximately 0 for all polar angles; at 0^{o} polar angle and 0.5 μ the sky's contribution decreases to approximately 10% of the total.

(3) Data showing the sky's contribution were recorded for a clear blue sky. When the sky is overcast or cloudy, the percent radiation from the sky will be greater than for a clear blue sky.

Since the sky radiation is often significant, we will retain it and place restrictions on the reflectance that allow us to equate voltage and reflectance ratios. Examination of equation 9 shows that if ρ' is constant with respect to $\theta_i\phi_i$ we can take it out of the integral. Also, by the reciprocity theorem [22], we have $\rho'(\theta_i\phi_i, \theta_r\phi_r) = \rho'(\theta_r\phi_r, \theta_i\phi_i)$, so that ρ' is also constant with respect to $\theta_r\phi_r$; thus, ρ' is a constant. Equation 9 then becomes

$$\frac{V_1}{V_2} = \frac{\rho_1'(H \cos \theta_s + N_i \cos \theta_i \, d\Omega_i)}{\rho_2'(H \cos \theta_s + N_i \cos \theta_i \, d\Omega_i)}$$

$$\frac{V_1}{V_2} = \frac{\rho_1'}{\rho_2'} \tag{11}$$

Assuming that ρ' is constant is equivalent to assuming the material is a Lambertian reflector. It is useful to categorize all materials as either specular or diffuse reflectors. A

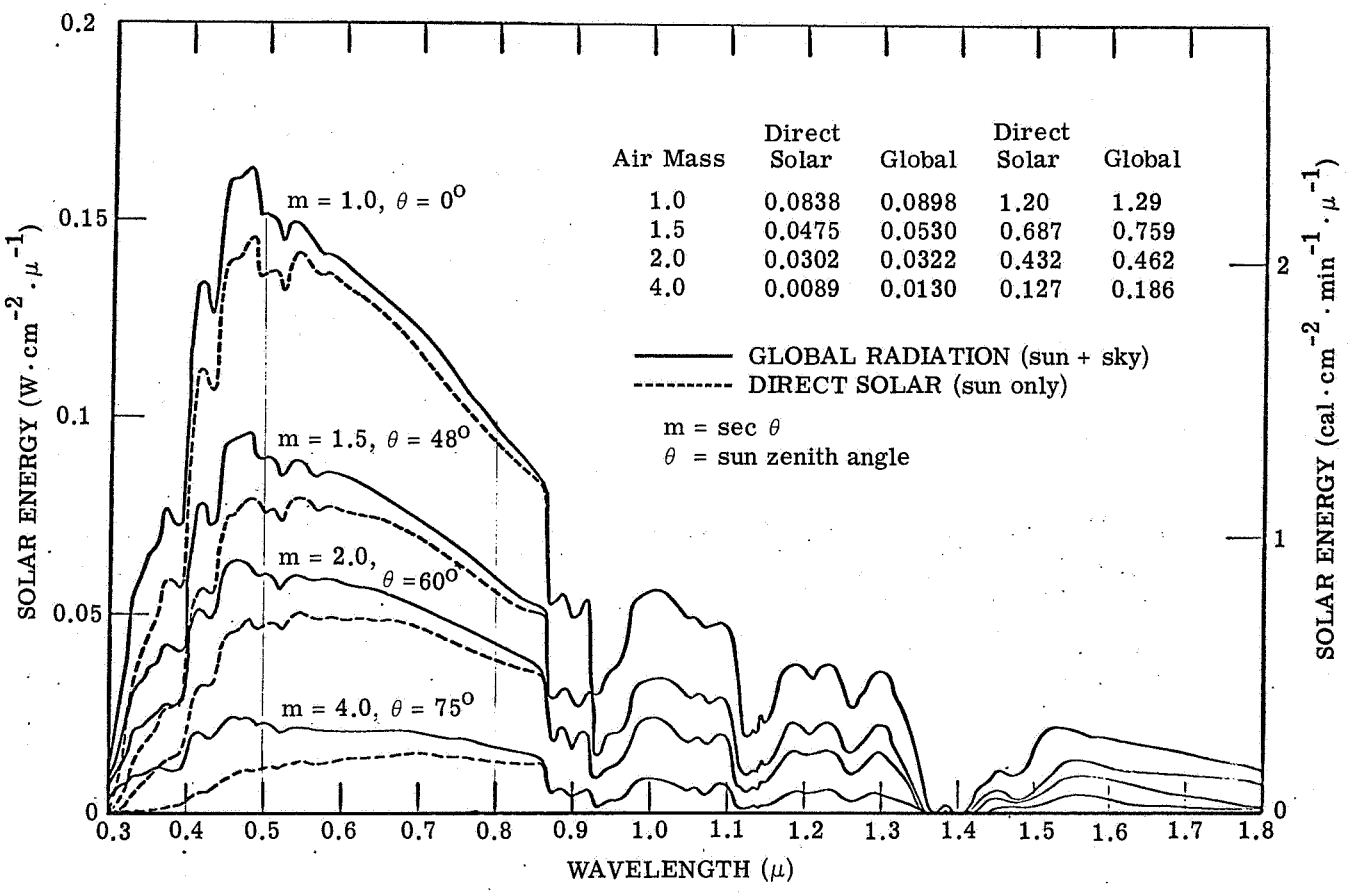

FIGURE 50. TOTAL ENERGY ON HORIZONTAL SURFACE [17]

specular reflector is one for which the angle of reflection equals the angle of incidence. A diffuse reflector is any reflector that is not specular. A Lambertian reflector is a diffuse reflector with a constant bidirectional reflectance per steradian, ρ'.

The measurements reported in reference 27 show that at least some naturally occurring materials are not Lambertian reflectors. They show that the reflectance of wheat, grass, and beets in sandy soil changes considerably with the angle of the radiation source. From these limited data we cannot say that most naturally occurring materials are non-Lambertian; we have demonstrated only that some are definitely not Lambertian.

Appendix II
DATA HANDLING EQUIPMENT

The objective of the data-handling equipment is to furnish data from the scanners in a form acceptable to IBM 700/7000 series computers such as are available at The University of Michigan and at Purdue University. It is intended that this be done by using available equipment as much as possible to lower the cost of this operation. For this purpose, a means of making the scanner data acceptable to the A-D equipment already at The University of Michigan is required and is the principal subject of the design.

II.1. A-D CONVERTER

The general characteristics of the available converter are described briefly. The equipment accepts a serial or parallel input and sequentially samples, holds, and converts the signal into digital form and records this on tape in 7-bit form at a density and rate (556 bits/in., 75 ips) acceptable to IBM equipment. However, the equipment cannot sample and hold an input signal from the 12 channels for a single resolution element as is needed for our data; consequently, a parallel sample-and-hold operation must be performed prior to using this equipment. Furthermore, since we are using two recorders which contain 12- and 4-channel data on 1-in. and 1/2-in. tape, respectively, and only 1/2-in. tape is needed, the data on the 1-in. tape should be converted to the 1/2-in. tape machine, i.e., it must be serialized. This sampling, holding, and serial multiplexing of the data must be performed by equipment not available at this time.

II.2. CHARACTERISTICS OF THE SAMPLED DATA

The data to be sampled are conventional scanner data obtained from either a 12-channel source, a 4-channel source, or two single-channel sources. Thus, the information required will be sampled 12, 4, or 1 at a time, serially entered on a tape channel (FM) along with identification information and synchronization pulses in other channels. In this form, the data can be accepted by the A-D conversion system.

To obtain an idea of the data which may be processed by this technique, it is useful to consider the form of the processing. The quantities of interest are the sampling rate and sampling density. The sampling rate is determined by the A-D converter and the number of channels. For example,

$$r = s \times \frac{1}{n} = 20 \times 10^3 \times \frac{1}{12} = 1.67 \times 10^3 \text{ samples/sec}$$

where n = number of channels

s = frequency capability of the A-D converter

Once the tape has been slowed down, however, the effective sampling rate will run up to as high as 53 kHz.

The sampling density, or the number of samples per radian of scanner motion, is a function of sampling rate, scanner angular velocity, and tape speed:

$$d = r \times \frac{1}{w} \times \frac{60}{t} \text{ samples/rad} = \frac{20 \times 10^3}{12} \times \frac{60}{3000 \times 2\pi} \times \frac{60}{t}$$

$$= \frac{50}{3\pi} \times n = 5.3 \times n \text{ samples/rad} = \frac{50}{3\pi} \times n \times \frac{\pi}{2} = 8.3 \times n \text{ samples/quadrant}$$

where r = samples/sec

w = rad/sec

t = tape playback speed, ips

60 = normal recording speed, ips

n = record/playback speed ratio

The sampling densities readily obtainable may range from 8.3 to 266 per quadrant as tape speed is changed from 60 ips to 1 7/8 ips in playback. This may be expressed as 5.3 to 170 samples/rad or as one sample per 189 mrad or per 5.9 mrad.

The ground sampling density is worth noting and is computed from the aircraft speed, 120 knots. These densities range, then, between 208 and 6650 samples per 100 ft of flight. The sampling density, however, will probably be chosen on the basis of obtaining sufficient angular sample resolution.

The angular resolution is of interest also. If a ground swath 300 ft wide is assumed at altitudes of 500 ft, 2000 ft, and 10,000 ft, the following sample densities are available per scan line along the length of the field:

Altitude	Low Density (60)	High Density (1 7/8)
500 ft	3.1 samples	99 samples
2,000 ft	0.79 samples	25.5 samples
10,000 ft	0.16 samples	5.1 samples

The high density seems reasonable and should allow satisfactory operation.

Of these data, which are probably typical, only 10%, 2% and 0.5%, respectively, of the actual scan angle is required for storage. The digitizing process, however, samples all the data and provides a very inefficient set of data which should be further processed. This will

require simple editing of the tape by a computer to obtain a masked, edited, repacked tape for direct use in programs without imposing the need for an editing program on each user of the data.

II. 3. DESIGN OF THE SERIALIZER

Following the process of serialization described, changing tape speeds and digitization allow a satisfactory range of sampling density. Since only the addition of a serialization process to the data recorded in the aircraft is required to make it acceptable to the A-D converter, the serializer can be considered necessary. Moreover, equipment similar to that needed is already designed and fabricated to handle the 12-channel calibrated information.

The data-handling process can be visualized as in figure 51. On the basis of previous remarks, it seems most efficient to retain data in only the original analog form or final edited form since only 2% to 10% of the intermediate tape is actually desired data.

The general block diagram of the serializer is shown in figure 52. Data are sampled at a constant rate of 20 kHz and multiplexed into a single FM channel of a tape recorder. A sync pulse is supplied to control the A-D converter. A stop/start pulse is supplied to control the IBM 729 tape handler and to increment the recorder number; this may be a single bipolar level change or burst of positive or negative pulses. A code is supplied on four channels to allow continual identification of data. This is set up to allow "1 of 4" coding so that masking may be simplified to sorting on a single bit. The start of a scan may be determined from the first occurrence of data and there is no coding for angular location; the angular location may be determined by counting the number of samples and determining angle from the known sampling rate and speed of rotation of the scanner. This will have to be known and supplied as additional data.

A detailed sketch of the formats of the tape generated in the process is given in figure 53. The sequence of sampling is 13 counts long, one sample interval, and 12 serially multiplexed analog samples of the input channels. At each sample, the data are encoded with identification bits as shown with the S interval coded as (0000) since it is an interval of change and allows an insertion of a $0 \rightarrow 1$ transfer to locate the first element of the 12 vector.

The digital tape will start on command and insert a record number at the beginning of the data, ignoring information on the analog tape. At the end of this operation, the record will commence with a randomly located sample point shown in figure 53 as point #10. Thus, in general, a certain amount of data must be thrown away since the sample point is not known and the location within the scan angle is not known. The tape could be encoded for this, but the search operation required can be performed more easily in the computer.

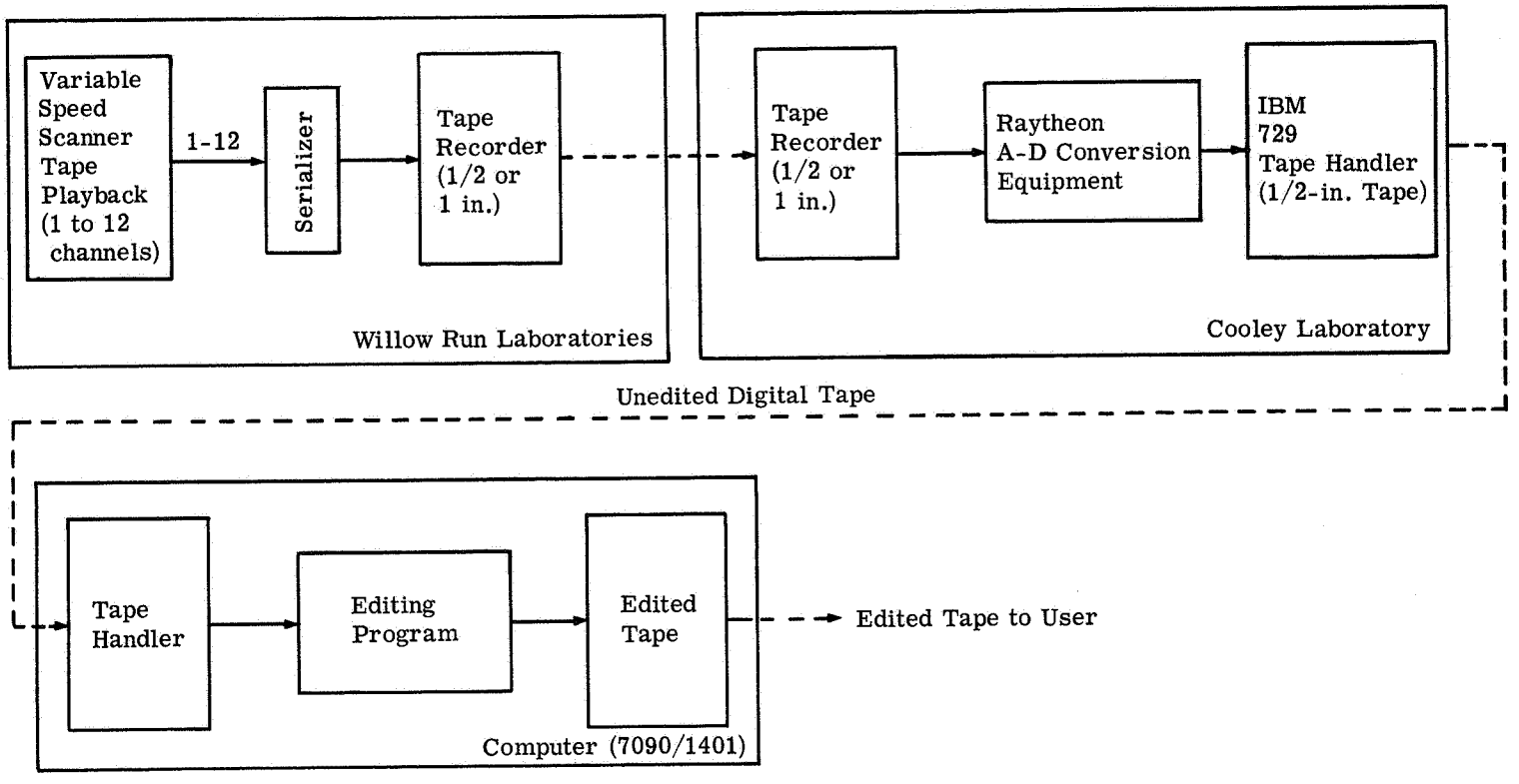

FIGURE 51. BLOCK DIAGRAM OF DATA-HANDLING PROCESS

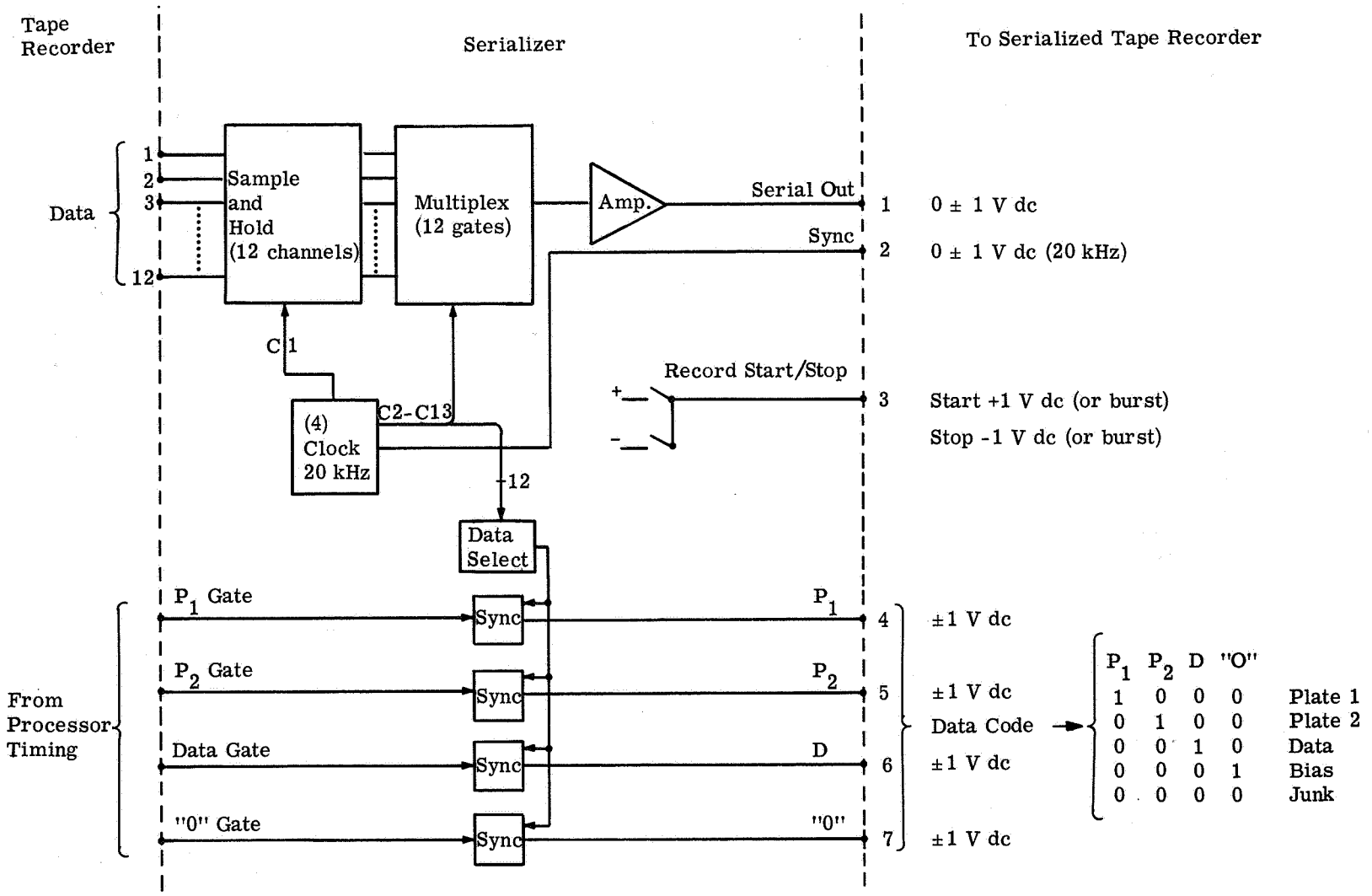

FIGURE 52. SERIALIZER BLOCK DIAGRAM

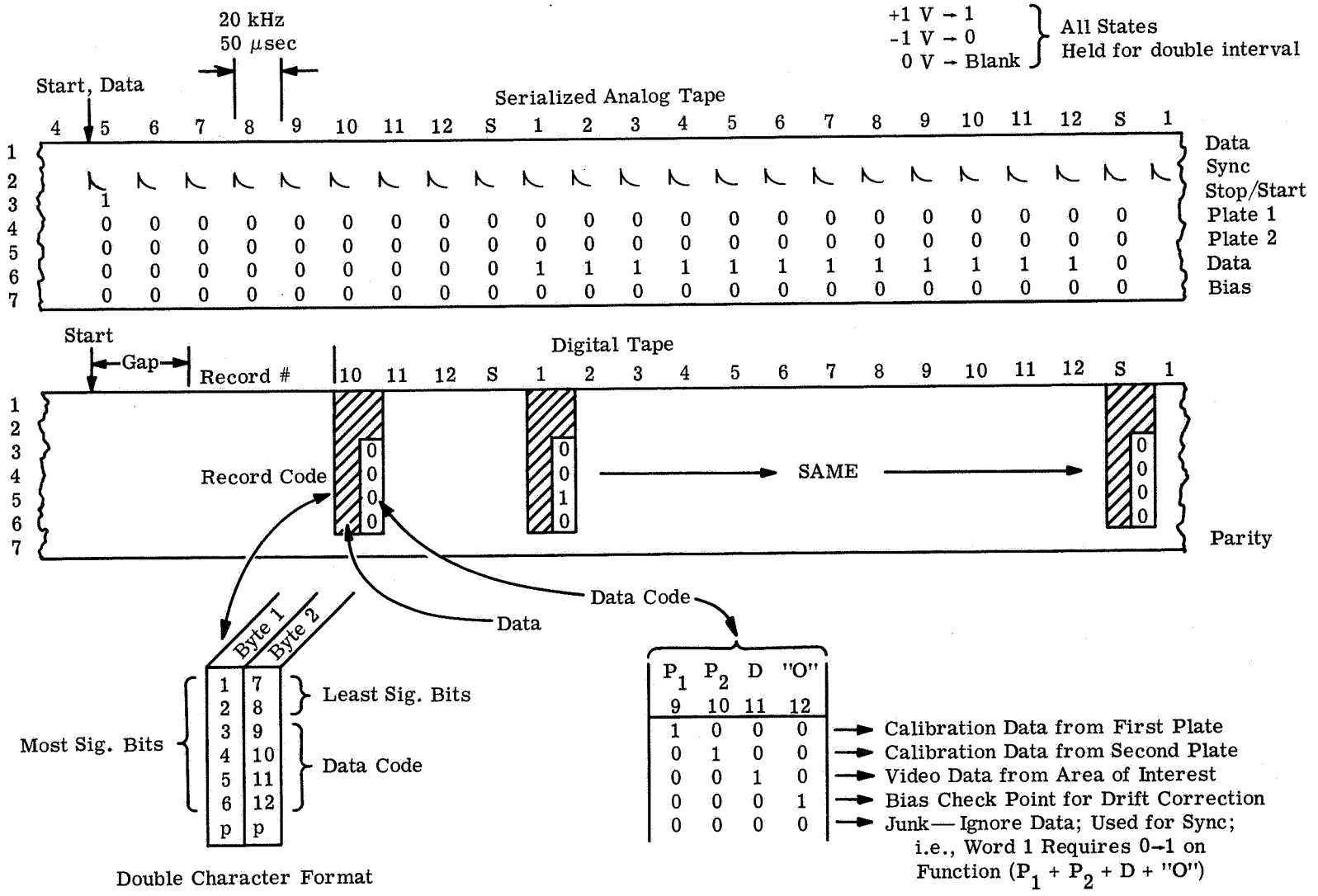

FIGURE 53. DETAILED FORMAT OF ANALOG AND DIGITAL TAPES

Finally, the overall appearance of the data will be as shown in figure 54. Each record will have a sequentially coded record number followed by data derived from calibration points and ground radiation interspersed with "junk" and starting at a random point within the field of interest and ending at another random point within the field of interest. The packing will be poor in terms of the percentage of data in the tape (2% to 10%), but it may be collated and unpacked simply. It appears best to do this unpacking and collating with the computer before supplying the data to any user. This requires the preparation of a simple program to mask the data to eliminate junk and to unpack the 12-bit characters and repack them into 36-bit words, at the same time adding whatever additional information is needed either on the tape or on cards. The exact form for the final tape should be determined by the analysts to assure a satisfactory set of data tapes. This final step should be made, however, to avoid buying and storing 10 to 50 times the amount of tape really needed.

II.4. RÉSUMÉ OF PROCESSING

In order to process the data as described above, a considerable amount of equipment is required (fig. 55). The new equipment needed, beyond the normal processing equipment, has been minimized as much as possible in order to build a serializer for which similar modules are already designed and built.

The operations required may now be described in terms of figure 55. The tape is run at a normal rate to locate the areas to be serialized and digitized as noted on the C-scan CRO. The location then is made from the tape footage indicator (and the CRO as a check). The specific area and the calibration points are then gated by location along the scan line to allow their encoding. When all areas are properly located, the tape is then run at a suitable speed to obtain the desired sampling density and the record start signal is given as determined by visual observation. The serialization continues until the record stop is given. A gap of tape is then run into the #2 recorder to separate the records as needed and the process is repeated for the second field.

At the same time the recording CRO is operated and a record of the area serialized is obtained for one channel. This may be expanded, of course, to afford a fuller picture than only the area serialized if this is desired.

II.5. CONCLUSION

The processing equipment described appears to be a simple method of obtaining digital records from the scanner data and should be compatible with the scanner data and the A-D equipment. It should also afford digital data acceptable by both WRL and Purdue computing equipment.

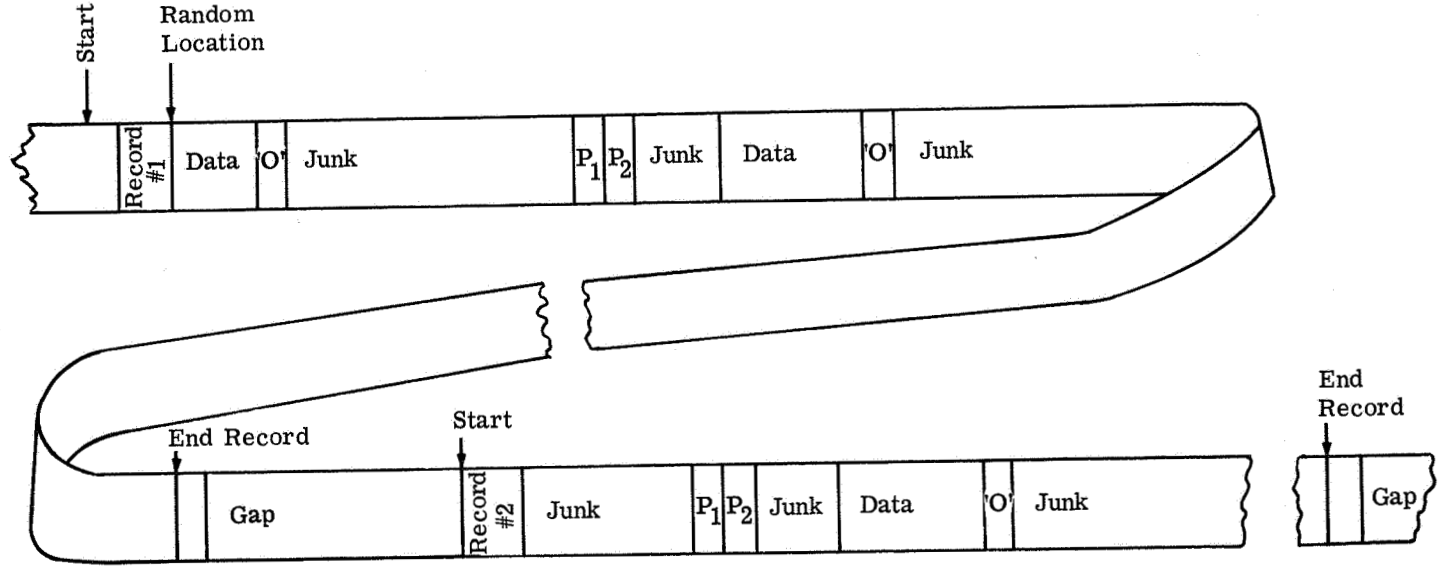

FIGURE 54. SIMPLIFIED OVERALL SKETCH OF RAW DATA TAPE

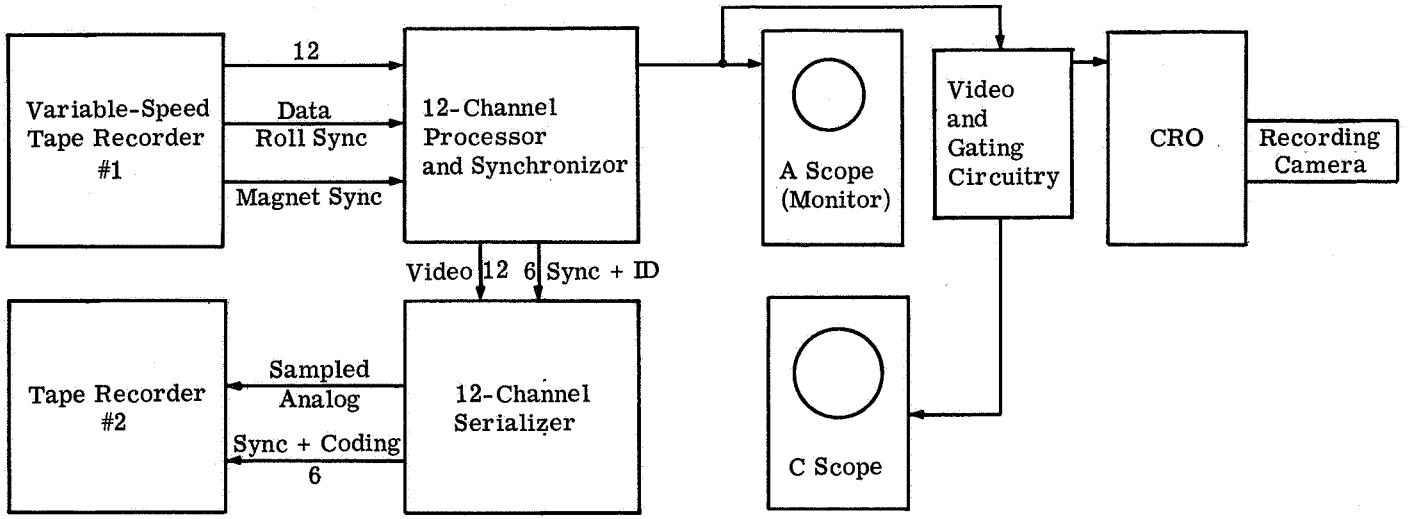

FIGURE 55. BLOCK DIAGRAM OF COMPLETE PROCESSOR

REFERENCES

1. M. Holter, D. Lowe, and R. Shay, Investigation of a Method for Remote Detection of Life on a Planet, Report No. 6590-1-P, Institute of Science and Technology, The University of Michigan, Ann Arbor, November 1964.

2. L. D. Miller, The Investigation of a Method for Remote Detection and Analysis of Life on a Planet (Final Report), Report No. 6590-4-F, Willow Run Laboratories of the Institute of Science and Technology, The University of Michigan, Ann Arbor, November 1965.

3. R. M. Hoffer, Purdue University, Lafayette, Ind., and L. D. Miller, Willow Run Laboratories of the Institute of Science and Technology, The University of Michigan, Ann Arbor, "Potential Applications of Remote Multispectral Sensing in Agriculture," presented at 30th Semi-Annual Convention of the American Society of Photogrammetry, Dayton, Ohio, 24 September 1965.

4. M. Holter and W. Wolfe, "Optical-Mechanical Scanning Techniques," Proc. IRE, Vol. 47, 1959, p. 1546.

5. M. A. Romanova, Air Survey of Sand Deposits by Spectral Luminance, Consultants Bureau, New York, 1964.

6. N. A. Raspolozhenskiy, "An Airborne Spectrometer for the Study of the Spectral Brightness of Landscape Features," Geodesy Aerophot., Vol. 6, 1964, p. 358.

7. R. R. Legault and F. C. Polcyn, "Investigations of Multi-Spectral Image Interpretation," Proceedings of the Third Symposium on Remote Sensing of Environment, October 14, 15, 16, 1964, Report No. 4864-9-X, Institute of Science and Technology, The University of Michigan, Ann Arbor, February 1965, AD 614 032, pp. 813-821.

8. C. E. Molineaux, "Multiband Spectral System for Reconnaissance," Photogrammetric Eng., Vol. 31, 1965, p. 131.

9. D. S. Lowe, F. C. Polcyn, and J. R. Shay, "Multispectral Data Collection Program," Proceedings of the Third Symposium on Remote Sensing of Environment, October 14, 15, 16, 1964, Report No. 4864-9-X, Institute of Science and Technology, The University of Michigan, Ann Arbor, February 1965, AD 614 032, pp. 667-680.

10. R. J. P. Lyon and E. A. Burns, "Infrared Spectra Analysis of the Lunar Surface from an Orbiting Spacecraft," Proceeding of the Second Symposium on Remote Sensing of Environment, 15, 16, 17 October 1962, Report No. 4864-3-X, Institute of Science and Technology, The University of Michigan, Ann Arbor, February 1963, AD 299 841, pp. 309-327.

11. D. S. Lowe and J. G. N. Braithwaite, "A Spectrum-Matching Technique for Enhancing Image Contrast," Appl. Opt., Vol. 5, 1966, p. 893.

12. D. S. Lowe, J. Braithwaite, and V. L. Larrowe, An Investigative Study of a Spectrum-Matching Imaging System (Final Report), Report No. 8201-1-F, Willow Run Laboratories of the Institute of Science and Technology, The University of Michigan, Ann Arbor, October 1966.

13. E. L. Krinov, Spectral Reflectance Properties of Natural Formation, National Research Council translation, 1953.

14. J. E. Carson, Soil, Temperature, and Weather Conditions, Report No. ANL-6470, Argonne National Laboratories, Argonne, Ill., November 1961.

15. W. R. Van Wijk, Physics of the Plant Environment, North Holland Publishing Co., Amsterdam, 1963.

16. Handbook of Geophysics, Macmillan, 1961, pp. 16-26.

17. D. Gates, "Spectral Distribution of Solar Radiation at the Earth's Surface," Science, Vol. 151, No. 3710, 1966; also unpublished data.

18. Azimuths of the Sun, 15th ed., Hydrographic Office, U. S. Navy Department, U. S. Government Printing Office, 1952.

19. W. D. McClellan, J. P. Meiners, and D. C. Orr, "Spectra Reflectance Studies on Plants," Proceedings of the Second Symposium on Remote Sensing of Environment, 15, 16, 17 October 1962, Report No. 4864-3-X, Institute of Science and Technology, The University of Michigan, Ann Arbor, February 1963, AD 299 841, pp. 403-413.

20. W. E. K. Middleton, Vision through the Atmosphere, University of Toronto Press, 1958.

21. M. J. Mazurowski and D. R. Sing, "Attenuation of Photographic Contrast by the Atmosphere," J. Opt. Soc. Am., Vol. 43, 1953.

22. F. E. Nicodemus, "Directional Reflectance and Emissivity of an Opaque Surface," Appl. Opt., Vol. 4, No. 7, 1965, p. 767.

23. H. R. Condit and F. Grum, "Spectral Energy Distribution of Daylight," J. Opt. Soc. Am., Vol. 54, No. 7, 1964, p. 937.

24. Atmospheric Optical Measurements in Western Florida, Flight 112, Part III, Sky Radiance (Blue), Visibility Laboratory, Scripps Institution of Oceanography, University of California, San Diego, November 1960.

25. Atmospheric Optical Measurements in Western Florida, Flight 112, Part IV, Sky Radiance (Blue), Visibility Laboratory, Scripps Institution of Oceanography, University of California, San Diego, November 1960.

26. Quantitative Spectral Measurements of Radiation in the 0.55 to 3 Micron Region from Clouds, Horizons and Blue Sky, NAVORD Report No. 3645, Naval Ordnance Test Station, China Lake, Calif., 31 March 1955.

27. D. Steiner and H. Haefner, "Tone Distortion for Automated Interpretation," Photogrammetric Eng., Vol. 31, 1965.

DISTRIBUTION LIST

Copy No.	Addressee
1-6	Office of Grants and Research Conctacts Code SC, NASA Washington, D. C.
7-8	Purdue Research Foundation, Executive Building Purdue University Lafayette, Indiana 47907